工 學 博 士 學 位 請 求 論 文

Biological Studies of Kaempferol from Green Tea Seed by Enzymatic Hydrolysis and Their Application to Cosmeceuticals

녹차씨 효소가수분해로 얻은 캄페롤의 피부에서의 효능 및 이를 활용한 코스메슈티컬 제품 연구

2013년 8월

서울大學校 大學院

化學生物工學部

姜 炳 永

Biological Studies of Kaempferol from Green Tea Seed by Enzymatic Hydrolysis and Their Application to Cosmeceuticals

녹차씨 효소가수분해로 얻은 캄페롤의 피부에서의 효능
및 이를 활용한 코스메슈티컬 연구

指導敎授 : 金 秉 祺

이 論文을 工學博士 學位論文으로 提出함

2013年 8月

서울大學校 大學院

化學生物工學部

姜 炳 永

姜 炳 永 의 工學博士 學位論文을 認准함

2013 年 8 月

委 員 長	_____
副委員長	_____
委 員	_____
委 員	_____
委 員	_____

Biological Studies of Kaempferol from Green Tea Seed by enzymatic hydrolysis and their Application to Cosmeceuticals

A Thesis

Submitted to the Faculty of Seoul National University

By

ByungYoung Kang

In Partial Fulfillment of the Requirements

for the Degree of Doctor of Philosophy

Advisor: Professor Byung-Gee Kim, Ph.D.

August, 2013

School of Chemical and Biological Engineering

Seoul National University

ABSTRACT

Kaempferol, one of the flavonols in green tea, has many biological activities, but the kaempferol of plant origin is too expensive to be used in commercial products. Recently, it has been confirmed that green tea seed (GTS) contained fairly good amount of kaempferol glycoside. After conducting structural analysis, two forms of kaempferol glycosides i.e. kaempferol-3-O-[2-O-β-D-galactopyranosyl-6-O-α-L-rhamnopyranosyl]-β-D-glucopyranoside (compound 1) and kaempferol-3-O-[2-O-β-D-xylopyranosyl-6-O-α-L-rhamnopyranosyl]-β-D-glucopyranoside (compound 2) were identified. To obtain pure kaempferol in large quantity, their enzymatic hydrolysis was attempted. Through screening of commercially available enzymes, β-galactosidase and hesperidinase were selected and, their mixing ratio was optimized. At the optimized condition, over 95% pure kaempferol was produced.

The purified kaempferol and its glycosides were subjected to various examinations of biological effects. In terms of antioxidant effect on skin anti-aging, Kaempferol was a more efficient scavenger of DPPH radicals and a better inhibitor of xanthin/xanthine oxidase than the compound 1 and compound 2. Kaempferol showed inhibitory effect on lipid peroxidation which was induced by t-butyl hydroperoxide (t-BHP) in keratinocytes. Kaempferol treatment significantly inhibited ultraviolet (UV)-induced matrix metalloproteinase-1 (MMP-1) in mono-culture of normal human fibroblasts or keratinocytes/fibroblasts co-cultured system. However, kaempferol did not change the level of type I pro-collagen

synthesis in fibroblasts. Since TNF-α is another inducer of skin-aging and stimulate MMP-1 in fibroblasts, another explanation is that kaempferol inhibits TNF-α production, which in turn repress MMP-1 in keratinocytes/fibroblasts co-culture.

When the effect of kaempferol on the skin wrinkles was examined *in vivo*, kaempferol showed to decrease wrinkles induced by squalene-hydroperoxide in hairless mice. In addition, topical application of the emulsion containing kaempferol for 8 weeks decreased wrinkles in photo-aged skin area such as crow's feet area.

To elucidate its effects on the skin further, the transcriptional profiles of kaempferol-treated HaCaT cells were examined using cDNA microarray analysis. 147 genes exhibited significant changes in expression. Among them, 18 genes were up-regulated and 129 genes were down-regulated. These genes were then classified into 12 categories according to their function: cell adhesion/cytoskeleton, cell cycle, redox homeostasis, immune/defense responses, metabolism, protein biosynthesis/modification, intracellular transport, RNA processing, DNA modification/replication, regulation of transcription, signal transduction and transport. The promoter sequences of the differentially-regulated genes was analyzed, and then over-represented regulatory sites and candidate transcription factors (TFs) for gene regulation by kaempferol were identified as such c-REL, SAP-1, Ahr-ARNT, Nrf-2, Elk-1, SPI-B, NF-κB and p65. In addition, the microarray results and bioinformatic analysis were validated by conventional methods such as real-time PCR and ELISA-based

transcriptional factor assay. The inhibitory effect of kaempferol on NF-κB and RelB in HaCaT cells and normal human epidermal keratinocytes (NHEKs) irradiated with UVB was shown by ELISA-based transcription factor assay. Since PPAR activation is one of several mechanisms which could account for the decrease of NF-κB activities, the effect of kaempferol to increase the transcriptional activity of PPARs in HaCaT cells was investigated. Kaempferol stimulated PPAR transcriptional activity in HaCaT cells transiently transfected with the PPRE-*tk*-Luc reporter gene, suggesting that kaempferol acts as a regulator of epidermal differentiation in human skin. To investigate whether or not kaempferol promotes the differentiation of keratinocytes, BrdU incorporation experiment and a Western blot analysis against transglutamase-1 protein were performed. Kaempferol treatment inhibited BrdU incorporation, and induced transglutamase-1 protein in keratinocytes, suggesting that kaempferol could be an inducer of epidermal keratinocytes differentiation.

In conclusion, kaempferol is demonstrated as a very effective anti-aging reagent that can be used as an anti-aging ingredient, and a possible candidate of cosmeceutical products.

Key words: Kaempferol, skin, aging, anti-oxidation, DNA microarray, wrinkle

Student number: 2003-30270

CONTENTS

LIST OF TABLES

LIST OF FIGURES

CHAPTER 1

Introduction

1. Introduction

1.1 Overview

In recent years cosmetic, pharmaceutical and chemical industries have become increasingly interested in antioxidants. Recent research efforts on antioxidants have focused on flavonoids that show strong free radical scavenging effects and metal ion chelating properties. In addition to their antioxidant activity, flavonoids have been reported to inhibit various enzymes such as cyclooxygenase and lipoxygenase related to inflammation [1]. Evidence for the presence of flavonoids in ancient remedies for burns and inflammation has been reported and these substances, which have been isolated, are presently used in commercial products [2, 3]. Therefore, flavonoids have attracted attention for potential beneficial effects on humans.

Flavonoids represent the single, most widely occurring group of phenolic phytochemicals. Approximately 5,000 flavonoids have been reported in the literature. According to the oxidation level of their central C ring, these variations define the families of anthocyanidin, flavone or flavonol (i.e. 3-hydroxyflavone), flavanone and proanthocyanidin oligomers of the monomeric flavan-3-ols. Flavonols are a specific class of flavonoids that are widely distributed in plants where they function as antioxidants, antimicrobials, photoreceptors, visual attractors and light screeners. Their chemical structure allows them to have a multitude of substitution patterns on the benzene and heterocyclic rings thus giving rise to different subgroups. The major flavonols in human diet are quercetin, kaempferol and myricetin. Interestingly, flavonols conents are about 13% in

green tea. Though flavan-3-ols, known as catechins, have attracted more attention from researchers, they need to be stabilized for commercial uses. In contrast, flavonols are structurally more stable than flavan-3-ols. The main flavonols in tea species are glycosides of quercetin and kaempferol. Quercetin and kaempferol have exhibited a wide range of biological activities including antioxidant, radical scavenging, anti-inflammatory, anti-atherosclerotic, anti-tumoral and anti-viral effects [4-6]. Concerning the commercial use of flavonols for other industrial purposes, the production of pure flavonols obtained from plant sources is not easy. Recently, several research groups reported commercial production of quercetin with purity of 95%. On the contrary, there has not been any report to produce the commercial grade of kaempferol.

The five top cosmetic non-surgical procedures are botulinum toxin injection, microdermabrasion, filler injection, laser hair removal, and chemical peeling [7]. But those non-surgical treatments have unexpected side effects and restlessness, and there are a lot of people still prefer the cosmetics. Thus, finding an effective and safe anti-skin aging ingredient is an important issue in cosmetic industry. For example, retinoid is a most potent ingredient that reduces wrinkle, but it can induce irritation. Many efforts have been performed to decrease such side effect. Recently, Lee et al [8] showed adding a bark extract of Alstonia scholaris R. Br. reduced retinoid-induced irritation.

In this study, it is identified that Kaempferol has potent anti-oxidative activities, and also has anti-skin aging effects. Kaempferol is

prepared from proper enzymatic reactions from green tea seed extract. Many biological activities have been proven from *in vitro* to *in vivo* (including clinical test) assays. As a further study, DNA microarray has been performed to find a specific molecular target of kaempferol in epidermal keratinocytes. Because of its high potency, kaempferol might be used as a safe and effective cosmetic product.

1.2 Flavonoid and Kaempferol

Tea [Camellia sinensis (L.) O. Kuntze, Theaceae] has been cultivated widely in Asia for centuries. *Camellia sinensis* is the plant used to make green tea. It is believed to provide a number of medicinal effects and the flavonoids are probably the most important of its many bioactive substances in this respect. These include the biologically-active polyphenols, which exhibit anti-carcinogenic, anti-inflammatory, cytostatic, apoptotic, anti-oxidant and anti-angiogenic activities [9-11]. The majority of flavonoids from green tea are catechins such as epicatechin (EC), epigallocatechin (EGC), epicatechin gallate (ECG) and epigallocatechin gallate (EGCG), the latter being the focus of most research. EGCG not only induces apoptosis selectively in tumor cells and abnormal human epidermal keratinocytes, it also inhibits UVB-induced AP-1 expression and accelerates keratinocyte differentiation and wound healing [12].

Epidemiological studies suggest that the consumption of tea provides protection against cancers in humans. Tea is generally consumed in one of three forms: green, oolong, or black. Approximately 3.0 million metric tons of dried tea is produced annually, of which 20% is green tea, 2% is oolong, and the remainder is black tea.

To produce green tea, after the leaves are picked, the young leaves are rolled and steamed to minimize oxidation. Recently, as popularity of green tea has increased, production of green tea seed (GTS) also has been increased. As tea contains a number of chemical constituents possessing medicinal and pharmacological properties, GTS contains many biologically active compounds such as saponins, flavonoids, vitamins, and oils [13]. The

major polyphenols present in teas are the flavan-3-ols and flavonols. Flavan-3-ols form about 77% of phenolic compounds in green tea, while flavonols make up 13%. Therefore, flavan-3-ols have attracted more attention from researchers. However, flavonols are structurally more stable than flavan-3-ols, and it has been shown that tea is a major dietary source of these compounds. The main flavonols in tea are glycosides of quercetin and kaempferol with lower levels of myricetin [13]. Concerning the commercial using of flavonols for other industrial purposes, the production of pure separated flavonols from plant sources such as tea is not easy.

The flavonoid kaempferol represents 22-29% of the total dietary flavonoid intake from a variety of diets [14] and is easily absorbed by the digestive tract. Its antioxidative properties have been demonstrated in cell-free systems, as well as in a variety of cell types. It exhibits strong radical-scavenging activity [15] and inhibits formation of superoxide anion radicals by xanthine oxidase [16]. Chemical stress-induced ROS production is decreased by kaempferol in various cell types [17, 18]. Kaempferol has also been shown to have cytoprotective and anti-apoptotic activities [15, 17] and to inhibit damage to DNA by certain hormones [19] and H_2O_2 [20].

1.3 Skin Aging

1.3.1 Skin and Skin-Aging

Skin is the outermost organ that functions physical and chemical protection of the body. It is the primary barrier against pathogen invasion

and dehydration [21]. It comprises a complex mosaic of cells of diverse embryonic origin that, under normal conditions, coexist side by side. Skin consists of three layers: epidermis, dermis and subcutaneous tissue (**Figure 4**). It also contains hair follicles, sebaceous glands and sweat glands. The epidermis consists primarily of keratinocytes and melanocytes, and forms the thin outer layer. The epidermis as the borderline to the environment is dependent on its highly controlled homeo-dynamic property critically balancing between proliferation, differentiation, desquamation and apoptosis [22]. The epidermis, a cell-rich layer, is composed mainly of differentiating keratinocytes, which are the most numerous cell type of the skin, which ultimately form the skin's external protective barrier to the environment. The epidermis also comprises pigment producing melanocytes and antigen presenting Langerhans cells.

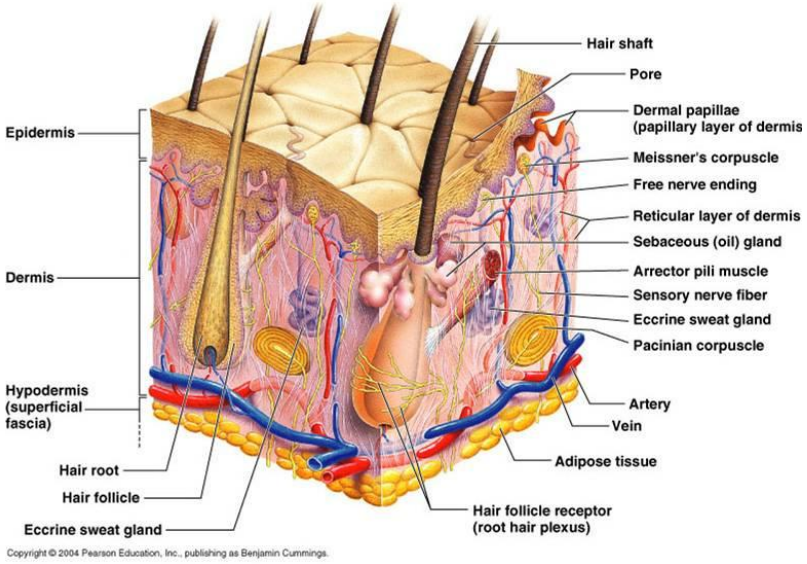

Figure 1.3.1 Structure of Skin (Pearson Education, Inc., publishing as Benjamin Cummings)

The basement membrane separates the epidermis from the dermis - the dermis comprised primarily of extracellular matrix proteins, which are produced by fibroblasts. Vascular supply to the skin also resides in the dermis. Subcutaneous tissue consists of adipose (fat) cells, which support the connective tissue framework. Type I collagen is the most abundant protein of the skin connective tissue. This tissue also contains other types of collagen (III, V, VII), elastin, proteoglycans, fibronectin and extracellular matrix proteins. Newly synthesized type I pro-collagen is secreted into the dermal extracellular space where it undergoes enzymatic processing, which results in the formation of collagen bundles responsible for the strength and resiliency of the skin [23-27].

This balance is progressively impaired during aging. Skin aging begins with a redistribution of fat, a decreased dermal elasticity, and a loss of bone mass, resulting in gravitational changes such as enhanced nasolabial fold, and continues with a progressive impairment of the regeneration of connective tissue components such as collagen and hyaluronate [28-30]. Intrinsically aged skin is thin, pale, wrinkled and less elastic, and has flattened dermal–epidermal junction [22]. The dermis is the deeper layer, forming the main bulk of the skin. Its function is to provide a tough matrix to support the blood vessels, nerves and appendages that are embedded in it [31].

Skin aging is a complex phenomenon induced by endogenous (chronological) and exogenous (extrinsic) factors. Chronological aging is a genetically programmed, unavoidable process, while extrinsic influences (e.g., sunlight, wind, heat, cigarette smoke, or exposure to chemicals) could be at least partially controlled by the individual [32-34]. Among the

extrinsic factors, ultraviolet (UV) irradiation (sunlight, tanning beds) is the single most important cause of skin aging [32, 35]. UV exposure leads to numerous changes in the skin, including epidermal and dermal thinning, a decline in collagen production and in the functionality of the dermal elastic network, and an uneven distribution of pigment deposition, all resulting in an aged-skin phenotype. Additionally, UV exposure is a major factor in the development of skin cancer. Most skin cancers are induced by the cumulative exposure to UV irradiation, and therefore appear mainly on aged skins [36].

1.3.2 Facial wrinkle on the skin

Human perception is based on visualization of surfaces. Because we cannot look inside, we define objects through their interfaces. This of course holds true for human skin. The interface, which meets our eyes, is the stratum corneum, the dead outer layer of the epidermis. The human skin surface is not smooth and is characterized by a specific relief [37]. The microstructure of the skin surface, determined by the epidermis, is composed of very fine lines intersecting one another. This structure resembles a net-like structure consisting of polygonal forms, most often triangles or quadrangles. The edges of the triangular or the quadrangle forms define the location of furrows or micro lines, and the curved surfaces surrounded by furrows define the ridges [38].

Aging of the skin is a complex biological process involving both genetically determined and environmental factors and can be divided into intrinsic and extrinsic aging [39, 40]. Intrinsic aging, which is largely

genetically determined, affects the skin in a manner similar to most internal organs. Extrinsic aging, more commonly termed photoaging, is caused by environmental exposure, primarily ultraviolet radiation [41, 42]. Besides UV radiation, the contribution of tobacco smoking to premature skin aging has been studied recently [43-45].

Wrinkles in facial skin are one of the most characteristic morphological changes of aging. Therefore, many quantification methods to analyze wrinkles have been developed. Nowadays, bioengineering applications have emerged rapidly, and the scientific community is witnessing the development of novel techniques with greater accuracy and descriptive properties. Different non-invasive methods for monitoring skin functions have been introduced, offering the advantages of being precise and non-invasive [46].

The considerable interest in the concept of eternal youth with minimum signs of aging has led to a large market for skin care products claiming to exert anti-wrinkle effects. These products may have physiological actions on the skin, as well as generating pleasant emotions during their use [47]. With the advancement of skin research, the present-day consumer has increased access to technological information about skin care products. As a result, the demand for proof of efficacy, especially for anti-aging products, is rapidly increasing [48]. Because of its decreased mechanical properties, aged skin not only shows typical signs of aging, like wrinkles and furrows, but also tends to a higher violability by mechanical exposure and skin diseases [38, 39]. For this reason skin aging has to be understood not only as a cosmetic problem but also, especially in an aging population, as a serious medical problem [49].

1.3.3 Methodology of skin surface replica

The skin surface ‘messages’ result mainly from the organization of the dermis and its collagen and elastin networks, but the state of the epidermis and stratum corneum can also play a role. The problem is more complex as the structure is three-dimentional and needs a minimum of geometric parameters; it is therefore difficult to make a simple description and interpretation.

Skin surface replica: Applied to skin relief, this method carried the following constraints. The mold had to be white (as snow), matte, and opaque. Among the brands studied at the time, the silicon resin SILFLO from Flexco fit that needs. It guaranteed reliable reproduction, the absence of further deformation, and documented artifacts. The fact that the samples could be stored for about 2 years was an added advantage [50, 51].

1.3.4 Skin visiometer analysis

Skin visiometer is a w well established, accurate, very economical and easy to handle measurement method to evaluate the topography of the skin surface by light transmission of a very thin, special blue dyed silicone. The very viscous two part silicone, mixed under vacuum to avoid bubbles, fills even smallest skin depths and reproduces them in detail.

The device features a parallel light source and a b/w CMOS-camera with 640 x 480 pixels. The replica is placed between these. The light absorption of the blue color is known. When the light penetrates the

replica, it is absorbed according to the thickness of the silicone material. The replica reproduces the heights and depths of the skin as a negative, i.e. wrinkles are higher in the replica as the silicone is thicker in this place (**Figure 5**).

An image digitalization unit which is in the same housing as the light transmission unit and connected to the computer via a USB interface and shows the heights and depths of the replica by a corresponding classification on a grey scale (256 different grey values), thus the depths of each pixel can be calculated in μm by the special software. This special measurement method allows many functions and the calculation of various different skin parameters within one second: A coloured 3D image can be displayed quickly. Other displays of the image (e.g. relief, false colour, etc.) are possible. Lines can be drawn on the images and the profile and the results are shown immediately.

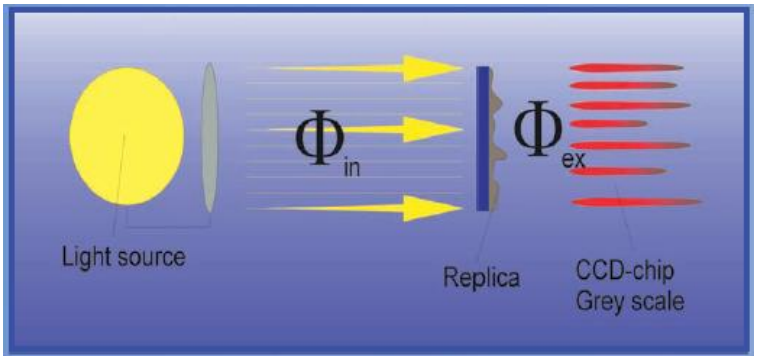

Figure 1.3.2 Principle of Visiometer analysis

(The amount of absorbed light is calculated by Lambert and Beer's Law:

$$\Phi ex = \Phi in \bullet e\text{-}kd$$

The outgoing light is proportional to the incoming light, the thickness of the material and the material constant k.)

1.4 DNA microarray

1.4.1 What is the DNA microarray?

Skin is the most accessible target for testing new treatments of human diseases, from topical medications for local cutaneous symptoms, to patches that treat systemic problems, and even for gene therapy. Because of their accessibility, skin cells were among earliest targets of DNA microarray studies [52]. DNA microarray analysis allows simultaneous monitoring of expression of multiple genes in different cells and tissues [53]. Its applications for pharmaceutical and clinical research include identification of disease-related genes, as well as targets for therapeutic drugs [54]. The RNA from the skin surface can even be recovered using tape stripping, an easy, non-invasive procedure. However, as in DNA microarray studies of other organs, the presence of many different cell types in skin has created difficulties. Skin samples from patients, potentially very informative, differ in proportions of various cell types, sample age and body sites, as well as concerns even more difficult to standardize, such as history of sun exposure, presence of underlying disease, and lifestyle. To avoid the confounding effects of various cell types, many researchers have used monocultures of keratinocytes, fibroblasts or melanocytes, or cell lines derived from these cells. Occasionally, co-cultures have been used to study the effects of cell-cell interactions. One of the first dermatologically relevant and most exciting studies using DNA microarrays was the analysis of the response of dermal fibroblasts to the addition of serum [52]. This experimental model, first starving the cells and then re-feeding them with a serum-containing medium, causes synchronous

cell division and thus serves as a paradigm for mammalian cell cycle studies. As expected, the authors found cell cycle regulators to be induced by serum. The unanticipated additional finding was that the fibroblasts initiated the expression of wound healing response proteins. In the dermis, serum is present only after wounding and therefore the fibroblasts interpreted the presence of serum as a signal that wounding occurred. Of course, it was possible to identify the induction of several wound healing response proteins individually using classical molecular biology methods; however, only DNA microarray-based transcriptional profiling could provide the global overview that made it possible to gain comprehensive insight into the new and exciting role of fibroblasts in wound repair.

A large number of DNA microarray studies followed, focused on various aspects of epidermal differentiation, skin cancers, inflammatory diseases, wound healing, ageing and stem cells. Specific for skin has been a series of studies on the effects of UV light, the harmful environmental agent that targets skin almost uniquely [55, 56]. A skin-specific cDNA array, named DermArray and containing >4000 gene probes has recently become commercially available [57]. A set of keratinocyte-specific house-keeping genes has been characterized [58, 59]. Recent review articles describe various aspects of the use of transcriptional profiling in dermatology and skin biology [60, 61] accumulation of large volume of bioinformatics data relevant to skin led to the coinage of the term Skinomics [62]. Figure 1.4.1 shows scheme of DNA microarray.

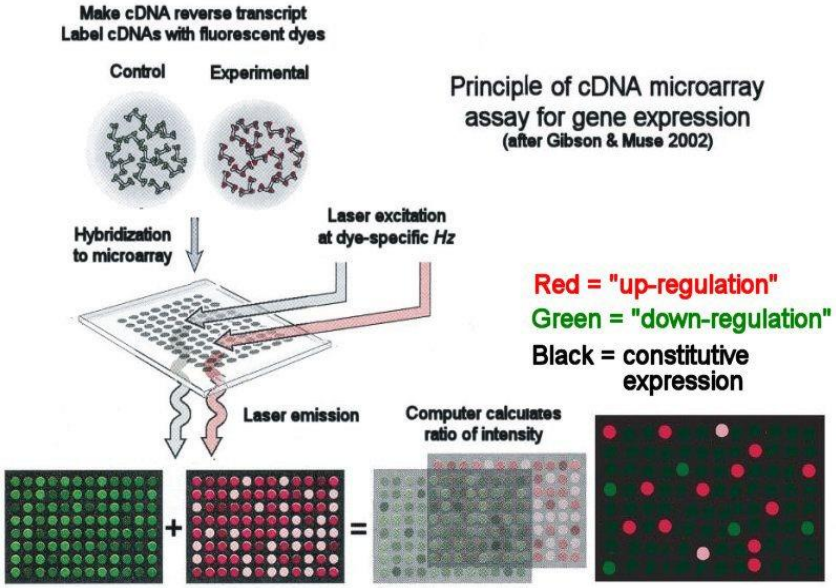

Figure 1.4.1 Schematic diagram of micro-array (Gibson & Muse 2002; Text Material © 2011 by Steven M. Carr)

Brifely, a microarray is a set of short Expressed Sequence Tags (ESTs) made from a cDNA library of a set of known (or partially known) gene loci. The ESTs are spotted onto a cover-slip-sized glass plate. A complete set of mRNA transcripts is prepared from an experimental treatment or condition. Complementary DNA (cDNA) reverse transcripts are prepared and labelled with a [red] fluorescent dye. A control library is constructed from an untreated source, labelled with a different fluorescent [green] dye. The experimental and control libraries are hybridized to the microarray. A Dual-Channel Laser excites the corresponding dye, and the fluorescence intensity indicates the degree of hybridization that has occurred. Relative gene expression is measured as the ratio of the two fluorescences.

After microarray experiment, confirmation by PCR is usually performed. Figure 1.4.2. shows PCR scheme and comparison between RT-PCR and qPCR. The purpose of a PCR (Polymerase Chain Reaction) is to make a huge number of copies of a gene. There are three major steps (Denaturation, annealing, and extension) in a PCR, which are repeated for 30 or 40 cycles. The principle of SYBR real-time PCR is a standard PCR reaction carried out in the presence of a dye, SYBR, which fluorescence when intercalated in the DNA helix. The fluorescence will increase as the amount of the PCR product increases and is quantified after each completed PCR cycle. The cycle at which the fluorescence exceeds a detection threshold, the Ct (threshold cycle) correlates to the number of target cDNA molecules present in the added cDNA.

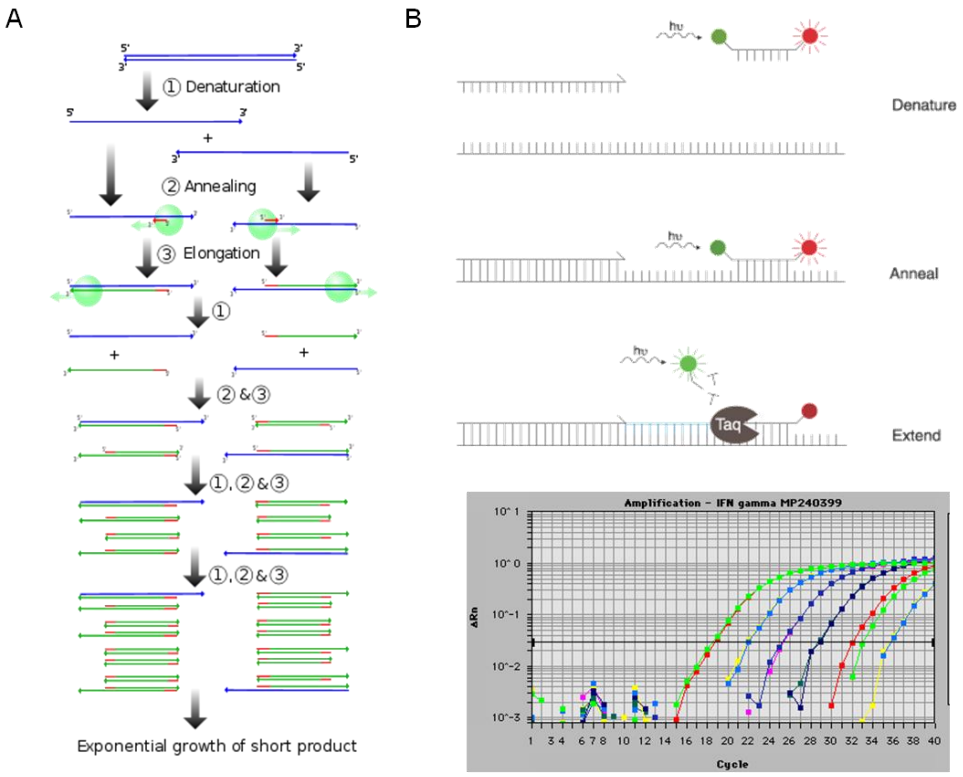

Figure 1.4.2 Schematic diagram of PCR and real-time PCR (Madeleine Price Ball, Actual Data found using the TaqMan® probe at Davidson College, respectively)

1.4.2 Keratinocyte differentiation

Epidermal keratinocytes differentiate through a multistage process creating a unique three-dimensional structure. In addition, keratinocytes must respond to a large variety of extracellular stimuli from the environment and from nearby cells. Consequently, keratinocytes have a relatively large transcriptome, that is, express many genes. A large study compared the transcriptomes of skin, differentiating 3D-cultured skin substitute (CSS), cultured keratinocytes, and non-keratinocyte cell types [58]. The comparison identified which genes are intrinsic to all keratinocytes, which are specific for their differentiation and 3D architecture, and which are induced in epidermis by other cutaneous cell types. Epidermal keratinocytes intrinsically express many proteases and protease inhibitors. Skin and the three-dimensional CSS, but not keratinocytes in monolayers, express epidermal differentiation markers, such as filaggrin, involucrin, loricrin, small proline-rich proteins and other cornified envelope components. Skin, but not CSS, specifically expresses a higher number of receptors, secreted proteins, and transcription factors.

Surprisingly, the mitochondrial genes were significantly suppressed in skin, suggesting a low metabolic rate. Cultured keratinocytes express many cell-cycle and DNA replication genes, as well as integrins and extracellular matrix proteins. These results define the intrinsic, the architecture-specific, and the paracrine-regulated genes in keratinocytes [63].

Vitamin D and calcium also promote epidermal differentiation. Transcription profiling studies identified a set of genes regulated by vitamin

D in keratinocytes [64]. Specifically, peptidylarginine deiminases, kallikreins, serine proteinase inhibitors, Kruppel-like factor 4, and c-Fos were found to be vitamin D-responsive genes with potential roles in epidermal differentiation. A subset of calcium-induced and suppressed genes in human keratinocytes has also been identified [65].

Retinoic acid, its metabolites and analogs inhibit epidermal differentiation. Preliminary studies on the effects of retinoids on keratinocytes identified a number of regulated genes not previously associated with inhibition of differentiation [66]. DNA microarray analysis identified Rho as another signaling molecule that suppresses expression of differentiation markers [67]. Similarly, E6 onco−protein from human papillomavirus type 16 inhibits keratinocyte differentiation and suppresses a large number of differentiation markers, including genes encoding small proline-rich proteins, transglutaminase, involucrin, elafin, and keratins [68]. E6 regulates cellular genes by both p53-dependent and in- dependent mechanisms and modulates certain effects of the viral protein E7 on cellular gene expression. Different classes of human papillomaviruses have distinct effects on cellular transcription patterns during infection [69].

Cultured primary keratinocytes have limited replication potential and eventually senesce. The senescence can be delayed or even prevented by culturing in the presence of fibroblast feeder cells. Comparison of the two culture methods show that in the absence of feeder cells keratinocytes express higher levels of migratory genes and reduced levels of differentiation markers; the expression of urokinase plasminogen activator receptor and p16INK4a were also increased in the migratory cells [70].

The overall picture that emerges from these studies identifies

several independent regulators of epidermal differentiation, both positive and negative. Furthermore, they discovered a large set of epidermal differentiation markers not known before. However, it also appears that there are different classes of differentiation markers. While some are always associated with epidermal differentiation, others can be expressed under a variety of conditions.

1.4.3 Effects of UV and other environmental stress

The epidermis is our first line of defense from ultraviolet light (UV), the major environmental carcinogen. Skin is uniquely the target of photodamage, which results in thinning, wrinkling, keratosis, and malignancy. Therefore, several groups used DNA microarrays to analyze the transcriptional effects of UV light in human epidermal keratinocytes [56, 71, 72]. Focusing on UVB, the most harmful component of the UV spectrum, the DNA microarray results show keratinocytes respond by inducing a cell repair program to repair the damage. Keratinocytes, being the primary cells exposed to UV, also act to protect the underlying organism. The early changes in gene expression, within the first 2 h, affect transcription factors, signal transducing, and cytoskeletal proteins that change cell phenotype from a normal, fast-growing cell to a “paused” phenotype. Presumably, this allows for the assessment of damage and its repair to take place. At 4–8 h post-irradiation, keratinocytes produce secreted growth factors, cytokines, and chemokines to alert the surrounding tissues to the UV damage. Later, at 16–24 h after treatment, components of the cornified envelope are produced, as keratinocytes enhance the

epidermal protective covering, while simultaneously terminally differentiating thus removing a carcinogenic threat [55]. UV light also induced the expression of genes involved in transcription, splicing and translation and enzymes that synthesize raw materials for DNA repair. In addition, expression of mitochondrial proteins was boosted, while the genes for metabolism, transport and adhesion proteins were down-regulated to provide cells with additional energy. Some of these responses had been expected, but others provided fresh views into the protective role of epidermis.

Interestingly, when keratinocytes were exposed to gamma irradiation or x-rays, the transcriptional changes were similar to those found in the UV-treated cells [73, 74]. Specifically, the genes involved in cell energy metabolism appeared to be particularly responsive. Both treatments caused an in- crease in mitochondrial ATP-synthases, while suppressed the genes that belong to energy requiring pathways. This resulted in a 50% increase of intracellular ATP in irradiated keratinocytes. The transcription factor ATF3 may be involved in the response to X-rays, as it was found to be strongly and specifically induced by the treatment.

1.5 Objectives

Firstly, in order to develop kaempferol commercially available, biotransformation of kaempferol glycosides from green teas seeds by enzymatic hydrolysis was performed. For the optimum enzymatic hydrolysis of green tea seed extract, several glycosylation enzymes were investigated.

Secondly, after preparation of kaempferol, various biological efficacy tests were performed: especially, anti-oxidation and dermal anti-aging effect on skin such as MMP-1. And then, effect of kaempferol on skin wrinkle improvement was investigated in animal (hairless mouse) and clinical test. For cosmeceutical application, kaempferol was tested in *in vivo* model, focusing on wrinkle decrease effect.

Lastly, DNA microarray analysis was applied to investigate the molecular mechanisms underlying the beneficial effects of kaempferol on the skin. It was investigated that changes in the transcriptional profiles of immortalized human keratinocytes (HaCaT cells) following treatment with kaempferol. Bioinformatics tools were used to analyze the promoter sequences of differentially regulated genes for the purpose of identifying meaningful transcription regulators. Using this approach, it was identified a genetic regulatory network that responds to kaempferol.

CHAPTER 2

Materials and Methods

2. Materials and Methods

2.1 Materials

Green tea seed (*Camellia sinensis* (L.) O. Kuntze, Theaceae) was purchased from Zhejiang Chemicals, China. The following enzymes and chemicals were obtained from Sigma Chemical Co. (St. Louis, MO, USA): a hesperidinase from *Penicillium* sp. (18 units/g), a β-glucosidase from almonds (2.4 units/mg), a cellulase from *Aspergillus niger* (5.1 units/mg), a β-glucuronidase from *Helix pomatia* (338 units/mg), a pectinase from *Rhizopus sp.* (490 units/g), a β-galactosidase from *Aspergillus oryzae* (8.7 units/mg), an amyloglucosidase from *Aspergillus niger* (51 units/mg), an α-amylase from human saliva (type XIII, A, 40 units/mg), a dextranase from *Penicillium* sp. (425 units/mg), a β-xylosidse from *Aspergillus niger* (8.5 units/mg), a xylanase from *Thermomyces lanuginosus* (285 units/mg), Kaempferol, 1,1-Diphenyl-2 -picrylhydrazyl (DPPH), sodium nitroprusside (SNP), xanthine, xanthine oxidase (XO) grade I from buttermilk (EC 1.1.3.22), phenazine methosulfate (PMS), β-nicotinamide adenine dinucleotide (NADH) and nitroblue tetrazolium chloride (NBT). All organic solvents used were of analytical grade and purchased from Fisher Scientific UK (Loughborough, Leics, UK.)

2.2 Preparation of Kaempferol

2.2.1 HPLC and TLC Analysis

The analysis of extracts and enzyme reactants were carried out by the following HPLC and TLC methods. The HPLC system consisted of a Waters 2695 separation module and a 2996 PDA detector. A 250 × 4.6 mm i.d Mightysil C18 reverse phase column (Kanto Chemical, Japan) was employed. The detector wavelength was set at 263 nm. The mobile phase used for the analysis of samples was a mixture of distilled water (A) and acetonitrile (B) with gradient elution. The gradient elution was 15 – 80% B in 60 min at a flow rate of 1 mL/min. TLC analysis was performed on Merck Kieselgel 60 F_{254} silica gel plates using *n*-butanol-acetic acid-water (3: 1: 1, v/v/v). The separated hydrolysates on TLC plates were visualized by dipping the plates into 5% (v/v) H_2SO_4 in methanol containing 0.3% (w/v) *N*-(1-naphthyl) ethylenediamine, followed by drying and heating for 10 min at 121℃.

2.2.2 LC/MS and NMR analysis

LC-MS-APCI analyses were made using a Thermo Finnigan (Surveyor) HPLC with a PDA detector coupled to a Thermo Finnigan (LCQ Classic) quadrupole ion trap mass spectrometer equipped with an APCI source. Chromatographic separations of material were performed on a 250 × 4 mm i.d., 5 μm, Merck LiChrosphere C18 column using a 1 mL/ min solvent gradient of 20–100% aqueous methanol (containing 1% acetic acid) in 40 min. The MS interface was set to positive ion mode (vaporizer tube temperature: 550℃, needle current: 5 μA (approx. 3.6 kV), sheath and auxiliary nitrogen gas pressures: 80 and 20 psi, heated capillary temperature: 150℃. Mass spectra were acquired in the range of (full) *m/z* 125–1200

(MS–MS ion isolation width: 5 Da, MS–MS collision energy: 45%, MS–MS scan range: *m/z* of parent ion – ca. 1/3 *m/z* parent ion). To determine the structure of the isolated compound from GTSE, ^{1}H, ^{13}C- NMR spectra were recorded on a Varian GEMINI-300BB (300MHz) spectrometer.

2.2.3. Isolation of Kaempferol glycosides from green tea seed

GTS was ground for extraction in a FM-680T grinder (Food Mixer, Han il, Korea) and crushed GTS (100g) was defatted three times with *n*-hexane (3 L) for 3 h. After removal of the solvent by filtration, defatted and dried GTS (78.5g) was extracted with 2 L of 70% ethanol in a Soxhlet apparatus for approximately 6 h and was then filtered. Evaporation of the solvent under reduced pressure provided the GTS extract (11.2g). The GTS extract (11.2g) was subjected to medium-pressure liquid chromatography (MPLC) system (Yamazen Co. Japan) using a gradient elution system of distilled water (DW) and acetonitrile gradient with acetonitrile from 15% to 50% acetonitrile in 60 min at a flow rate of 30 mL/min. The pressure of system was 3 Mpa. A 300×37 mm i.d, 50 μm, Ultra pack-ODS-S-50C column (Yamazen Co., Japan) was used. The detector wavelength was set at 263 nm. The fraction volume was 30 mL. 10 fractions were collected and monitored by HPLC. The fractions were combined [fr. 1~4 (7.5 g), fr. 5 (0.25 g), fr. 6~7 (1.9 g), fr. 8 (0.31 g), fr. 9~10 (1.24 g)] and compounds **1** (fr. 5) and **2** (fr. 8) were isolated in yields of 0.25 g and 0.31 g, respectively. To determine the structure of the isolated compounds, LC/MS and NMR analysis was conducted. Acid hydrolysis was conducted for the analysis of carbohydrate residues.

2.2.4 Compound 1

LC/MS *m/z* 756.9 [M + H]; NMR δ_H (CD_3OD, 300MHz): 8.02 (2H, d, *J* = 8.7 Hz, H-2′, H-6′), 6.90 (2H, d, *J* = 9.0 Hz, H-3′, H-5′), 6.37 (1H, d, *J* = 1.8 Hz, H-8), 6.17 (1H, d, *J* = 1.8 Hz, H-6), 5.33 (1H, d, *J* = 7.8 Hz, H1-Glc), 4.70 (1H, d, *J* = 7.5 Hz H1-Gal), 4.47 (1H, d, *J* = 0.9 Hz H1-Rha), 3.2 - 3.8 (16H, m), 1.08 (3H, d, *J* = 6.3 Hz); NMR δ_C (CD_3OD, 75MHz): 179.48 (C-4), 166.59 (C-9), 163.02 (C-7), 161.47 (C-5), 159.25 (C-2), 158.60 (C-4′), 134.72 (C-3), 132.37 (C-2′, 6′), 122.94 (C-1′), 116.24 (C-3′, 5′), 105.57 (C-10), 104.48 (C_{Gal}-1), 101.12 (C_{Glu}-1), 102.21 (C_{Rha}-1), 100.19 (C-6), 95.06 (C-8), 82.05 (C_{Glu}-2), 78.28 (C_{Glu}-3), 77.87 (C_{Gal}-5), 77.82 (C_{Glu}-5), 76.95 (C_{Gal}-3), 75.38 (C_{Gal}-2), 73.86 (C_{Rha}-3), 72.30 (C_{Rha}-2), 72.07 (C_{Glu}-4), 71.40 (C_{Rha}-4), 71.27 (C_{Gal}-4), 69.71 (C_{Rha}-5), 68.22 (C_{Glu}-6), 62.59 (C_{Gal}-6), 17.85 (C_{Rha}-6); all these data corresponded to that in the literature for camelliaside A [13].

2.2.5 Compound 2

LC/MS *m/z* 726.9 [M + H]; NMR δ_H (CD_3OD, 300MHz): 8.00 (2H, d, *J* = 8.7 Hz, H-2′, H-6′), 6.80 (2H, d, *J* = 9.0 Hz, H-3′, H-5′), 6.34 (1H, d, *J* = 2.1 Hz, H-8), 6.14 (1H, d, *J* = 2.1 Hz, H-6), 5.35 (1H, d, *J* = 7.2 Hz, H1-Glc), 4.73 (1H, d, *J* = 7.5 Hz H1-Xyl), 4.45 (1H, d, *J* = 1.2 Hz H1-Rha), 3.2 - 3.8 (15H, m), 1.09 (3H, d, *J* = 6.3 Hz); NMR δ_C (CD_3OD, 75MHz): 179.43 (C-4), 165.91 (C-9), 163.04 (C-7), 161.36 (C-5), 158.70 (C-2), 158.47 (C-4′), 134.83 (C-3), 132.35 (C-2′, 6′), 122.92 (C-1`), 116.17 (C-3′, 5′), 105.73 (C-10), 105.13 (C_{Xyl}-1), 100.83 (C_{Glu}-1), 102.14 (C_{Rha}-1),

99.92 (C-6), 94.85 (C-8), 81.93 (C_{Glu}-2), 78.21 (C_{Glu}-3), 77.05 (C_{Xyl}-3), 76.84 (C_{Glu}-5), 74.68 (C_{Xyl}-2), 73.85 (C_{Rha}-3), 72.27 (C_{Rha}-2), 71.42 (C_{Glu}-4), 72.06 (C_{Rha}-4), 70.99 (C_{Xyl}-4), 69.70 (C_{Rha}-5), 68.11 (C_{Glu}-6), 66.54 (C_{Xyl}-5), 17.85 (C_{Rha}-6); all these data corresponded to that in the literature for camelliaside B [13].

2.2.6 Acid hydrolysis of compounds 1 and 2

Compounds **1** (10 mg) and **2** (10mg) dissolved in 1 mL 2 M HCl was heated at 100˚C for 1 h in a sealed tube. The reactant was centrifuged and separated insoluble (precipitant) and soluble parts (supernatant). The insoluble part was washed several times with a distill water and dried in vacuo. The soluble part was neutralized with 1 mL of 2 M NaOH. Then stored frozen for analysis.

2.2.7 Enzymatic hydrolysis of green tea seed extract

GTSE (0.5 g) in 8 ml 0.02 M sodium-acetate buffer (pH 5.0) with 2 ml of several glycolytic enzyme solutions was incubated with stirring at 37˚C for fixed time. The amount of each enzyme was adjusted to provide a final concentration in the mixture of 50 units/g of GTSE. Each sample and blank was used as a reaction control. All samples were prepared in duplicate. After incubation, each aliquot (200 μl) was extracted with ethanol (800 μl) and centrifuged at 12000g (4˚C) for 10 min. Supernatants were transferred to new tubes and dried completely in vacuum. It was stored frozen for analysis

2.3 Effects of Kaempferol on Sking aging *in vitro*

2.3.1 DPPH assay

DPPH radical-scavenging assay was as follows. The reaction mixture containing various concentrations of the test samples, final concentration of 10, 25, 50, 100, 500 and 1000 μM, and 0.2 mM DPPH methanolic solution was incubated at room temperature for 30 min in the dark after which the absorbance was measured at 517 nm (Jasco V-550 spectrophotometer). The scavenging activity was expressed as a percent compared to control DPPH solution (100%). The synthetic antioxidant Trolox and L-ascorbic acid were included in experiments as a positive control.

2.3.2 Xanthine oxidase inhibition assay

Superoxide anions were generated by the xanthine/xanthine oxidase (XO) system, following the described procedure. The reaction mixture consisted of xanthine (0.5 mM), NBT (0.5 mM) and test samples at the concentration of 31, 63, 125, 250 and 500 μM, in a final volume of 100 μL. Xanthine and NBT were dissolved in phosphate buffer 200 mM with 0.25 mM EDTA, pH 7.5. The reaction mixture were preincubated at room temperature for 2 min, and initiated by the addition of 100 μL of XO (50 mU/mL). The mixture (200 μL) was kept for 30 min at 37°C. To detect Superoxide, the coloring reagent (final concentration of 300 μg/mL sulfanilic acid, 5 μg/mL of *N*-(1-naphthyl)-ethylenediamine

dihydrochloride, and 16.7% (v/v) acetic acid) was added after the incubation. The mixture was allowed to stand for 30 min at room temperature, and the absorbance at 550 nm was measured (Ceres UV 900 Hdi). Different concentrations of compounds were analyzed and then the half-minimal inhibitory concentration (IC_{50}) was calculated by linear regression analysis.

2.3.3 Assay of uric acid generated by xanthine oxidase

The effect of compounds on xanthine oxidase activity was evaluated by measuring the formation of uric acid from xanthine. The reaction mixtures contained the same proportion of components as in assay for superoxide anion, except NBT. The reaction mixture consisted of xanthine (0.5 mM), dissolved in phosphate buffer 200 mM with 0.25 mM EDTA, pH 7.5, and test samples at the concentration of 31, 63, 125, 250 and 500 μM, in a final volume of 100 μL. The reaction mixture were preincubated at room temperature for 2 min, and initiated by the addition of 100 μL of XO (50 mU/mL). The mixture (200 μL) was kept for 30 min at 37˚C. The reaction was stopped with HCl (20 μL, 5 M). The production of uric acid was determined specrophotometically at 295 nm (Ceres UV 900 Hdi).

2.3.4 Cell viability assay

The effect of kaempferol on cell viability was measured using the MTT (3-(4,5-Dimethylthiazol-2-yl)-2,5-dipheynltetrazolium bromide) assay.

Briefly, MTT (50ul of 2mg/ml) dissolved in culture media was added to cells, and the cells were incubated for 3h in a 37^{o}C incubator. The medium was removed and formazan crystals of these cells were solubilized in 200ul DMSO by gentle shaking for 10 min. The amount of formazan was quantified in an ELISA reader at 540nm.

2.3.5 Lipid peroxidation inhibition

Add test sample 0.1ml and ethyl linoleate 10 uM to an incubation medium (4.89ml) containing 2% sodium dodecyl sulfate, 1uM ferrous chloride and 0.5mM hydrogen peroxide. Keep the incubation medium at 55^{o}C for 16h. Transfected each reaction mixture (0.3ml) into test tube, which was followed by the addition of 4% BHT (50ul) in order to prevent further oxidation. Add 1ml of 0.67% TBA to the reaction mixture. Vortex the sample and incubate at 95^{o}C for 30min. After cooling, add 4ml of a 15% methanolic butanol solution and stir the solution. Centrifuge the reaction mixture for 10 min at 2,500 rpm and measure the absorbance of the supernatant at 532nm. The extent of lipid peroxidation is determined by measuring the quantity of the TBA reactive substance (TBARS). 1,1,3,3-tetraethoxypropane is used at the standard, and the lipid peroxide concentration is expressed as the amount of malondialdehyde, and is shown as the percentage inhibition of MDA formation. Finasteride is used as a positive control.

2.3.6 HaCaT-Normal human fibroblast co-culture

A HaCaT–fibroblast co-culture system was established in which HaCaT and fibroblasts were grown in the upper and lower chamber, respectively. Thirty-milimeter Transwell (SPL, Korea) culture plate inserts with 0.4-μm pore sizes were used in the co-culture experiments. HaCaT cells (5×10^4 cells/ml) were seeded on the inserts with DMEM in 10% fetal bovine serum (FBS). In a separate 24-well plate (3×10^4 cells/ml), fibroblasts were seeded with DMEM in 10% FBS. The cells were incubated for 24 h, and then the two cultures were assembled as a co-culture, with the lower chamber containing fibroblasts on the plastic 24-well plate and the upper chamber with the insert containing HaCaT or fibroblasts. An insert with just the fibroblasts was used as a control.

2.3.7 MMP-1 ELISA

After UVB exposure, serum-free DMEM containing kaempferol at the indicated concentrations was added to the cells, and culture medium was harvested after 24 h. MMP-1 sandwich ELISA assays were performed according to the manufacturer's protocols (RPN 2610, Amersham Bioscience, USA) using pre-coated 96-well immunoplates, rabbit anti-human MMP-1 antibodies, and anti-rabbit horseradish peroxidase conjugate. 3, 3, 5, 5-Tetramethylbenzidine was used as the peroxidase substrate. The absorbance was read at 450 nm using a microtiter plate reader (Molecular Devices, USA).

2.3.8 TNF-α ELISA

After UVB exposure, serum-free DMEM containing kaempferol at the indicated concentrations was added to the co-cultured HaCaT/fibroblast cells, and culture medium was harvested after 24 h. TNF-α sandwich ELISA assays were performed according to the manufacturer's protocols

2.3.9 Procollagen I ELISA

The levels of type I procollagen protein in cell-free supernatants were determined by ELISA (Takara, Japan). The supernatants of cultured fibroblast treated with various concentrations of kaempferol were harvested, and stored at -70^{o}C. The ELISA was performed according to the manufacturer's instructions accompanying the product.

2.3.10 UVB irradiation

For each experiment, cells were maintained in culture medium with 1% Fetal Bovine Serum (FBS) and kaempferol at the indicated concentration for 24h. Pre-treated cells were washed twice with phosphate-buffered saline (PBS) (Welgene, Daegu, Korea) and exposed to UVB irradiation (UVB lamp: G15TBE, SANKYO DENKI, Japan). The total energy dose of UVB irradiation was 100mJ/cm^{2}.

2.4 Effects of kaempferol on skin aging *in vivo*

2.4.1 Application Studies in Mouse

The application study was performed in long-term topical application of kaempferol on the dorsal skin of SqOOH treated mice for 3 weeks. This study was conducted in conformity with the policies and procedures of the Institutional Animal Care and Use Committee of the AmorePacific R&D Center. Female albino hairless mice (Skh: hr-1) purchased from Charles River Laboratories (Wilmington, Mass, USA) were used for the application of a kaempferol (1%) and the vehicle solution (polyetyleneglycol 400). Skin damage were induced by SqOOH (squalene monohydroperoxide).

2.4.2 Generation of Replicas, and Image Analysis

Replicas of mouse dorsal skin were obtained using SILFLO resin (Cuderm, USA). A photograph of the dorsal skin of each mouse was taken just before the animals were sacrificed. Image analysis of the replicas was performed by IEC Korea (Suwon, Korea). The impression replicas were set on a horizontal sample stand, and wrinkle shadows were produced by illumination with light of a fixed intensity at an angle of 20° using an optical light source (Minebea, China). The shadow images were photographed with a CCD camera (Samsung, Korea) and analyzed by Skin-Visiometer SV 600 software (CK electronic GmbH, Germany). Arbitrary units were as- signed to each sample, R1—R5, based on the principle of measuring the depth of furrows according to shadow size and brightness due to inflection under illumination. Skin roughness, referred to as R1, is defined as the difference between the highest crest and lowest furrow. To exclude the possibility of artifact, the program cut the line into five equal

parts. R3 represents an average of the maximum distance (R1) derived from each of the five parts of the line; R2 represents the largest value of these five distances. R4 represents the mean area surrounded by a horizontal line drawn at the highest crest and the furrows profile. R5 stands for the mean deviation of the furrow's profile to the middle line. Skin specimens obtained from dorsal skin sacrificed at the end of the study. Dorsal skin were fixed in 10% buffered formalin, embedded in paraffin and sectioned (3~4mm) for light microscopy. Sections were stained with Masson-Trichrome for collagen fiber evaluation.

2.5 Effects of kaempferol on skin aging: Clinical test

2.5.1 Clinical test: Subjects

27 Korean female volunteers in good health (30-60 years old, 46.03±5.48 years old) participated in this study. All subjects are included in the standard body portions or BMI 18.5-25.0. Formal informed consent was obtained in all cases. In order to avoid environmental influences, volunteers were allowed to relax in the examination room maintained at the temperature of 20±2℃ and a relative humidity of 40±2% for 30 minutes, after washing their faces with soap. Then, measurement of the wrinkle improvement was performed by replica analysis at 4 and 8 weeks.

2.5.2 Clinical test: Method

The subject was instructed to apply a quantity of product to the area typically, twice daily in morning and in the evening. The typical test site for the sampling was the periorbital canthus (crow's feet area).

2.5.3 Clinical test: Wrinkle measurement

At each visit, negative replicas were obtained from crow's feet wrinkles using Silflo resin (Cuderm, Dallas, TX, USA) and analysed by Visiolinea VL650 (Courage+Khazaka Electronic GmbH.). Replicas were analysed using the values of size and length.Also, subject's periorbital wrinkles were evaluated with a double-blind test by two dermatologists. The dermatologists evaluated subjects' periorbital wrinkles at weeks 0 (baseline), 4, and 8 weeks.

2.5.4 Statistical analysis

SPSS® 18.0 (SPSS Inc., Chicago, USA) was used for statistical analysis. Differences among skin physical parameters in region of interest were analyzed with the two-independent t-test. P values smaller than 0.05 were considered statistically significant.

2.6 DNA microarray

2.6.1 Cell culture

The spontaneously-transformed human keratinocyte cell line HaCaT (N.E. Fusenig, Deutsches Krebsforschungszentrum, Heidelberg,

Germany) [75] was grown in DMEM containing 10% FBS and antibiotics (100 mg ml-1 streptomycin and 100 IU ml-1 penicillin). Cells (1 × 10^5) were grown in tissue culture flasks (75 cm^2) at 37°C in 5% CO2 and 95% air for 24 h, followed by serum starvation for 24 h. Kaempferol was then added and the cells were incubated for the time periods indicated. Control cultures were maintained in medium supplemented with a 1 : 10,000 dilution of vehicle (DMSO), which produced no apparent growth or differentiation effects. NHEKs were derived from neonatal foreskin as previously described [76]. Briefly epidermis was isolated from newborn foreskins by incubation in Dispase, and a suspension of keratinocytes was obtained by incubation in 10 mM EDTA and subsequent trypsinization. Cells thus obtained were cultured with serum-free keratinocyte growth medium (KGM, Clonetics, San Diego, CA) and used for experiments after 2 or 3 passages.

2.6.2 RNA preparation

Following kaempferol treatment, HaCaT cells were washed twice with PBS and total RNA was isolated using Trizol reagent (GibcoBRL Life Technologies, Grand Island, NY), according to the manufacturer's instructions. The RNA concentration was determined photometrically and its quality was observed using agarose gel electrophoresis.

2.6.3 cDNA microarray analysis

It was used a human 10K cDNA microarray that comprised 10,336

cDNA spots, as described previously [77]. Housekeeping genes and yeast DNA were spotted as negative controls. cDNA microarray analyses were performed four times for each time point. Fluorescence-labeled cDNA probes were prepared from 20 mg total RNA using an Amino Allyl cDNA labeling kit (Ambion, Austin, TX), as described previously [78]. The Cy3- and Cy5-labeled cDNA probes, corresponding to control and kaempferol-treated cells, respectively, were mixed and hybridized to the microarrays at 55^{o}C for 16 h. The two fluorescent images (Cy3 and Cy5) were scanned separately using a GMS 418 Array Scanner (Affymetrix, Santa Clara, CA) and image data were analyzed with the ImaGene v. 4.2 (Biodiscovery, Santa Monica, CA) and MAAS (Gaiagene, Seoul, Korea) software packages [79]. For each hybridization, emission signal data were normalized by multiplying the Cy3 signal values by the mean Cy3 to Cy5 signal intensity ratios for all spots on the array. Values ≥ 2-fold higher than background intensity was considered significant. It was calculated the median value of the gene expression ratio from four independently-repeated microarray experiments, then used modified *t*-tests (significance analysis of microarrays, SAM) to evaluate the statistical significance of changes in gene expression [80]. Significant genome-wide changes in expression were selected at SAM(d) = 0.66 and we adopted a 2.0-fold change cutoff, based on our previous experience. Genes exhibiting significant differences in expression level were classified into Gene Ontology (GO)-based functional categories (The Gene Ontology. http://www.geneontology.org), with some modifications. It was applied hierarchical clustering to genes using the weighted pair-group method with a centroid average, as implemented in the CLUSTER program [81]. The results were analyzed using Tree View

software (M. Eisen; http://www.microarrays.org/software).

2.6.4 Real time RT-PCR

It was selected a subset of differentially-expressed genes for independent confirmation of microarray results. It was performed SYBR green-based real-time RT-PCR using the gene encoding b-actin as an internal reference. Reverse transcription was performed on 4 mg total RNA in a 25 ml reaction mixture containing MuLV reverse transcriptase (2.5 U), RNAse inhibitor (1 U), 5 mM MgCl2, 50 mM KCl, 10 mM Tris-HCl, (pH 8.3), 2.5 mM oligo (dT) primer and 1 mM dNTPs. The reaction mixture was incubated at 42^{o}C for 60 min, then denatured at 85°C for 5 min. Using an ICycler (BioRad, Hercules, CA), cDNA was amplified in 50 ml reaction mixtures containing 1 U AmpliTaq DNA polymerase (Perkin Elmer, Shelton, CT), 50 mM Tris (pH 8.3), 0.25 g/L BSA, 3 mM MgCl2, 0.25 mM dNTPs, 1/50,000 dilution of SYBR green I (Molecular Probes, Eugene, OR) and 0.25 mM of the requisite PCR primers. Primer sequences were as follows in **Table 6**. The following reaction conditions were used: one cycle of denaturing at 95^{o}C for 5 min, followed by 30 cycles of 95^{o}C for 30 s, 60^{o}C for 45 s and 72^{o}C for 1 min. Relative RNA levels were determined by analyzing the changes in SYBR green I fluorescence during amplification, according to the manufacturer's instructions. b-actin was amplified in parallel; the results were used for normalization. PCR product sizes were confirmed by 2% agarose gel electrophoresis and staining with ethidium bromide. The purity of PCR products was determined by melting point analysis using the Cycler software (BioRad, Hercules, CA)

Table 2.6.1 PCR primer set

Gene symbol	Forward	Reverse
nuclear factor of kappa light polypeptide gene enhancer in B-cells 2 (NF-κB2)	5'-TCCACCTTTAAGTTGCCCTG-3’	5'-TCTGCTCTCGTCATGTCACC-3’
phospholipase A2-activating protein (PLAA)	5'-TTAAACACCCACCCACCAAG-3’	5'-CGAAAGCCTGGAGGTAAAGA-3’
signal transducer and activator of transcription 3 (STAT3)	5'-TCAGACCCATCATCAAGCAA-3’	5'-ATGACAGGTAAATGGGCGAG-3'
TNFα	5'-TGCACCACAGTTTAAACCCA-3’	5'-GACTCCTTCAGGTGCTCAGG-3’
peroxisome proliferator-activated receptor alpha (PPARα)	5'-GTGGCTGCTATAATTTGCTGTG-3’	5'-GAAGGTGTCATCTGGATGGGT-3’
PPAR-gamma (PPARγ)	5'-CAAGACTACCCTTTAAGTGAA-3'	5'-CTACTTTGATCGCACTTTGGT-3'
β-actin	5'-GGGTCAGAAGGACTCCTATG-3’	5'-GTAACAATGCCATGTTCAAT-3'

2.6.5 Promoter analysis

Promoter analysis was performed using oPOSSUM v1.3 [82], a web-based tool for analyzing sets of co-expressed genes. It incorporates cross-species comparisons, PSSM-based promoter motif detection and statistical methods for identification of over-represented transcription factor binding sites (TFBSs) using a pre-computed database. The database was constructed from an initial set of 14,083 orthologs from both human and mouse, which were obtained by selecting only 'one-to-one' human-mouse orthologs from Ensembl [83]. It was analyzed 2,000 bp upstream and downstream of the transcription start site (TSS) for each differentially-expressed gene. The level of conservation with the aligned orthologous mouse sequence was set to level 1 (the top 10 percentile of non-coding conserved regions with an absolute minimum percent identity of 70%). Two measures of statistical over-representation were used: a Z-score and a one-tailed Fisher exact probability.

2.6.6 UVB irradiation and NF-κB (p65/RelB) assay

HaCaT cells and NHEKs pretreated with kaempferol or vehicle were washed with PBS, after which fresh PBS was added and the cells were exposed to UVB radiation (40 mJ/cm2) delivered through a bank of FS40 lamps (Westinghouse, Pittsburgh, PA) with a UVB emission maximum at 313 nm. UV wavelengths not normally present in natural incident solar radiation were blocked using a Kodacel cellulose filter (Eastman Kodak Co., Rochester, MN), as described previously [84]. Following irradiation, the culture medium was reintroduced and cells were incubated for a further 6 h.

Kaempferol treatment occurred 6 h prior to and following UVB irradiation. Following treatment of cells with kaempferol and/or UVB, nuclear extracts were prepared and assayed using a TransFactor extraction kit (BD Bioscience CLONTECH, San Jose, CA) according to the manufacturer's instructions. Nuclear extracts were spun at 20,000 *g* for 5 min at 4^{o}C, after which the supernatants were assayed for p65 or RelB content. Equal amounts of nuclear lysate were added to incubation wells pre-coated with the DNA-binding consensus sequence and the presence of translocated p65 or the RelB subunit was assayed.

2.6.7 Plasmids and reporter gene assays

The reporter plasmid PPRE-*tk*-Luc, which contains captor expression plasmid pCMX-mPPAR, has been described previously [85, 86]. A modified calcium phosphate precipitation procedure was used for transient transfection [87]. In brief, HaCaT cells (1×10^5/well) were seeded into a 12-well culture plate and transfected with DNA mixtures (1.3 mg/well) containing carrier DNA (pBluescript), reporter plasmid (0.1 mg), β-galactosidase (β-gal) expression vector (0.2 mg) and pCMX-mPPAR expression vector (10 ng), using Lipofectamine Plus (GIBCO BRL, Grand Island, NY). The cells were treated for 24 h with test compounds, after which luciferase activity was determined using a luminometer, according to the manufacturer's instructions. Luciferase activity was normalized for transfection efficiency using the corresponding β-gal activity.

2.6.8 BrdU incorporation assay

The proliferation of keratinocyte cells was evaluated from the cellular incorporation of 5-bromo-2_-deoxyuridine (BrdU). Keratinocytes on 96-well culture plates were treated with the test drugs in RPMI 1640 containing 1% (v/v) FBS at 37℃ in 5% CO_2. After 24 h, BrdU (10 uM) was added to the culture medium and then incubated for another 16 to 18 h. The keratinocytes were fixed and BrdU incorporation was determined with a Cell Proliferation Enzyme-Linked Immunosorbent Assay (ELISA) kit (Roche Applied Science, Mannheim, Germany) using peroxidase-conjugated anti-BrdU Fab fragments according to the manufacturer's instructions. The results are presented as a percentage of the value for control culture conditions.

2.6.9 Western Blotting

After UVB (100mJ/cm^2) exposure, 1% FBS-medium 106 containing kaempferol at the indicated concentration was added to the cells. Cells were harvested 6 days later. Western blotting was performed as described previously [88]. Blotting proteins were visualized by enhanced chemiluminescence (Novex ECL, Invitrogen, CA, USA) and LAS3000 (Fuji Film, Tokyo, Japan). For sequential detection, membranes were stripped using Restore Western Blot Stripping buffer (Thermo scientific, Rockford, USA). To confirm equal protein loading in each well, cytosolic proteins were separated on 4-12% SDS-PAGE gels and the probe antibodies used were the anti-actin (Santa Cruz Biotechnology, CA, USA).

2.6.10 Statistical analysis

ANOVA tests were performed using SigmaStat (SPSS Inc., Chicago, IL); $P < 0.05$ was considered to be statistically significant.

CHAPTER 3.

Kaempferol and Anti-aging effects

3.1. Preparation of Kaempferol

3.1.1 Purification and identification of compounds in green tea seed

As shown in **Figure 3.1.1A**, HPLC analysis of green tea seed extract (GTSE) gives just two peaks, compounds **1** and **2**. For the structure analysis of these compounds, GTSE was further purified by MPLC. The fractions were combined after monitoring HPLC and compounds **1** and **2** were isolated in yields of 250 mg (0.25%) and 310 mg (0.31%), respectively. To determine the structure of the isolated compounds **1** and **2**, acid hydrolysis, LC/MS and NMR analysis was conducted. Compound **1** was obtained as a pale yellow amorphous powder. Upon acid hydrolysis of **1**, kaempferol, galactose, glucose and rhamnose were identified by TLC. The ^{1}H NMR spectrum showed four kinds of aromatic protons [δ 8.02 (2H, d, J = 8.7 Hz, H-2′, H-6′), 6.90 (2H, d, J = 9.0 Hz, H-3′, H-5′), 6.37 (1H, d, J = 1.8 Hz, H-8) and 6.17 (1H, d, J = 1.8 Hz, H-6)] indicating the kaempferol skeleton with three anomeric protons [δ 5.33 (1H, d, J = 7.8 Hz, H1-Glc), 4.70 (1H, d, J = 7.5 Hz H1-Gal), 4.47 (1H, d, J = 0.9 Hz H1-Rha)]. Furthermore, 31 carbon signals were observed in the ^{13}C NMR spectrum. Among them 13 carbon signals were assigned to the kaempferol and three carbon signals [δ 104.48 (C_{Gal}-1), 101.12 (C_{Glu}-1) and 102.21 (C_{Rha}-1)] to anomeric carbons of the sugar moiety. Compound **2** was also obtained as a pale yellow amorphous powder. Acid hydrolysis of **2** gave kaempferol, glucose, rhamnose and xylose. The ^{1}H NMR spectrum showed four kinds of aromatic protons [δ 8.00 (2H, d, J = 8.7 Hz, H-2′, H-6′), 6.80 (2H, d, J =

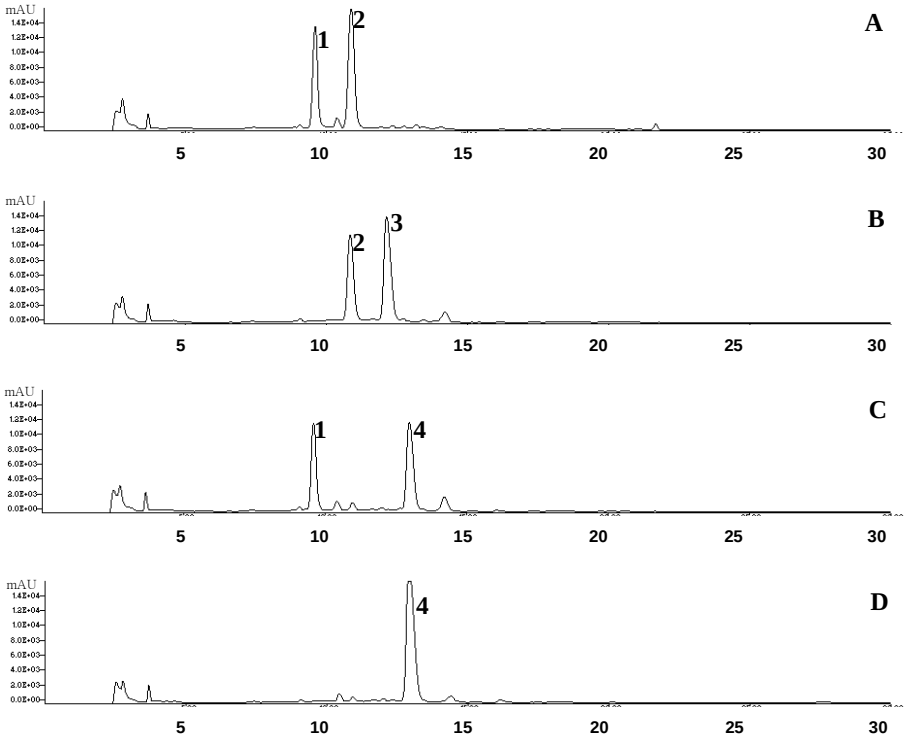

Figure 3.1.1 HPLC profile of green tea seed extract and the hydrolysis of GTSE with the commercial glycolytic enzymes

(A) Green tea seed extract; (B) reaction with hesperidinase; (C) reaction with cellulase; (D) reaction with β-galactosidase;

Key to peak identity: 1, kaempferol-3-*O*-[2-*O*-β-D-galactopyranosyl-6-*O*-α-L-rhanmopyranosyl]-β-D-glucopyranoside; 2, kaempferol-3-*O*-[2-*O*-β-D-xylopyranosyl-6-*O*-α-L-rhanmopyranosyl]-β-D-glucopyranoside; 3, kaempferol-3-O-β-D-galactopyranosyl (1→2)-β-D-glucopyranoside; 4, kaempferol-3-O-α-L-rhanmopyranosyl (1→6)-β-D-glucopyranoside

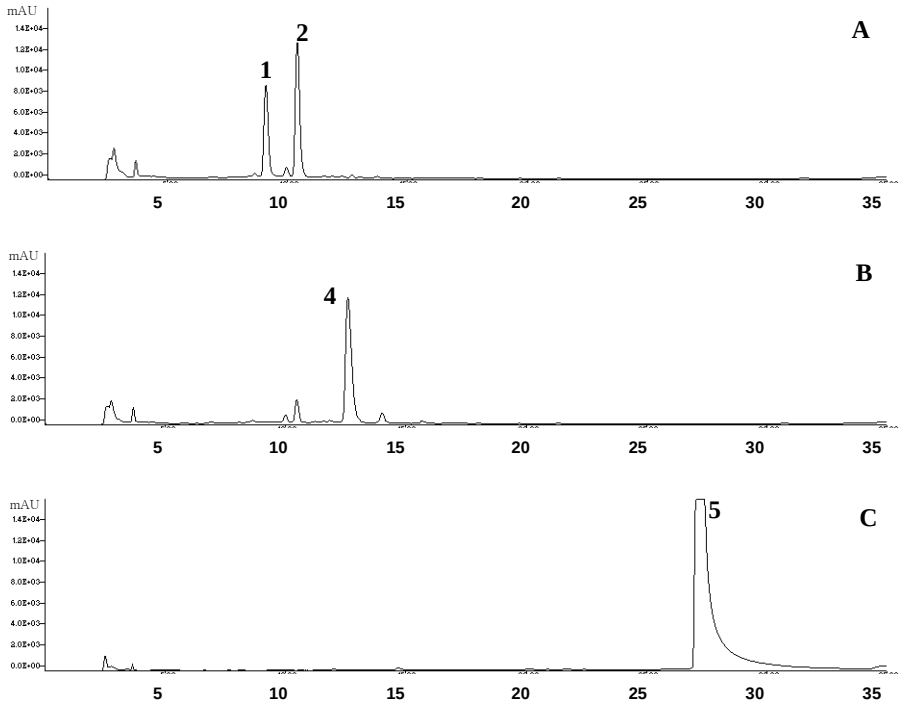

Figure 3.1.2 HPLC profile of hydrolysate of GTSE using mixed enzyme reaction

(A) Green tea seed extract; (B) reaction with β-galactosidase; (C) reaction with (D) and hesperidinase; Key to peak identity: 1, compound **1**; 2, compound **2**; 4, compound **4**; 5, compound **5**(kaempferol)

9.0 Hz, H-3′, H-5′), 6.34 (1H, d, *J* = 2.1 Hz, H-8) and 6.14 (1H, d, *J* = 2.1 Hz, H-6)] indicating the kaempferol skeleton with three anomeric protons [δ 5.35 (1H, d, *J* = 7.2 Hz, H1-Glc), 4.73 (1H, d, *J* = 7.5 Hz H1-Xyl) and 4.45 (1H, d, *J* = 1.2 Hz H1-Rha)]. In addition, 30 carbon signals were observed in the ^{13}C NMR spectrum. Among them, 13 carbon signals were assigned to the kaempferol and three carbon signals [δ 105.13 (C_{Xyl}-1), 100.83 (C_{Glu}-1) and 102.14 (C_{Rha}-1)] were due to the anomeric carbons of the sugar moiety. Based on the analysis data, compounds 1 and 2 were thus identified as kaempferol-3-*O*-[2-*O*-β-D-galactopyranosyl-6-*O*-α-L-rhanmopyranosyl]-β-D-glucopyranoside and kaempferol-3-*O*-[2-*O*-β-D-xylopyranosyl-6-*O*-α-L-rhamnopyranosyl]-β-D-glucopyranoside, respectively. All these data corresponded to that in the literature for camelliaside A and camelliaside B, respectively [13]. Although these compounds have been already reported as constituents in 'tea seed cake' prepared from tea seeds, because ‘tea seed cake’ is mixed material usually produced by tea seed which is fruits born from a tea plant belonged to the *Camellia* family, this is the first report on the isolation of these compounds from natural green tea seeds, *Camellia sinensis* solely.

3.1.2 Kaempferol production from GTSE using glycolytic enzymes

Because conventional chemical hydrolysis inevitably produced side reactions, glycolytic enzymes have traditionally been used for the process of deglycosylation of products [89]. To select enzyme for the concurrent bioconversion of kaempferol glycosides in GTS to kaempferol, the hydrolyzing ability of several glycolytic enzymes based on the

glycosidic moiety of compounds **1** and **2**, hesperidinase, β-glucosidase, cellulase, β-glucuronidase, pectinase, β-galactosidase, amyloglucosidase, α-amylase, β-xylosidase, xylanase and dextranase, were evaluated. For this purpose individual kinetics of hydrolysis of 50 mg/ml GTSE were carried out incubating each glycolytic enzyme at 37°C for 24 hr. The enzyme amount was adjusted to 50 units/g of GTSE. All reactions were monitored by HPLC and TLC analysis. Though some hydrolysed compounds were produced on reaction with cellulase, amyloglucosidase, β-galactosidase, β-xylosidase, Xylanase, hesperidinase, complete hydrolysis to kaempferol was not achieved in any case (**Figure 3.1.1**). In the case of the reaction with hesperidinase (**Figure 3.1.1B**), kaempferol-3-*O*-β-D-galactopyranosyl (1→2)-β-D-glucopyranoside (compound **3**, peak 3) was produced by hydrolyzing the rhamnosyl moiety of compound **1**. The reaction with β-xylosidase, xylanase, cellulase and amyloglucosidase gave the same hydrolysis pattern. **Figure 3.1.1C** shows the result of hydrolysis using cellulase. Kaempferol-3-*O*-β-D-rhamnopyranosyl (1→6)-β-D-glucopyranoside (compound **4**, peak 4) was produced by hydrolysing the xylosyl moiety of compound **2**. In general, cellulase and amyloglucosidase was cleaved glycosidic bond from some natural glycosides such as daidzin and genistin. But, in these results they showed xylosyl bond cleaved activity, perhaps due to the different activities and longer incubation time. In the case of the reaction with β-galactosidase (**Figure 3.1.1D**), compound **4** was also produced by hydrolyzing the galactosyl moiety of compound **1** and the xylosyl moiety of compound **2**. However, kaempferol was not formed in any reaction. Furthermore, other glycolytic enzymes except mentioned

above, β-glucosidase, β-glucuronidase, pectinase, α-amylase, and dextranase, were not formed any hydrolysis product. Though the flavonoids with glucose at the C-3 and C-7 position can be a substrate for β-glucosidase, the deglycosylation of other sugar such as rhamnose and rutinose depend on the structure of the flavonoids, the position of the sugar substituent and the species of the sugar moieties. It was therefore carried out a novel enzymatic approach, which is the mixed enzyme reaction method, to complete deglycosylation of compounds **1** and **2** in GTSE simultaneously for kaempferol production. After various enzyme combination reactions according to their individual kinetic behavior, it was able to observe the optimum combination of the enzymes, hesperidinase and β-galactosidase. **Figure 3.1.2** shows the results of GTSE hydrolysed with hesperidinase and β-galactosidase. When two enzymes were mixed for the reaction, compounds **1** and **2** were converted to kaempferol (peak 5) completely. This means that bioconversion of compounds **1** and **2** to kaempferol requires two enzyme reactions. Thus, β-galactosidase hydrolyses the xylosyl and galactosyl moiety of compounds **1** and **2** and the following reaction with hesperidinase removes the remaining rhamnosyl-glucoside residue. **Figure 3.1.3** shows the structures of the compounds **1** and **2** and their enzymatic hydrolysis products, compounds **3**, **4** and **5**.

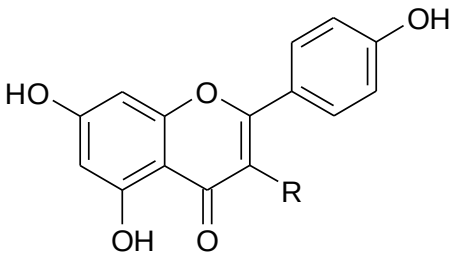

Compound	R
Compound **1**	Gal(1→2)[Rha(1→6)]Glc
Compound **2**	Xyl(1→2)[Rha(1→6)]Glc
Compound **3**	Gal(1→2)Glc
Compound **4**	Rha(1→6)Glc
Compound **5**	H

Figure 3.1.3 Structure of glycosidic flavonoids isolated from green tea seed and its enzymatic hydrolysed product, kaempferol

Glc: glucopyranoside, Gal: galactopyranoside, Xyl: xylopyranoside, Rha: rhamnopyranoside

3.2 Effect of Kaempferol *in vitro*

3.2.1 DPPH scavenging activities of two tea seed flavonoids and kaempferol

Most of the beneficial health effects of flavonoids are attributed to their antioxidant and chelating abilities. For comparing the antioxidation activity of tea seed flavonoids and its aglycone, kaempferol, the GTSE hydrolysate (GTSE-H) was further purified because the kaempferol content of GTSE-H was about 20% (w/w). After simple purification, centrifugation of GTSE-H and re-extraction of precipitation, we obtained the highly purified kaempferol in above 95% purity. The free radical scavenging activity of tea seed flavonoids and kaempferol, its aglycone, was tested by DPPH radical scavenging assay. The DPPH test is a non-enzymatic method currently used to provide basic information on the reactivity of compounds to scavenge free radicals [90]. **Table 3.2.1** shows the DPPH radical scavenging activity of the two tea seed flavonoids, compounds **1** and **2**, and compound **5**, its aglycone. Compound **5**, kaempferol, inhibited DPPH formation by 50% at a concentration of 59.2 ± 1.7 μM (IC50), whereas the two tea seed glycosides showed weak DPPH radical scavenging activity.

3.2.2 Xanthine oxidase (XO) inhibition activities of two tea seed flavonoids and kaempferol

The enzyme XO catalyses the oxidation of xanthine to uric acid. During the reoxidation of XO, oxygen molecules act as electron acceptors, producing superoxide radicals and hydrogen peroxide. Consequently, XO is considered to be an important biological source of superoxide radicals.

These are involved in many pathological processes such as inflammation, cancer and aging [91-93]. To compare the anti-superoxide effect of tea seed flavonoids and kaempferol, both inhibition of XO and the scavenging effect on the superoxide anion were measured in one assay. For comparison of inhibition effect of these compounds, allopurinol, the most well-studied xanthine oxidase inhibitor, was used as positive control. Inhibition of XO results in a decreased production of uric acid, which can be measured specrophotometically, and a decreased production of superoxide was measured by the nitrite method **(Figure 3.2.1)**. For each compounds tested two IC_{50} values can be calculated by linear regression analysis: 50% inhibition of XO, which is calculated by 50% decrease of uric acid production and 50% reduction of the superoxide level. Each IC_{50} value of the compounds is listed in **Table 3.2.2**. Though all the compounds showed less activity than allopurinol, the compound **5**, kaempferol, showed higher activity than its *O*-glycosides, compounds **1** and **2**. Presence of an OH group in 5 and 7 positions in both the compounds makes them potential candidates for superoxide reaction [94]. Free radical scavenging by flavonoids is highly dependent on the presence of a free 3-OH [95].Usually, aglycones are more potent antioxidants that their corresponding glycosides [96]. In this case, our result confirmed that *O*-glycosylation at C-3 reduced the activity of superoxide reaction although the kaempferol glycosides have a free OH group in both 5 and 7 positions.

Table 3.2.1 DPPH radical scavenging activity of tea seed flavonoids and kaempferol

Samples	IC_{50} (μM)*
Compound **1**	>1000
Compound **2**	>1000
Compound **5** (Kaempferol)	59.2 ± 1.7
Trolox	51.3 ± 2.1
L-Ascorbic acid	48.8 ± 2.7

*IC_{50} denote the antioxidant concentration causing 50% reduction of the free radical form of DPPH in methanol after 30 min with an each samples, respectively. It was calculated from regression line using different concentrations in triplicate experiments

3.2.3 Lipid peroxidation inhibitory effect of kaempferol

Tert-butyl hydroperoxide (t-BHP) is a ROS generation agent that causes lipid peroxidation. t-BHP has been known to decrease cellular proliferation life span and increase the proportion of cells' positive senescence-associated enzyme activity. Thus, t-BHP has been used for the induction of stress-induced premature senescence [97]. As shown in this study, kaempferol has an anti-oxidative effect, and it was found that kaempferol inhibited t-BHP induced lipid peroxidation (**Figure 3.2.2**).

Flavonoids generally occur in foods as *O*-glycosides with bound sugars, usually at the C-3 position. Recently, it has been reported that the aglycone is likely to have a greater biological effect than the glycoside *(9)*. *O*-glycosylation at C-3 of compounds **1** and **2** had a negative influence on the radical scavenging activity. The presence of a large substituent at C-3 reduced the activity probably the steric hindrance.

Two kaempferol glycosides, kaempferol-3-*O*-[2-*O*-β-D-galactopyranosyl-6-*O*-α-L-rhamnopyranosyl]-β-D-glucopyranoside and kaempferol-3-*O*-[2-*O*-β-D-xylopyranosyl-6-*O*-α-L-rhamnopyranosyl]-β-D-glucopyranoside, were isolated from the GTS. From these compounds, a commercially and biologically useful flavonoid, kaempferol, was produced by enzymatic hydrolysis using two O-glycolytic enzymes, β-galactosidase and hesperidinase. After a simple separation process, we obtained a highly purified kaempferol. It was also compared the antioxidant effect of these two GTS flavonoids and its aglycone, kaempferol. Kaempferol is a more efficient scavenger of DPPH radicals and a better inhibitor of xanthine/xanthine oxidase than the two glycosides.

Lipid peroxidation is a universal feature of oxidative stress, causing loss of cellular structure and function [98]. Like all other free radical chain reactions, lipid peroxidation must be initiated by a free radical, (i.e., by a one-electron oxidation) in this case abstracting an allylic hydrogen from a polyunsaturated side chain to create a lipid radical (L·). The protonated form of superoxide, the hydroperoxyl radical (HO_2·), can serve as an intiating radical due to its lipophilicity and redox potential:

$$HO_2\cdot + LH \rightarrow H2O2 + L\cdot$$

The lipid radical L· adds molecular oxygen extremely rapidly to produce a lipid dioxyl radical, which is a sufficiently good oxidant to abstract an allylic hydrogen from another unsaturated side chain, producing a lipid hydroperoxide (LOOH) and propagating the chain. Typically *in vivo* these two reactions cycle about 15 times, such that each initiating event results in the oxidation of about 15 polyunsaturated fatty acid molecules [98]. Thus the inhibitory effect of kaempferol on t-BHP induced lipid peroxidation indicated that kaempferol could protect cell damage that is generated from oxidative stress.

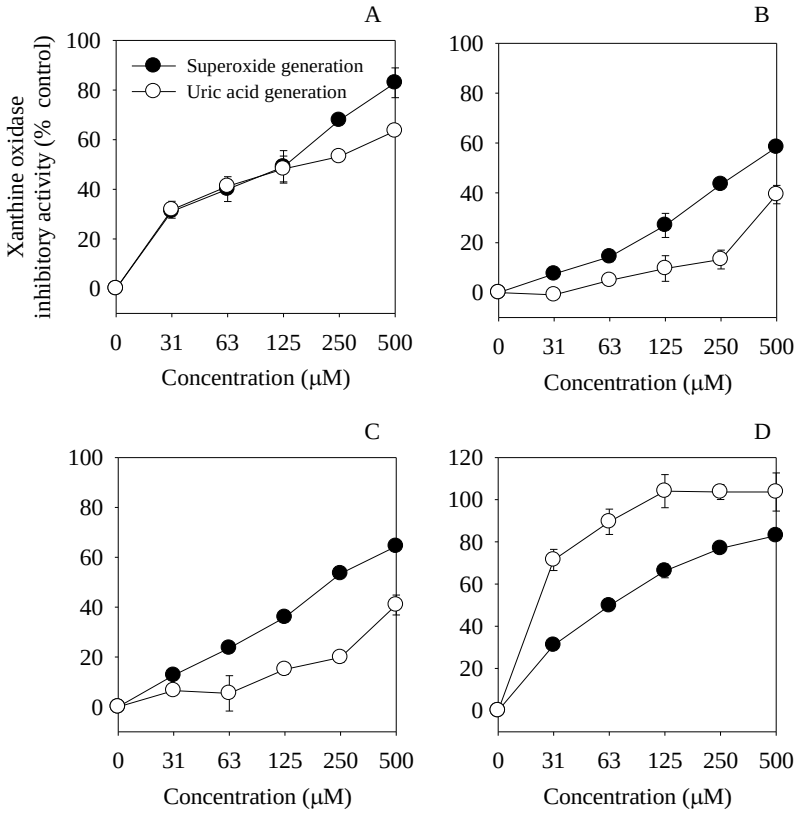

Figure 3.2.1 Antioxidation effect of tea seed flavonoids and kaempferol on xanthine/xanthine oxidase system.

(A) compound 5(kaempferol), (B) compound 1, (C) compound 2, (D) allopurinol; Open circles are indicated the uric acid generation activity and closed circles are indicater the superoxide generation activity

Table 3.2.2 Xanthine oxidase inhibitory activity of tea seed flavonoids and kaempferol

Samples	Xanthine oxidase inhibitory activity (IC_{50}*, μM)	
	Superoxide generation inhibition	Uric acid generation inhibition
Compound 1	337.7 ± 18.0	660.2 ± 6.1
Compound 2	223.4 ± 3.3	386.9 ± 5.9
Compound 5 (Kaempferol)	108.7 ± 9.4	159.1 ± 4.9
Allopurinol	63.1 ± 1.2	19.2 ± 3.2

*For each test two IC_{50} was calculated by linear regression analysis: 50% inhibition of xanthine oxidase (=50% decrease of uric acid production) and 50% reduction of the superoxide level.

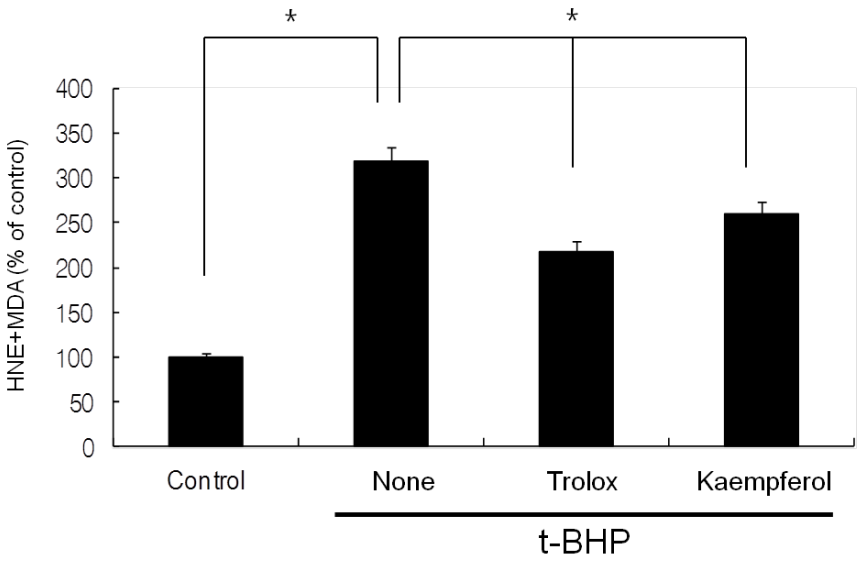

Figure 3.2.2 Inhibition of t-BHP-induced lipid peroxidation

Tert-Butyl hydroperoxide (t-BHP) was treated for lipid peroxidation. Trolox and kaempferol signnificanlty inhibited t-BHP-induced lipid peroxidation in keratinocytes. Three-independent experiments were performed and one of representative was shown in here.

3.2.4 Effect of kaempferol on UVB-induced MMP-1 expression, and procollagen biosynthesis

Before further experiment, cellular toxicity should be examined. As shown in **Figure 3.2.3**, kaempferol was not cytotoxic to HaCaT (**Fig. 3.2.3A**) or NHFs (**Fig. 3.2.3B**) at the indicated doses.

NHFs were first irradiated with UVB 40mJ/cm^2 and then treated with the indicated doses of kaempferol for 24 h followed by MMP-1 expression determination in the culture medium by ELISA. ELISA analysis revealed that MMP-1 levels were elevated by 160% upon irradiation compared to the basal level of UVB untreated cells. Treatment with kaempferol blocked the up-regulation of MMP-1 which is induced by UVB irradiation (**Fig. 3.2.4A**). It was also used the HaCaT-NHF co-culture system, and UVB was only irradiated to HaCaT keratinocytes. In this system, UVB irradiation increased MMP-1 expression more, so than it did in the NHF mono-culture only. In a co-culture system, treatment with kaempferol also significantly inhibited MMP-1 expression in the same manner (**Fig. 3.2.4B**).

Because of its skin anti-aging potency on extracellular matirx, further experiment was performed on collagen. However, kaempferol did not induce type I procollagen synthesis. TGF-β was used as a positive control in this experiment (**Fig. 3.2.5**).

3.2.5 Inhibition of TNF-α production in HaCaT/NHF co-culture

MMP-1 Metalloproteinase-1 can be induced by IL-1β, IL-6, IL-17, IL-21,

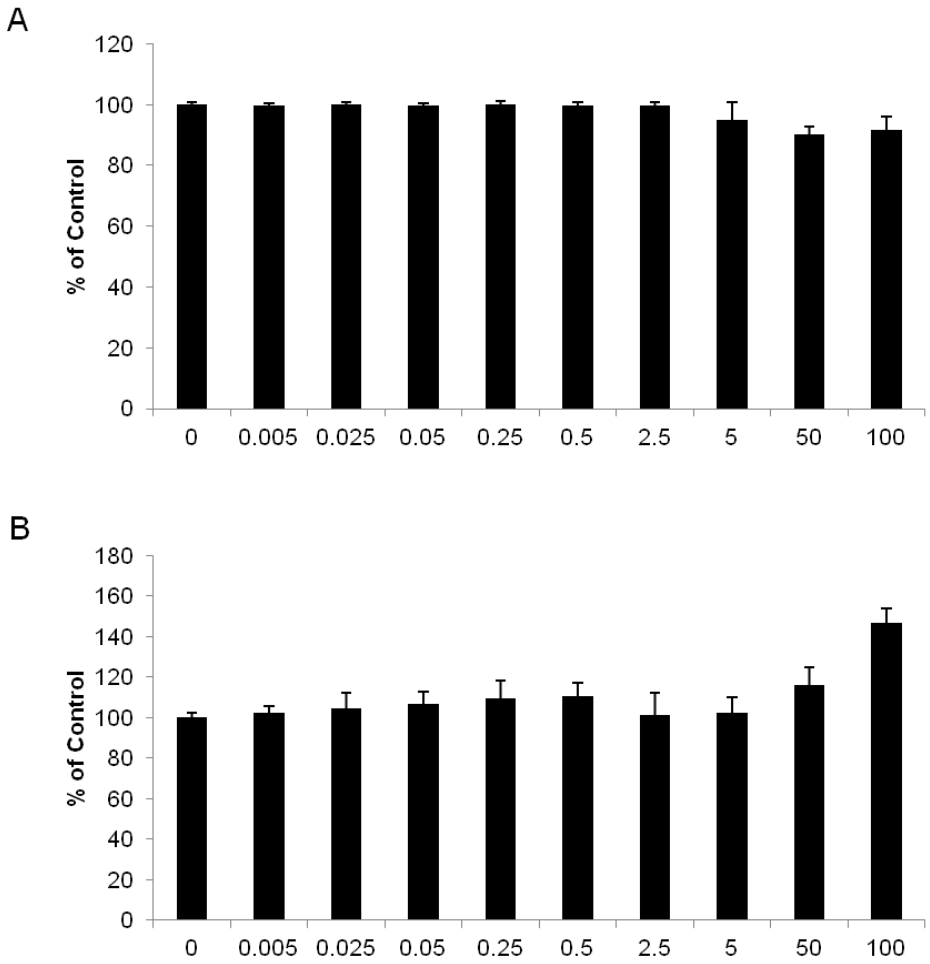

Figure 3.2.3 Cytotoxicity of kaempferol on HaCaT and Normal human fibroblasts

HaCaT, a keratinocyte cell line and normal human fibroblasts were treated with kaempferol at the indicated doses, and after 48h, cytotoxicity was measured for further experiments.

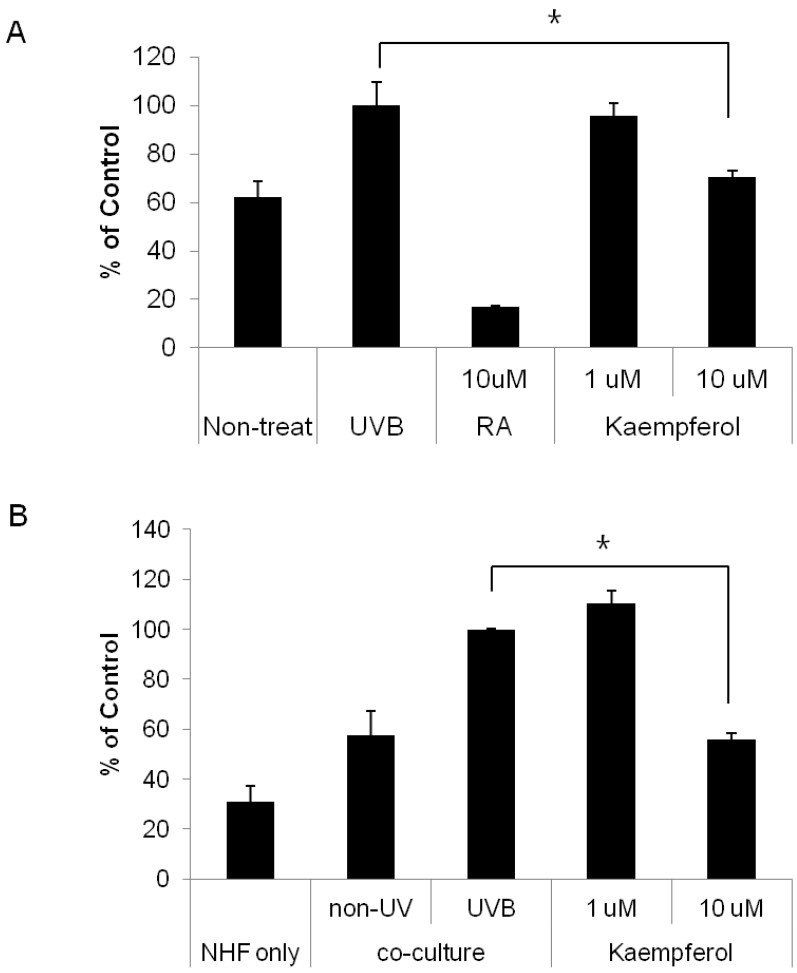

Figure 3.2.4 MMP-1 expression inhibition of kaempferol

After serum starvation for 24 h, cells were treated with UV irradiation and then media changed fresh media containing amentoflavone at the indicated concentration. And then further cultured for 24h. MMP-1 expressions were analyzed by ELISA kit in culture media. These ELISA results are representative of three independent experiments. (A) fibroblastsonly culture system (B) fibroblast and HaCaT coculture system.

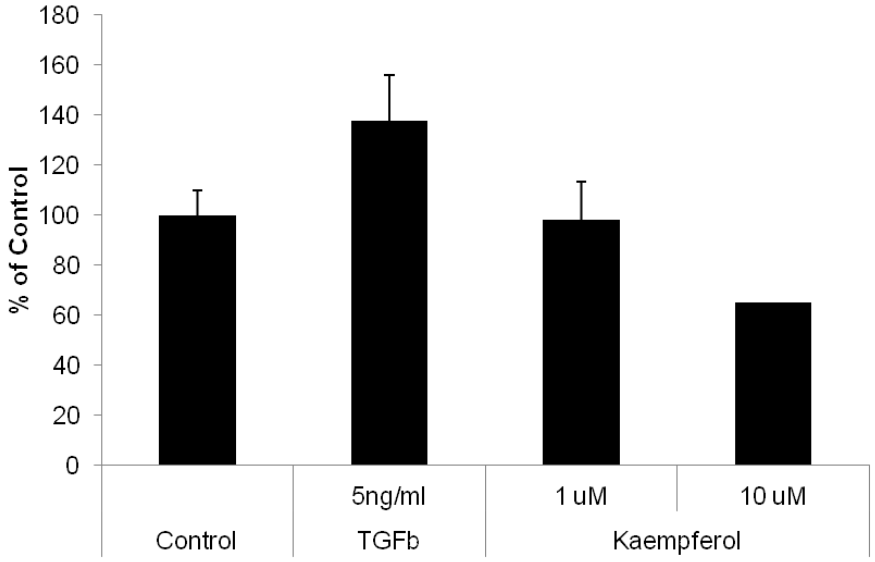

Figure 3.2.5 Effect of kaempferol on procollagen synthesis

Normal human fibroblasts were treated with TGFβ or kaempferol for the indicated doses for 48h and supernatant was harvested for type I procollagen assay.

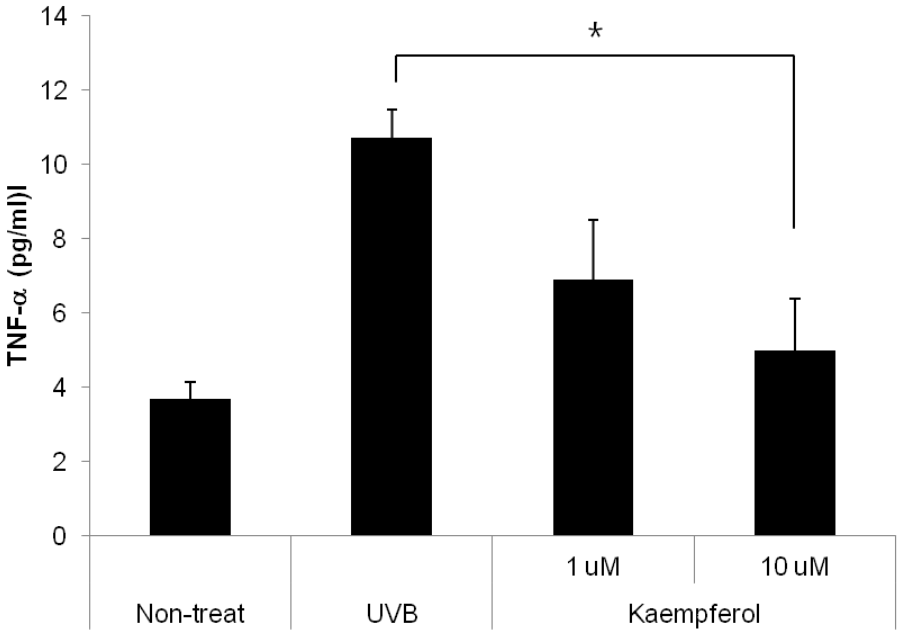

Figure 3.2.6 Inhibitory effect of kaempferol on TNF-α production

In HaCaT/Normal human fibroblasts co-culture system, UVB irradiation was used for TNF-α induction. Kaempferol was treated for 24h, and culture medium was harvested for further TNF-α assay.

TNF-α, and MIF or inhibited by TGF-β and TIMP-1 [99-101]. Previous report showed that mediator produced by NHEK cells under UVA irradiation post-conditions is responsible for stimulating MMP-1 in fibroblasts, data from qRT-PCR show that mRNA levels of IL-1α, IL-6 and TNF-α were significantly induced by UVA in NHEK cells. Also, only the patterns of TNF-α induction were similar to those of MMP-1 in fibroblasts grown in NHEK medium. This result indicated that TNF-α may be the factor from the NHEK media that stimulate MMP-1 in fibroblasts [102]. In this study, kaempferol dose-dependently inhibited TNF-α production when HaCaT/NHF cells were irradiated by UVB (**Fig. 3.2.6**).

Ultraviolet (UV) radiation has many effects on the skin, including inflammation, immunosuppression and alterations in the extracellular matrix (ECM), in addition to accelerated skin ageing [103]. Connective tissue damage in photoaged skin reflects both increased collagen destruction and decreased replacement of damaged connective tissue with newly synthesized collagen. Type 1 collagen is the primary constituent of the ECM and reduction of type 1 pro-collagen is closely related to skin aging [104-106]. Collagen degradation such as type I collagen results from repeated induction of matrix metalloproteinases (MMPs) by UV irradiation [107]. MMPs are a family of zinc-dependent endopeptidases that include MMP-1 (interstitial collagenase), MMP-3 (stromelysin-1) and MMP- 9 (92 kDa type IV gelatinase). In particular, MMP-1 is mainly responsible for the degradation of dermal collagen during the aging process of human skin [108-111]. Therefore analysis of MMP-1 expression levels along with collagen production has become a primary screening process for anti-aging

cosmetic ingredients.

Li et al [112] previously showed that fibroblasts co-cultured with keratinocytes are significantly higher in MMPs expression at gene and protein levels compared to mono-cultured fibroblasts [113]. Our data was also consistent with this finding that the basal MMP-1 protein expression in HaCaT-NHF co-culture was higher than in NHF mono-culture. UVB-irradiated HaCaT further induced MMP-1 protein expression, and it was also inhibited with kaempferol treatment. These results indicated that kaempferol could inhibit MMP-1 expression from UVB-irradiated NHF directly, and inhibit keratinocyte-mediated MMP-1 induction in NHF. Thus the effect of kaempferol was not limited to direct UVB-activated signal in NHF. It might affect keratinocyte-related intercellular factors on MMP-1 induction. In addition, in the HaCaT-NHF co-culture system, kaempferol was exposed to both cell types and was able to affect HaCaT and NHF.

3.3 Effect of Kaempferol *in vivo*

3.3.1 Decrease of SqOOH-induced wrinkle formation in hairless mouse

To investigate the effect of kaempferol on SqOOH-induced wrinkle formation, the dorsal skins of hairless mouse (Skh-1) were used. The cumulative effects of sub-erythema application of squalene monohydroperoxide (SqOOH), the initial products of UV-peroxidated squalene, to the skin of hairless mice were examined. Repeated topical application of 10mM SqOOH to hairless mice for 3 weeks induced definite skin roughness and crinkle formation. 3D surface parameter analysis revealed that changes in roughness parameters (number of furrows and crest, distance between a furrow and next crest, and irregularity) of the group treated with Sq-OOH compared to control group (**Figure 3.3.1**).

Retinoic acid (RA) is a well-known anti-wrinkle ingredient in cosmetics. Retinoids are derived from vitamin A, and can penetrate easily the epidermis with its lipid soluble property. Topical application of retinoids reduces skin wrinkles through induction of collagen biosynthesis and decrease of matrix metalloproteinases (MMPs)-mediated extracellular matrix degradation [114]. However, topical retinoids therapy could induce inflammation, known as retinoid dermatitis [115], and this phenomenon limits the wide usage of retinoids as cosmetic ingredients. Also, retinoids application is recommended in nighttime by dermatologists, because exposure to light causes retinoids degradation [116]. Besides photo-unstable characteristics, when topically applied retinoids meet sunlight, it might cause sunburn-like erythema. The metabolites and both isotretinoin

and its major metabolite showed phototoxic potential in controlled phototesting [117]. Thus, finding an effective and safe new anti-wrinkle ingredient is an important issue for cosmetic product. In this animal study, it was found that kaempferol reduced SqOOH-induced wrinkle formation effectively (**Figure 3.3.1**).

3.3.2 Clinical application of kaempferol on human skin

A replica from the right and left periorbital areas was taken at weeks 0 (baseline), 4, and 8 weeks and analysed based on five parameters using the Visiometer and dedicated software. **Table 3.3.1 and 3.3.2** compares R parameters at weeks 4 and 8 for kaempferol in clinical study. Visiometer R-values R1 through R5 decrease as wrinkles diminish. At week 8, a statistically significant difference in the R1 and R2 was observed in kaempferol-treated subjects on horizontal line analysis. R1 was significantly different even at 4 weeks treatment. In circular line analysis, R1, R2, R3, and R4 were differed at 8 weeks significantly (**Table 3.3.2**). This result indicated that topical application of kaempferol had potent effect on skin wrinkle improvement.

3.3.3 Investigator's assessment

Periorbital wrinkles were evaluated in a double-blind test by two dermatologists at weeks 0, 4, and 8, and analyzed by mann-whiteney u-test. As shown in **Table 3.3.3**, kaempferol-treated group showed significant wrinkle improvement at 8 weeks.

Wrinkling is one characteristic of aged skin, and has been attributed to age-dependent loss of skin hydration and to changes in the density and orientation of collagen fibers and keratin in the extracellular matrix [118]. Exposure of the human epidermis to ultraviolet (UV) irradiation leads to changes in the physiological and biochemical features of the skin. Photoaged skin is clinically characterized by wrinkled, dry, inelastic and irregularly pigmented skin. These phenomena usually result from the increase of epidermal thickness, reduction in collagen in the dermis, and increased numbers of keratinizing cysts in the lower dermis. Topical retinoid derivatives can repair UV-damaged skin *in vivo*, leading to the effacement of wrinkles [119].

Retinoic acid is the most bioactive form of the retinoids when topically applied to the skin, causing thinning of the stratum corneum, which leads to a smoother skin texture, and increased collagen content in photodamaged skin, which reduces fine wrinkles and increases skin tensile strength [120]. However, topical retinoic acids have a limited effect in the long-term treatment of ageing and photoageing due to side-effects such as irritation of the skin. Although retinol was developed to reduce such side-effects, it is photounstable and has a lower efficacy than other retinoids. This photoinstability and skin irritation potential is a major drawback for its use in cosmetics [121]. In this study, first it was proved that kaempferol had potency on anti-aging activities on skin such as MMP-1 inhibition, anti-inflammation and anti-oxidandation.

Lipid peroxidation has been suggested to play a key role in damaging biological processes resulting from excessive exposure to UV light. Aging of skin has been associated with increased peroxidation of skin

lipid. In particular, squalene, which is a main component of skin surface polyunsaturated lipids, is easily peroxidized. Squalene-monohydroperoxide (SqOOH), the initial product of peroxidized squalene, is produced at the human skin by natural exposure to sunlight during day time activities [122]. Recently, a few researchers reported on the damages of hairless mice skin by the topical application of SqOOH. Repeated application of SqOOH to the hairless mice induced the skin wrinkles with clear and fine appearance. Histologically were seen, more keratinocyte hypertrophy with Sq-OOH treated skin than with chronic UVB irradiated group in epidermis. In dermis, characteristics, found in UVB irradiated skin, such as the loss of polarity, fractured collagen bundle and elastosis, were not observed severely.

The alteration of epidermal layer might be the main factor for the formation of wrinkle caused by SqOOH. From the previous works, SqOOH is considered as an important source of damage in the early stage of aging process to result in epidermal wrinkle [123]. Thus, it is very important to minimize such damage that would be induced mainly by SqOOH against healthy skin condition. Therefore, in this study, kaempferol was used as a new anti-aging material for protecting skin damage by SqOOH.

The present study demonstrated a significant improvement in the treatment of fine photo ageing-induced wrinkles (Clinical) or chemical-induced wrinkle (animal) using topical application of kaempferol. It was analyzed images using replicas and visiometer, an objective technique to reproduce changes in photo-damaged skin. The image analysis using replicas was performed at week 4 and 8 (clinical study) and week 3 (animal).

In these *in vivo* animal and clinical studies, the overall wrinkle was

significantly improved with kaempferol treatment compared with treatment with placebo or retinoic acid. Clinical data based on subject and investigator assessment revealed a greater improvement in fine wrinkles using kaempferol than with a placebo.

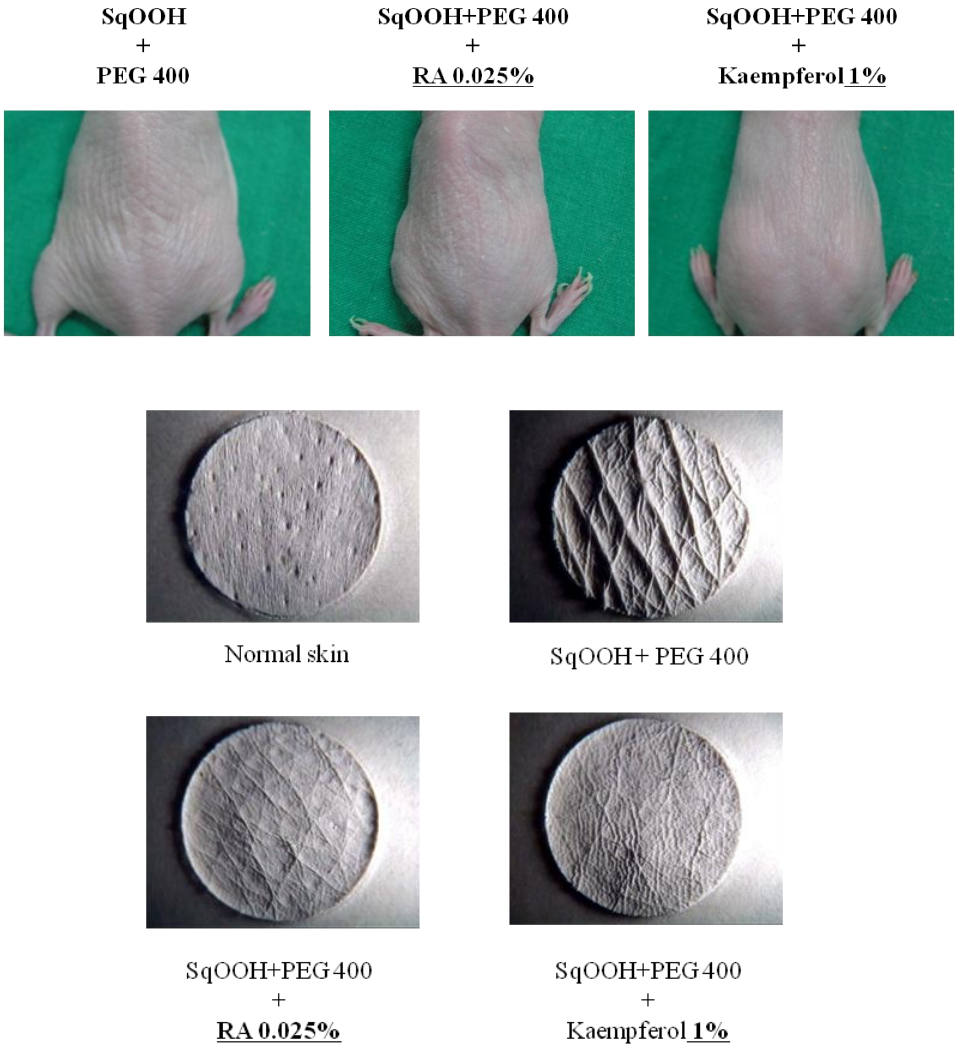

Figure 3.3.1 SqOOH-induced skin wrinkling and effect of kaempferol

The back skin of hairless mice was exposed to SqOOH, and vehicle (PEG-400), 0.025% retinoic acid, and 1% kaempferol was topically applied for 3 weeks.

Table 3.3.1 Replica analysis on Horizontal line

	4 weeks Δ(T4w-T0w)		8 weeks Δ(T8w-T0w)	
	Kaempferol	**Control**	**Kaempferol**	**Control**
R1	-0.1041* ±0.6213	0.2222 ±0.4874	-0.1741* ±0.7741	0.2502 ±0.4301
R2	-0.1026 ±0.5974	0.1826 ±0.4926	-0.1493* ±0.6904	0.1919 ±0.4258
R3	-0.0507 ±0.4623	0.1315 ±0.3603	-0.0796 ±0.5375	0.1567 ±0.3136
R4	-0.0126 ±0.1020	0.0385 ±0.0884	-0.0889 ±0.1275	0.0330 ±0.6591
R5	-0.0111 ±0.1992	0.0637 ±0.1650	-0.0007 ±0.2384	0.0741 ±0.1487

* p value, independent t-test, two-tailed, $p < 0.05$

Table 3.3.2 Replica analysis on Circular line

	4 weeks Δ(T4w-T0w)		8 weeks Δ(T8w-T0w)	
	Kaempferol	**Control**	**Kaempferol**	**Control**
R1	-0.0493 ±0.3698	0.8440 ±0.3094	-0.1152* ±0.4635	0.0452 ±0.2851
R2	-0.1259 ±0.6317	0.1863 ±0.5135	-0.2337* ±0.7916	0.2130 ±0.5227
R3	-0.0826* ±0.4669	0.1407 ±0.3309	-0.1422* ±0.5880	0.1722 ±0.3412
R4	-0.0052 ±0.1271	0.0363 ±0.1039	-0.1472* ±0.1521	0.0485 ±0.1043
R5	-0.0159 ±0.2372	0.0644 ±0.1665	-0.0304 ±0.2837	0.0881 ±0.1730

* p value, independent t-test, two-tailed, $p < 0.05$

Table 3.3.3 Wrinkle improvement analysis by dermatologist

	4 weeks Δ(T4w-T0w)		**8 weeks Δ(T8w-T0w)**	
	Kaempferol	Control	Kaempferol	Control
Dermatologist 1	-0.5±0.7	-0.6±0.6	-0.9±1.1	-0.9±1.1
Sig.	N.S.		N.S.	
Dermatologist 2	0.0±0.3	0.0±0.0	-0.5±0.6*	0.0±0.5
Sig.	N.S.		p=0.002	

* p value, independent t-test, two-tailed, $p < 0.05$

CHAPTER 4.

Molecular target search of Kaempferol by cDNA microarray

4. Molecular target search of Kaempferol by cDNA microarray

4.1. Identification of kaempferol-responsive genes

To identify genes regulated differentially by kaempferol, we compared the expression levels of *ca*. 10,000 genes from kaempferol- and vehicle-treated HaCaT cells. cDNA microarray analyses revealed a >2-fold difference in the expression of 147 transcripts, at one or more time points (**Table 4.1.1**). Of these, 18 and 129 were up- and down-regulated, respectively. Altered expression of the majority of down-regulated transcripts (117) occurred 3 h after kaempferol treatment. To provide independent validation of the microarray data, we performed real-time PCR analyses on expression of selected genes. In concordance with the results obtained from the microarray experiments, transcript levels for genes encoding NF-κB2, Plaa and Stat3 decreased following kaempferol treatment (**Table 4.1.2**).

4.2 Functional categorization and hierarchical clustering of differentially-expressed genes

The 147 transcripts were classified into 12 categories, according to their functional roles. The majority of down-regulated genes were involved in cell adhesion/cytoskeleton, cell cycle, DNA modification/replication, signal transduction, transcription regulation and transport (**Figure 4.2.1**). In contrast, up-regulated genes were involved in cellular redox homeostasis (**Figure 4.2.1**). The 147 transcripts were clustered into 3 distinct expression

Table 4.1.1 Kaempferol-treated HaCaT and its cDNA microarray data

GenBank No	Name	Symbol	Function	Cluster	Fold change		
					3h	6h	24h
BM787728	Actinin, alpha 1	ACTN1	cell adhesion and cytoskeleton	2	-2.5	-1.2	-1.4
BM783646	Desmoglein 2	DSG2	cell adhesion and cytoskeleton	2	-2.4	-1.1	-1.5
BF864858	Formin binding protein 4	FNBP4	cell adhesion and cytoskeleton	2	-2.4	-1.2	-1.4
BQ417219	Glycoprotein V (platelet)	GP5	cell adhesion and cytoskeleton	2	-2.7	-1.1	-1.4
BG752932	Neurofibromin 2 (bilateral acoustic neuroma)	NF2	cell adhesion and cytoskeleton	2	-2.4	-1.1	-1.5
BM925368	Stomatin	STOM	cell adhesion and cytoskeleton	2	-2.2	-1.2	-1.4
BM750409	Adaptor protein containing pH domain, PTB domain and leucine zipper motif 1	APPL	cell cycle	2	-2.4	-1.3	-1.5
BQ082207	Cell division cycle 2-like 5 (cholinesterase-related cell division controller)	CDC2L5	cell cycle	2	-2.5	-1.3	-1.5
BM783084	Radical fringe homolog (Drosophila)	RFNG	cell cycle	2	-2.5	-1.2	-1.2
BM752799	S-phase kinase-associated protein 2 (p45)	SKP2	cell cycle	2	-2.2	-1.7	-1.6
BM755446	Thioredoxin-like 4B	TXNL4B	cell cycle	2	-2.2	-1.3	-1.6
BM748933	Endoplasmic reticulum thioredoxin superfamily member, 18 kDa	TLP19	cell redox homeostasis	1	1.2	1.0	2.1
BM749654	Peroxiredoxin 3	PRDX3	cell redox homeostasis	1	1.4	1.2	3.4
BM799388	Thioredoxin reductase 1	TXNRD1	cell redox homeostasis	1	1.2	3.8	2.8
AI022345	Thioredoxin reductase 1	TXNRD1	cell redox homeostasis	1	1.4	2.9	1.9
BE872273	Nucleoredoxin	NXN	cell redox homeostasis	2	-2.3	-1.1	-1.3
BM761603	FOS-like antigen 1	FOSL1	defense and immune response	1	-1.2	2.1	2.5
BM759589	Stress-induced-phosphoprotein 1 (Hsp70/Hsp90-organizing protein)	STIP1	defense and immune response	2	-2.7	-1.3	-1.5
BM786490	DEAD (Asp-Glu-Ala-Asp) box polypeptide 51	DDX51	DNA modification and replication	2	-2.4	-1.3	-1.6
BM787857	Origin recognition complex, subunit 6 homolog-like (yeast)	ORC6L	DNA modification and replication	2	-2.3	-1.2	-1.4

Table 4.1.1 (Cont'd)

GenBank No	Name	Symbol	Function	Cluster	3h	6h	24h
BM757481	Polymerase (DNA directed) nu	POLN	DNA modification and replication	2	-2.3	-1.1	-1.4
BM787623	Topoisomerase (DNA) II binding protein 1	TOPBP1	DNA modification and replication	2	-2.5	-1.3	-1.4
BM793025	Topoisomerase (DNA) III alpha	TOP3A	DNA modification and replication	2	-2.1	-1.3	-1.6
BM756089	Clusterin (complement lysis inhibitor, SP-40,40, sulfated glycoprotein 2, testosterone-repressed prostate message 2, apolipoprotein J)	CLU	defense and immune response	1	1.2	1.2	2.3
AF027706	Receptor-interacting serine-threonine kinase 2	RIPK2	defense and immune response	1	1.9	1.4	3.3
BM757316	Sp2 transcription factor	SP2	defense and immune response	1	1.4	1.4	2.6
BM791916	Cathepsin S	CTSS	defense and immune response	2	-2.1	-1.1	-1.4
BM751205	CD68 antigen	CD68	defense and immune response	2	-2.2	-1.2	-1.5
BM785914	Glucose phosphate isomerase	GPI	defense and immune response	2	-2.1	-1.1	-1.4
BM784811	Interferon (alpha, beta and omega) receptor 1	IFNAR1	defense and immune response	2	-2.5	-1.5	-1.6
BM750766	Nuclear factor of kappa light polypeptide gene enhancer in B-cells 2 (p49/p100)	NFKB2	defense and immune response	2	-2.3	-1.2	-1.4
BM761120	Nuclear factor of kappa light polypeptide gene enhancer in B-cells inhibitor, beta	NFKBIB	defense and immune response	2	-2.4	-1.3	-1.5
BM786517	Signal transducer and activator of transcription 3 (acute-phase response factor)	STAT3	defense and immune response	2	-2.2	-1.2	-1.4
BM742118	Signal transducer and activator of transcription 3 (acute-phase response factor)	STAT3	defense and immune response	2	-2.8	-1.2	-1.6
BM741126	Transcription factor 7 (T-cell specific, HMG-box)	TCF7	defense and immune response	2	-2.1	-1.3	-1.4
BM794187	Interferon, alpha-inducible protein (clone IFI-15K)	G1P2	defense and immune response	3	-1.4	-1.7	-2.6
BM790031	Interferon-induced protein with tetratricopeptide repeats 3	IFIT3	defense and immune response	3	-1.0		-3.3
BM763771	Toll-like receptor adaptor molecule 1	TRIF	defense and immune response	3	-1.4	-1.5	-2.0
BM759632	Adaptor-related protein complex 1, mu 1 subunit	AP1M1	intracellular transport	1	1.4	-1.0	2.7
BM758517	Adaptor-related protein complex 1, sigma 3 subunit	AP1S3	intracellular transport	2	-2.7	-1.3	-1.5
BM750940	Adaptor-related protein complex 3, sigma 2 subunit	AP3S2	intracellular transport	2	-2.6	-1.2	-1.5

Table 4.1.1 (Cont'd)

GenBank No	Name	Symbol	Function	Cluster	3h	6h	24h
BX647920	Golgi autoantigen, golgin subfamily a, 2	GOLGA2	intracellular transport	2	-2.5	-1.2	-1.5
BX105880	Intersectin 2	ITSN2	intracellular transport	2	-2.6	-1.0	-1.3
BI038938	Myosin, heavy polypeptide 9, non-muscle	MYH9	intracellular transport	2	-2.2	-1.3	-1.4
BM750459	Nudix (nucleoside diphosphate linked moiety X)-type motif 4	NUDT4	intracellular transport	2	-2.4	-1.2	-1.4
BM785614	Protective protein for beta-galactosidase (galactosialidosis)	PPGB	intracellular transport	2	-2.5	-1.3	-1.6
CB104873	RAB1B, member RAS oncogene family	RAB1B	intracellular transport	2	-2.8	-1.3	-1.5
NM_014999	RAB21, member RAS oncogene family	RAB21	intracellular transport	2	-2.5	-1.1	-1.4
AI379719	Sorting nexin 5	SNX5	intracellular transport	2	-2.5	-1.3	-1.5
AK126465	Trans-golgi network protein 2	TGOLN2	intracellular transport	2	-2.5	-1.2	-1.3
BM794327	Insulin induced gene 1	INSIG1	metablism	3	-1.3	-1.8	-2.1
BM767910	Aldehyde dehydrogenase 3 family, memberA1	ALDH3A1	metabolism	1	1.5	1.3	2.7
BM738976	Aldo-keto reductase family 1, member C2 (dihydrodiol dehydrogenase 2; bile acid binding protein; 3-alpha hydroxysteroid dehydrogenase, type III)	AKR1C1	metabolism	1	1.5	1.5	3.2
BM772580	Aldo-keto reductase family 1, member C3 (3-alpha hydroxysteroid dehydrogenase, type II)	AKR1C3	metabolism	1	1.7	1.4	4.3
BM749464	Phosphate cytidylyltransferase 2, ethanolamine	PCYT2	metabolism	1	1.1	1.3	2.5
BM787682	5'-nucleotidase, cytosolic II	NT5C2	metabolism	2	-2.1	-1.3	-1.2
BM789270	Aldehyde dehydrogenase 1 family, member B1	ALDH1B1	metabolism	2	-2.2	-1.3	-1.4
AK123877	Aldehyde dehydrogenase 3 family, member A2	ALDH3A2	metabolism	2	-2.3	-1.2	-1.4
AW674711	Fucokinase	FUK	metabolism	2	-2.1	-1.1	-1.5
AF145023	Hydroxysteroid (17-beta) dehydrogenase 7	HSD17B7	metabolism	2	-2.2	-1.1	-1.4
CK005113	Isocitrate dehydrogenase 1 (NADP+), soluble	IDH1	metabolism	2	-2.3	-1.1	-1.5
BM751331	Isopentenyl-diphosphate delta isomerase 2	IDI2	metabolism	2	-2.2	-1.3	-1.5

Table 4.1.1 (Cont'd)

GenBank No	Name	Symbol	Function	Cluster	3h	6h	24h
BM786493	Lipase, member H	LIPH	metabolism	2	-2.3	-1.0	-1.2
NM_000239	Lysozyme (renal amyloidosis)	LYZ	metabolism	2	-2.5	-1.2	-1.5
BM790413	Acetyl-Coenzyme A synthetase 2 (ADP forming)	ACAS2	metabolism	3	-1.3	-1.6	-2.8
BM788852	Lysozyme (renal amyloidosis)	LYZ	metabolism	2	-2.5	-1.0	-1.2
BM743201	ATP citrate lyase	ACLY	metabolism	3	-1.0	-2.0	-2.3
BM763995	Eukaryotic translation elongation factor 1 alpha 1	EEF1A1	protein biosynthesis and modification	1	-1.2	2.2	2.2
BM745910	Alanyl-tRNA synthetase like	AARSL	protein biosynthesis and modification	2	-2.5	-1.2	-1.6
AL039930	Deltex homolog 2 (Drosophila)	DTX2	protein biosynthesis and modification	2	-2.5	-1.3	-1.5
BM785042	Methionyl-tRNA formyltransferase, mitochondrial	MtFMT	protein biosynthesis and modification	2	-2.1	-1.1	-1.5
BM782100	Parkinson disease (autosomal recessive, juvenile) 2, parkin	PARK2	protein biosynthesis and modification	2	-2.4	-1.3	-1.7
BC030707	Peptidylprolyl isomerase D (cyclophilin D)	PPID	protein biosynthesis and modification	2	-2.4	-1.2	-1.5
BC013423	Procollagen-proline, 2-oxoglutarate 4-dioxygenase (proline 4-hydroxylase), alpha polypeptide II	P4HA2	protein biosynthesis and modification	2	-2.4	-1.2	-1.6
BM784581	Serine (or cysteine) proteinase inhibitor, clade A (alpha-1 antiproteinase, antitrypsin), member 1	SERPINA1	protein biosynthesis and modification	2	-2.0	-1.2	-1.5
BX449079	Serine (or cysteine) proteinase inhibitor, clade F (alpha-2 antiplasmin, pigment epithelium derived factor), member 2	SERPINF2	protein biosynthesis and modification	2	-2.9	-1.2	-1.6
BM745603	Source of immunodominant MHC-associated peptides	SIMP	protein biosynthesis and modification	2	-2.6	-1.2	-1.4
BM773413	Proteasome (prosome, macropain) 26S subunit, non-ATPase, 14	PSMD14	protein biosynthesis and modification	2	-2.1	-1.3	-1.3
BM750445	Transmembrane protease, serine 3	TMPRSS3	protein biosynthesis and modification	2	-2.3	-1.4	-1.5
BM769452	2'-5'-oligoadenylate synthetase-like	OASL	protein biosynthesis and modification	3	-1.4	-2.1	-3.4
BM784305	Heat shock 27kDa protein 1	HSPB1	protein biosynthesis and modification	3	-1.1	-1.6	-2.5
BM739650	Tryptophanyl-tRNA synthetase	WARS	protein biosynthesis and modification	3	-1.4	-1.7	-2.7
BM757476	Tryptophanyl-tRNA synthetase	WARS	protein biosynthesis and modification	3	-1.5	-1.4	-2.5

Table 4.1.1 (Cont'd)

GenBank No	Name	Symbol	Function	Cluster	3h	6h	24h
BM782879	Ubiquitin specific protease 9, X-linked (fat facets-like, Drosophila)	USP9X	protein biosynthesis and modification	3	1.1	-1.7	-2.5
BM749499	Exosome component 8	EXOSC8	RNA processing	1	1.8	1.2	3.1
BM750408	LUC7-like (S. cerevisiae)	LUC7L	RNA processing	2	-2.4	-1.3	-1.5
W72860	Ankyrin repeat and SOCS box-containing 8	ASB8	signal transduction	2	-2.4	-1.3	-1.4
BM787149	Calcium binding protein P22	CHP	signal transduction	2	-2.3	-1.4	-1.4
BQ321472	Calcium/calmodulin-dependent protein kinase kinase 2, beta	CAMKK2	signal transduction	2	-2.9	-1.2	-1.4
BM740193	Calcium/calmodulin-dependent serine protein kinase (MAGUK family)	CASK	signal transduction	2	-2.2	-1.2	-1.5
BM751912	Casein kinase 1, gamma 1	CSNK1G1	signal transduction	2	-2.6	-1.3	-1.5
BM761773	Caveolin 2	CAV2	signal transduction	2	-2.5	-1.3	-1.6
BE155243	G protein-coupled receptor kinase interactor 2	GIT2	signal transduction	2	-2.4	-1.2	-1.6
BM786945	LIM and senescent cell antigen-like domains 1	LIMS1	signal transduction	2	-2.2	-1.1	-1.2
AL110164	LIM and senescent cell antigen-like domains 1	LIMS1	signal transduction	2	-3.1	-1.2	-1.5
BM790133	Phosphatidylinositol 4-kinase, catalytic, beta polypeptide	PIK4CB	signal transduction	2	-2.7	-1.2	-1.6
BM767282	Phospholipase A2-activating protein	PLAA	signal transduction	2	-2.1	-1.1	-1.4
BM772207	Phospholipase A2-activating protein	PLAA	signal transduction	2	-2.0	-1.3	-1.4
BM785608	Protein kinase, AMP-activated, gamma 2 non-catalytic subunit	PRKAG2	signal transduction	2	-2.2	-1.2	-1.5
BM787878	PTK2 protein tyrosine kinase 2	PTK2	signal transduction	2	-2.1	-1.1	-1.4
BM793147	RAS protein activator like 1 (GAP1 like)	RASAL1	signal transduction	2	-2.1	-1.2	-1.4
BX648337	RasGEF domain family, member 1B	RASGEF1B	signal transduction	2	-2.4	-1.2	-1.5
BM752462	Rho-associated, coiled-coil containing protein kinase 2	ROCK2	signal transduction	2	-2.3	-1.2	-1.4
BM752511	Serine/threonine kinase 17b (apoptosis-inducing)	STK17B	signal transduction	2	-2.3	1.0	-1.4

Table 4.1.1 (Cont'd)

GenBank No	Name	Symbol	Function	Cluster	3h	6h	24h
AL832591	Serine/threonine/tyrosine interacting protein	STYX	signal transduction	2	-2.3	-1.3	-1.4
NM_013257	Serum/glucocorticoid regulated kinase-like	SGKL	signal transduction	2	-2.5	-1.3	-1.3
BM785530	Syndecan 1	SDC1	signal transduction	2	-2.5	-1.2	-1.4
AI089275	Syndecan 4 (amphiglycan, ryudocan)	SDC4	signal transduction	3	-1.3	-1.5	-2.4
AI475332	CCAAT/enhancer binding protein zeta	CEBPZ	transcription regulation	2	-2.2	-1.2	-1.4
BM783777	MYB binding protein (P160) 1a	MYBBP1A	transcription regulation	2	-2.4	-1.2	1.0
AK091308	NMDA receptor regulated 1	NARG1	transcription regulation	2	-2.3	-1.2	-1.4
BM738548	SEC14-like 2 (S. cerevisiae)	SEC14L2	transcription regulation	2	-2.2	-1.1	-1.3
BM747886	SMAD, mothers against DPP homolog 9 (Drosophila)	SMAD9	transcription regulation	2	-2.1	-1.3	-1.3
BM748522	SWI/SNF related, matrix associated, actin dependent regulator of chromatin, subfamily e, member 1	SMARCE1	transcription regulation	2	-2.3	-1.3	-1.4
NM_006284	TAF10 RNA polymerase II, TATA box binding protein (TBP)-associated factor, 30kDa	TAF10	transcription regulation	2	-2.5	-1.3	-1.0
BM788970	TAF15 RNA polymerase II, TATA box binding protein (TBP)-associated factor, 68kDa	TAF15	transcription regulation	2	-2.2	-1.1	-1.5
CB104801	Thyroid hormone receptor interactor 11	TRIP11	transcription regulation	2	-2.1	-1.3	-1.5
BM788650	A kinase (PRKA) anchor protein (yotiao) 9	AKAP9	transport	2	-2.2	-1.1	-1.4
BM742353	Low density lipoprotein receptor-related protein associated protein 1	LRPAP1	transport	2	-2.2	-1.1	-1.4
BM782262	Polymeric immunoglobulin receptor	PIGR	transport	2	-2.4	-1.1	-1.5
NM_031954	Potassium channel tetramerisation domain containing 10	KCTD10	transport	2	-2.1	-1.3	-1.5
BM744354	Potassium voltage-gated channel, isk-related family, member 3	KCNE3	transport	2	-2.4	-1.3	-1.4
BM788500	Solute carrier family 30 (zinc transporter), member 4	SLC30A4	transport	2	-2.3	-1.3	-1.2
BM756300	Solute carrier family 31 (copper transporters), member 1	SLC31A1	transport	2	-2.3	-1.1	-1.4
NM_001859	Solute carrier family 31 (copper transporters), member 1	SLC31A1	transport	2	-2.7	-1.3	-1.4

Table 4.1.1 (Cont'd)

GenBank No	Name	Symbol	Function	Cluster	3h	6h	24h
BM787821	Solute carrier family 31 (copper transporters), member 1	SLC31A1	transport	2	-2.3	-1.3	-1.5
BM772075	Solute carrier family 7, (cationic amino acid transporter, y+ system) member 11	SLC7A11	transport	2	-2.1	-1.1	-1.3
BM751070	Synaptotagmin XIII	SYT13	transport	2	-2.2	-1.2	-1.3
BM755434	Transmembrane 9 superfamily member 1	TM9SF1	transport	2	-2.4	-1.2	-1.4
BM787401	Coiled-coil-helix-coiled-coil-helix domain containing 1	CHCHD1	unknown	1	1.6	1.3	3.0
BM764394	CTCL tumor antigen se57-1	SE57-1	unknown	1	1.5	1.6	2.9
BM767070	Peroxisomal membrane protein 2, 22kDa	PXMP2	unknown	1	1.5	1.2	2.0
AF037630	Ankyrin repeat and sterile alpha motif domain containing 1	ANKS1	unknown	2	-2.2	-1.2	-1.5
BM749164	Chromosome 6 open reading frame 210	C6orf210	unknown	2	-2.2	-1.2	-1.4
BM743387	Chromosome 6 open reading frame 69	C6orf69	unknown	2	-2.4	-1.1	-1.3
BQ082124	Copine VIII	CPNE8	unknown	2	-2.3	-1.4	-1.3
BM763955	Hypoxia-inducible protein 2	HIG2	unknown	2	-2.0	-1.1	-1.4
BM782016	Interphase cyctoplasmic foci protein 45	ICF45	unknown	2	-2.3	-1.1	-1.6
BM751923	Intersex-like (Drosophila)	IXL	unknown	2	-2.5	-1.2	-1.4
BM759265	CD82 antigen	KAI1	unknown	2	-2.1	-1.2	-1.4
AY251274	Junctophilin 3	JPH3	unknown	2	-2.2	-1.1	-1.2
BM788543	PDZ domain containing, X chromosome	FLJ21687	unknown	2	-2.4	-1.3	-1.4
BM746149	PQ loop repeat containing 2	PQLC2	unknown	2	-2.5	-1.4	-1.6
BM751773	Small EDRK-rich factor 2	SERF2	unknown	2	-2.4	-1.2	-1.5
BM747039	Small EDRK-rich factor 2	SERF2	unknown	2	-2.4	-1.1	-1.5
BM754369	Thioredoxin interacting protein	TXNIP	unknown	2	-2.2	-1.7	-1.4

Table 4.1.2 Validation of microarray data by real-time PCR

GenBank ID	Unigene ID	Gene symbol	Microarray			Real time PCR		
			3h	6h	24h	3h	6h	24h
BM789388	Hs.337766	TXNRD1	1.2	3.8	2.8	1.8 ± 0.2*	5.2 ± 0.8**	5.0 ± 1.2**
BM749654	Hs.523302	PRDX3	1.4	1.2	3.3	1.5 ± 0.4	1.7 ± 0.2*	2.7 ± 0.6*
BM750766	Hs.73090	NF-kB2	0.44	0.86	0.74	0.30 ± 0.10*	0.80 ± 0.30	0.70 ± 0.10
BM767282	Hs.27182	PLAA	0.48	0.88	0.70	0.42 ± 0.21*	0.72 ± 0.10	0.66 ± 0.20
BM742118	Hs.463059	STAT3	0.35	0.86	0.64	0.47 ± 0.11*	0.78 ± 0.00	0.62 ± 0.20

HaCaT cells (1 × 10^5) were cultivated in medium containing 10% FBS for 24 h. Following subsequent 24 h serum starvation, kaempferol was added and incubation continued for the time periods indicated. Control cultures were maintained in medium supplemented with a 1 : 10,000 dilution of vehicle (DMSO). Total RNA was isolated and the relative mRNA expression levels of different genes were measured by real-time RT-PCR analysis with SYBR green. Data are expressed as fold changes (means ± SD) (n = 3), normalized to b-actin mRNA expression. The values for the control group were set at 1.00. Analyses were performed in triplicate for each group. *P < 0.05 compared with the control group. **P < 0.01 compared with the control group.

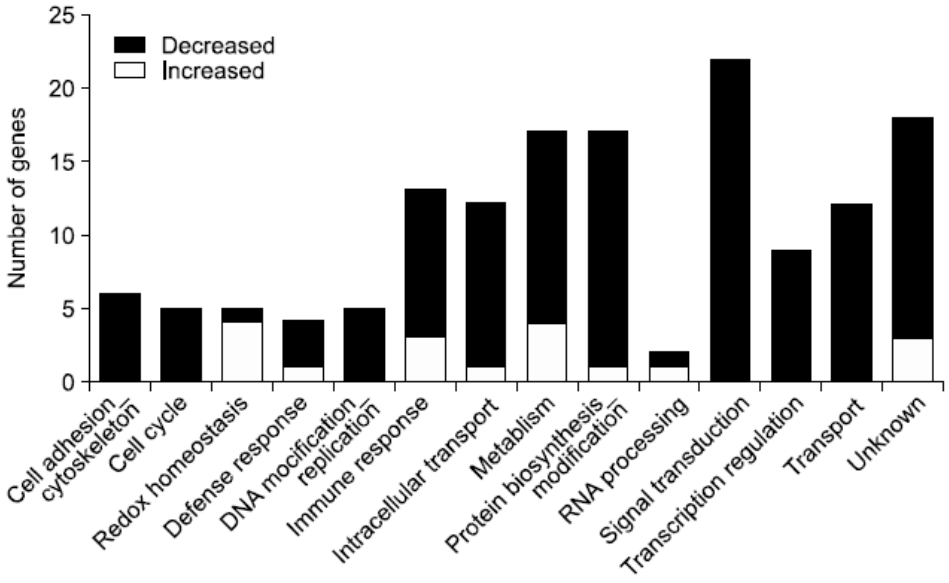

Figure 4.2.1 Global gene expression in functional categories.

Black and white bars represent the numbers of genes with decreased and increased expression, respectively, following kaempferol treatment.

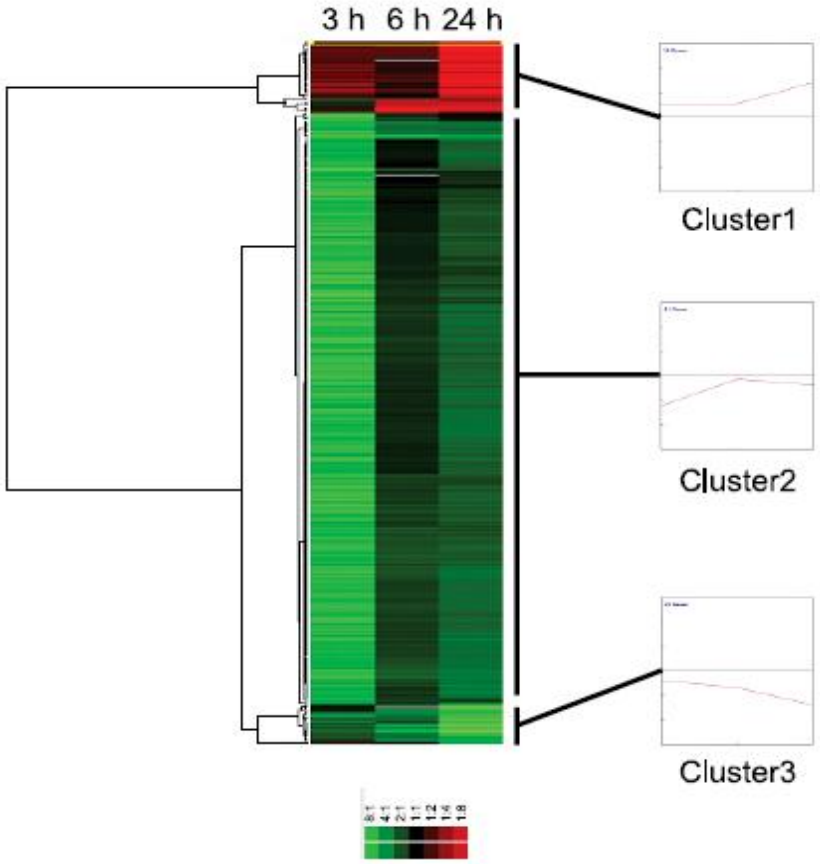

Figure 4.2.2 Hierarchical clustering of genes that were significantly up- or down-regulated by kaempferol treatment.

Differentially-expressed genes were clustered hierarchically based on similarities in their expression profiles. The expression pattern of each gene is displayed as a horizontal strip.

patterns, following a hierarchical clustering of similarity (**Figure 4.2.2**).

4.3 Promoter analysis of differentially-expressed genes

The nonredundant set of 147 differentially-expressed genes (based on GenBank accession number) was mapped computationally to 137 unique UniGene clusters. In order to identify biologically relevant transcription factor binding sites (referred to here as transcription regulatory elements or TREs), we performed promoter analyses on the regulatory regions of these genes (2,000 bp up- and downstream of the TSS) using oPOSSUM v1.3 [82]. The numbers of genes submitted to oPOSSUM, as well as the genes mapped to mouse orthologs and used for subsequent analyses, are presented in Table 2. It was used a Fisher *P* value cutoff of 0.05 to identify over-represented TREs. Over represented TREs for genes exhibiting altered expression following kaempferol treatment were as follows: increased expression, Ahr-ARNT; decreased expression, c-REL, SAP-1, Ahr-ARNT, Nrf-2, Elk-1, SPI-B, NF-κB and p65. The c-REL, p65 and NF-κB are all members of the NF-κB family of TFs, and these ranked first, seventh and eighth using Fisher *P* values (**Table 4.3.1**). The differentially expressed genes following kaempferol treatment with overrepresented Ahr-ARNT, p65, c-REL and NF-κB in their promoters are listed in **Table 4.3.2**.

Including this study, the beneficial effects of kaempferol have been demonstrated in cell-free systems and a variety of cell types [18, 20, 79, 86, 124]. However, its effects on gene expression in the skin have rarely been studied. Therefore, we used cDNA microarray analysis to examine its

effects on epidermal keratinocytes. It was assessed the levels of *ca*. 10,000 transcripts in kaempferol-treated HaCaT cells and observed marked alterations in the expression of 147 genes. These genes are involved in cytoskeleton, cell adhesion, redox homeostasis, immune and defense responses, metabolism, protein biosynthesis and modification, DNA modification and replication, regulation of transcription, signal transduction and transport in a wide range of biological systems, including human skin cells [125] (The Gene Ontology, http://www. geneontology.org). Following kaempferol treatment of HaCaT cells, it was observed a >2-fold upregulation of genes involved in redox homeostasis, such as an endoplasmic reticulum thioredoxin superfamily member (18 kDa), peroxiredoxin 3 and thioredoxin reductase 1. Tea-associated compounds are known to exhibit potent antioxidant activity and have been implicated in the alleviation of cancer-associated oxidative stresses [2, 9, 82]. In relation to such activities, flavonoids isolated from green tea leaves have been shown to regulate several genes differentially [1]. However, the regulatory effects of kaempferol on genes involved in cellular redox homeostasis in the skin have not yet been studied intensively. Our microarray data provide a starting point for unraveling the molecular mechanisms underlying the antioxidative action of kaempferol in skin cells.

It was observed decreased expression patterns in genes encoding proteins involved in inflammatory and immune responses, such as CD68 antigen, interferon (a, b, and w) receptor 1, nuclear factor of kappa light polypeptide gene enhancer in B-cells 2 (p49/p100), nuclear factor of kappa light polypeptide gene enhancer in B-cells inhibitor b, interferon-inducible protein (clone IFI-15K), interferon-induced protein with tetratricopeptide

repeats 3, Toll-like receptor adaptor molecule 1 and signal transducer and activator of transcription 3 (acute phase response factor). Several *in vitro* studies have investigated the inhibitory activity of flavonoids on NO and cytokine production in macrophage cell lines such as RAW264.7 [126-129] and J774.1 [130]. Kaempferol was shown to have an inhibitory effect on M-CSF-induced proliferation of macrophages obtained from bone marrow cultures [131]. In the primary macrophage cultures, it downregulated iNOS expression and inhibited LPS-induced TNFα secretion [131]. In osteoblasts, it downregulated TNFα-induced production of the osteoclastogenic cytokines IL-6 and monocyte chemoattractant protein-1 (MCP-1/CCL2) [132]. It has been suggested that the antioxidative/radical scavenging properties of flavonoids are related in part to their anti-inflammatory activities and specifically to inhibition of the NF-κB pathway [131]. These aspects should be considered in relation to the gene expression profiles revealed in our study. The regulatory regions of promoters from differentially-expressed genes have the potential to provide insight into coordinated regulation. Therefore, promoter analysis was performed using oPOSSUM v1.3 [58]. Two measures of statistical over-representation were used: a Z-score and a one-tailed Fisher exact probability. The Z-score compares the rate of occurrence of a TRE in the set of co-expressed genes to the expected rate estimated from the pre-computed background set [58]. Thus, Z-score indicates a significant difference in the rate of existence of sites, and is particularly useful for detecting increased prevalence of common sites. The Fisher exact test compares the proportion of co-expressed genes containing a particular TRE to the proportion of the non-target group that contains the site to determine the probability of a non-

random association between the target group and the TRE of interest [58].

A significant value for the Fisher exact probability indicates that there are a significant proportion of genes that contain the site, and is particularly good for rare TREs [58]. oPOSSUM analysis identified binding sites for transcription factors that play important roles in cell proliferation, differentiation and developmental processes. The Ahr-ARNT TRE was over-represented among both genes increased and decreased following kaempferol treatment. Several TFs have been shown to have transactivatory and suppressive properties simultaneously in the same type of cell under the same condition, depending on interacting partners and target genes. For example, a positive role for AP-1 in the estrogen-mediated induction of target genes is well established, but a role for AP-1 in gene repression is also elucidated in estrogen-treated cells. In that case, AP-1 interacts with estrogen receptor and corepressor NRIP1 [133]. Similarly, it might be possible that Ahr-ARNT TRE can have roles in the kaempferol-mediated induction and repression of target genes simultaneously. The c-REL, SAP-1, Nrf-2, Elk-1, SPI-B, NF-κB and p65 binding sites were over-represented in genes with decreased expression. The Fisher *P* values of TREs for members of the NF-κB family, such as c-REL, p65 and NF-κB, ranked highly. These bioinformatic analyses were consistent with the ELISA-based transcription factor assay, which indicated decreased NF-kB p65 and RelB activity in kaempferol-treated HaCaT cells and NHEKs. Therefore, the downregulation of genes in Clusters 2 and 3 may be attributed in part to reduced activity of members of the NF-κB-family. In addition, our observations are consistent with previous reports, which demonstrated that kaempferol blocked TNF-induced translocation of the NF-κB subunit p65

from the cytoplasm to the nucleus in mouse primary calvarial osteoblasts [132] and downregulate iNOS and TNF expression via NF-κB inactivation in aged rat gingival tissues [134]. Kim *et al*. showed the inhibitory effects of kaempferol against the aging process such as inflammation in gingival tissues and demonstrated the underlying molecular mechanisms. It was predicted the NF-κB family signal as one putative regulatory network from the epidermal genes regulated differentially by kaempferol using bioinformatic methods and confirmed the prediction with the ELISA-based transcription factor assay. Our result was consistent with Kim *et al*.'s result. Contrary to their hypothesis-driven approach, however, our unbiased approach gave comprehensive information about wide ranges of effects of kaempferol. Besides NF-κB family members, many transcription factors have to be validated. Kaempferol was shown to bind to the PPAR in a competition binding assay using Gst-PPAR LBD fusion protein and kaempferol-induced stimulation of PPAR transactivation activity was detected in transient transfection experiments employing the mouse macrophage cell line RAW264.7 [135]. In addition, PPAR activators have been reported to antagonize the NF-κB signaling pathway directly [90, 136]. Therefore, among the mechanisms that can account for decreased NF-κB activity, it was examined the activation of PPARs. Kaempferol stimulated PPAR transcriptional activity in HaCaT cells transiently transfected with the PPRE-*tk*-Luc reporter gene, suggesting that, at least in part, its mode of action may be mediated by PPAR pathways.

4.4 Proof-of-Concept: Target study of kaempferol

4.4.1 Effect of kaempferol on NF-κB activity

To verify the bioinformatic analyses, we used an ELISA-based transcription factor assay to examine the effect of 10 mM kaempferol on activation of NF-κB p65 and RelB in HaCaT cells and NHEKs irradiated with UVB (**Figure 4.4.1**). Although kaempferol treatment significantly inhibited activation of NF-kκ p65 elicited by UVB irradiation, it had no effect on basal activity in HaCaT cells (**Figure 4.4.1A**). In contrast to NF-κB p65, RelB was not activated by UVB irradiation in HaCaT cells and kaempferol treatment decreased RelB basal activity, as well as RelB activity in UVB-irradiated HaCaT cells (**Figure 4.4.1B**). Although UVB-induced NF-κB activation was shown in both HaCaT cells and NHEKs, HaCaT cells were found to contain a constitutive aberrant NF-κB activity that is not found in NHEKs [137]. Therefore, we examine the effect of kaempferol on activation of NF-kB in NHEKs. Similar to HaCaT cells, kaempferol treatment significantly inhibited activation of NF-κB p65 elicited by UVB irradiation in NHEKs (**Figure 4.4.1C**).

Table 4.3.1 Over-represented TREs in the promoters of differentially expressed genes following treatment with Kaempferol.

Cluster	Expression pattern	TRE	Z-score	Fisher *P* value
1	Genes increased (17 input; 5 analyzed)	Ahr-ARNT	4.055	4.124e-02
2	Genes decreased at 3 h (109 input; 67 analyzed)	c-REL	9.693	3.645e-04
		SAP1	5.692	1.170e-02
		Ahr-ARNT	1.272	1.260e-02
		Nrf-2	8.874	1.290e-02
		Elk-1	4.575	1.484e-02
		SPI-B	8.455	2.275e-02
		NF-κB	1.5	4.556e-02
		p65	5.987	5.099e-02
3	Genes decreased at 6 and/or 24 h (11 input; 5 analyzed)	NF-κB	5.957	2.522e-02

Table 4.3.2 Genes increased or decreased following kaempferol treatment

Overrepresented Ahr-ARNT, p65, c-REL and NF-κB in their promoters.

Cluster	Symbol	UGCluster	Name	TF
Cluster 1	*RIPK2*	Hs.103755	Receptor-interacting serine-threonine kinase 2	Ahr-ARNT
	PRDX3	Hs.523302	Peroxiredoxin 3	Ahr-ARNT
	AP1M1	Hs.71040	Adaptor-related protein complex 1, mu 1 subunit	Ahr-ARNT
	CLU	Hs.436657	Clusterin (complement lysis inhibitor, SP-40, 40, sulfated glycoprotein 2, testosterone-repressed prostate message 2, apolipoprotein J)	Ahr-ARNT
	FOSL1	Hs.283565	FOS-like antigen 1	Ahr-ARNT
Cluster 2	actn1	Hs.509765	Actinin, alpha 1	p65/c-REL/NF-κB
	aarsl	Hs.158381	Alanyl-tRNA synthetase-like	p65/c-REL/NF-κB
	anks1	Hs.132639	Ankyrin repeat and sterile alpha motif domain containing 1	c-REL/NF-κB
	cask	Hs.495984	Calcium/calmodulin-dependent serine protein kinase (MAGUK family)	p65/c-REL/NF-κB
	kai1	Hs.527778	CD82 antigen	p65/c-REL/NF-κB
	cdc2l5	Hs.233552	Cell division cycle 2-like 5 (cholinesterase-related cell division controller)	c-REL
	c6orf210	Hs.486095	Chromosome 6 open reading frame 210	c-REL/NF-κB
	c6orf69	Hs.188757	Chromosome 6 open reading frame 69	c-REL
	cpne8	Hs.40910	Copine VIII	NF-κB
	dtx2	Hs.187058	Deltex homolog 2 (*Drosophila*)	p65/c-REL/NF-κB
	git2	Hs.434996	G protein-coupled receptor kinase interactor 2	c-REL
	gp5	Hs.73734	Glycoprotein V (platelet)	p65/c-REL/NF-κB
	jph3	Hs.123450	Junctophilin 3	c-REL/NF-κB
	luc7L	Hs.16803	LUC7-like (*S. cerevisiae*)	c-REL
	myh9	Hs.474751	Myosin, heavy polypeptide 9, non-muscle	p65/c-REL/NF-κB
	nf2	Hs.187898	Neurofibromin 2 (bilateral acoustic neuroma)	p65/c-REL
	nfkb2	Hs.73090	Nuclear factor of kappa light polypeptide gene enhancer in B-cells 2 (p49/p100)	p65/c-REL/NF-κB
	nfkbib	Hs.9731	Nuclear factor of kappa light polypeptide gene enhancer in B-cells inhibitor, beta	p65/c-REL/NF-κB
	nxn	Hs.527989	Nucleoredoxin	p65/c-REL/NF-κB
	ppid	Hs.183958	Peptidylprolyl isomerase D (cyclophilin D)	p65/c-REL/NF-κB
	plaa	Hs.27182	Phospholipase A2-activating protein	c-REL
	pigr	Hs.497589	Polymeric immunoglobulin receptor	p65/c-REL/NF-κB
	kctd10	Hs.524731	Potassium channel tetramerisation domain-containing 10	p65/c-REL/NF-κB
	pqlc2	Hs.523036	PQ loop repeat-containing 2	p65/c-REL/NF-κB
	prkag2	Hs.549162	Protein kinase, AMP-activated, gamma 2 non-catalytic subunit	p65/c-REL/NF-κB
	rab1b	Hs.300816	RAB1B, member RAS oncogene family	p65/c-REL/NF-κB
	rab21	Hs.524590	RAB21, member RAS oncogene family	p65/c-REL/NF-κB
	rasgef1b	Hs.480068	RasGEF domain family, member 1B	c-REL
	rock2	Hs.58617	Rho-associated, coiled-coil-containing protein kinase 2	c-REL
	sec14l2	Hs.335614	SEC14-like 2 (*S. cerevisiae*)	p65/c-REL/NF-κB
	stat3	Hs.463059	Signal transducer and activator of transcription 3 (acute-phase response factor)	p66/c-REL/NF-κB
	slc30a4	Hs.162989	Solute carrier family 30 (zinc transporter), member 4	p65/c-REL/NF-κB
	slc31a1	Hs.532315	Solute carrier family 31 (copper transporters), member 1	NF-κB
	skp2	Hs.23348	S-phase kinase-associated protein 2 (p45)	c-REL
	stom	Hs.253903	Stomatin	p65/c-REL
	stip1	Hs.337295	Stress-induced-phosphoprotein 1 (Hsp70/Hsp90-organizing protein)	p65/c-REL/NF-κB
	smarce1	Hs.463010	SWI/SNF-related, matrix-associated, actin-dependent regulator of chromatin, subfamily e, member 1	p65/c-REL/NF-κB
	sdc1	Hs.224607	Syndecan 1	p65/c-REL/NF-κB
	tcf7	Hs.519580	Transcription factor 7 (T-cell specific, HMG-box)	p66/c-REL/NF-κB
	Tm9sf1	Hs.91586	Transmembrane 9 superfamily member 1	c-REL
	psmd14	Hs.369125	Proteasome (prosome, macropain) 26S subunit, non-ATPase, 14	p65/c-REL
	pik4cb	Hs.527624	Phosphatidylinositol 4-kinase, catalytic, beta polypeptide	c-REL/NF-κB
Cluster 3	usp9x	Hs.77578	Ubiquitin specific protease 9, X-linked (fat facets-like, *Drosophila*)	Nf-κB
	acly	Hs.387567	ATP citrate lyase	Nf-κB
	hspb1	Hs.520973	Heat shock 27 kDa protein 1	Nf-κB
	sdc4	Hs.252189	Syndecan 4 (amphiglycan, ryudocan)	Nf-κB

However, RelB showed a different response following UVB irradiation in NHEKs. RelB was activated by UVB irradiation and UVB-induced RelB activation was inhibited by kaempferol treatment in NHEKs (**Figure 4.4.1D**).

4.4.2 Effect of kaempferol on the transcriptional activity of PPARs

PPAR activation is one of several mechanisms that could account for decreased NF-κB activities. As PPAR activators have been reported to antagonize the NF-κB signaling pathway directly [124, 136], we tested whether or not kaempferol could activate the transcriptional activity of PPARs in HaCaT cells. It was performed transient transfection experiments using the PPRE-*tk*-Luc reporter gene [85]. When PPRE-*tk*-Luc was co-transfected with the PPARα, PPARβ/δ and PPARγ expression vectors, treatment with 10 mM kaempferol increased reporter activity by a factor of approximately 2.0, 2.6 and 3.0, respectively (**Figure 4.4.2**).

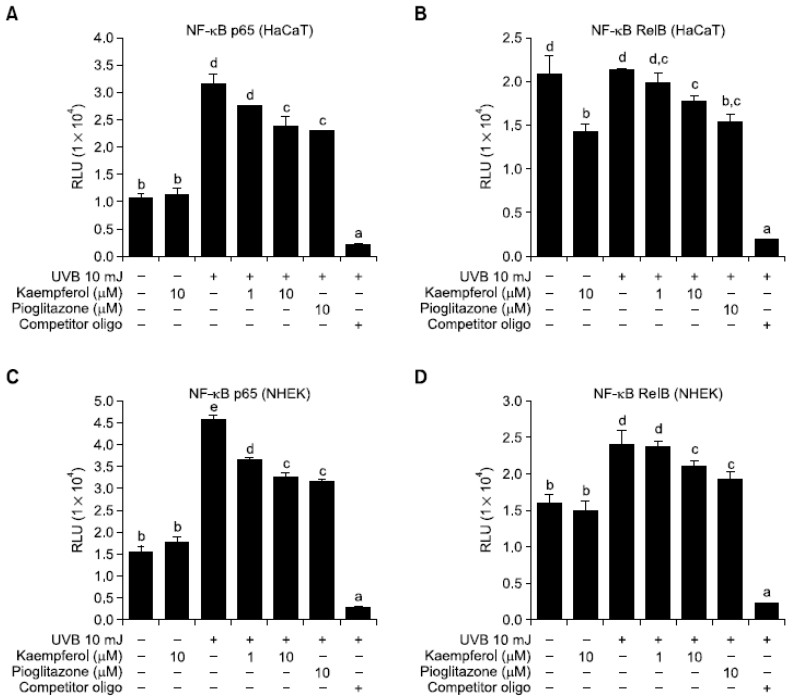

Figure 4.4.1 Effects of kaempferol on NF-κB activity in HaCaT cells and NHEKs.

Nuclear extracts of HaCaT cells were prepared and the presence of translocated p65 (A) or RelB subunit (B) was assessed using ELISA. Values represent means ± SD of 3 or 4 independent experiments. $P < 0.05$.

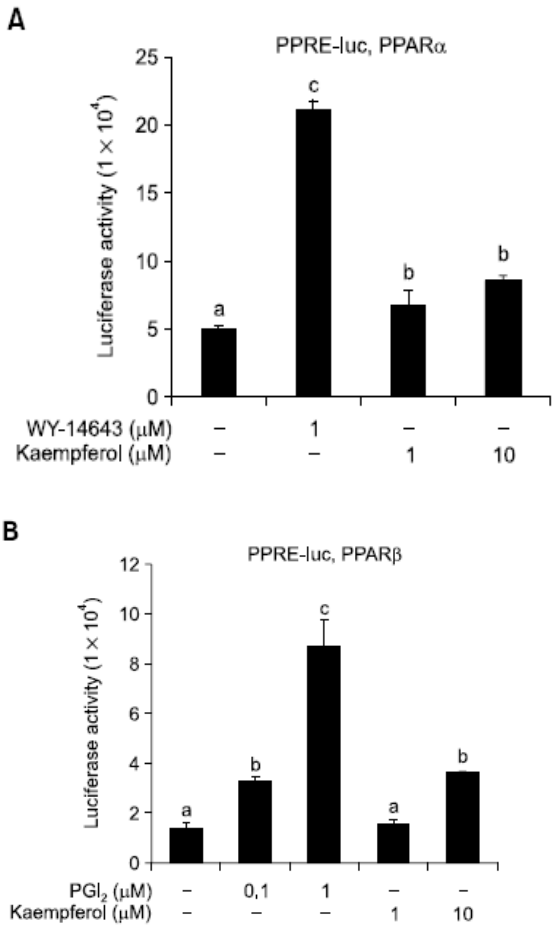

Figure 4.4.2 Effect of kaempferol on transcriptional activity of PPARs. Cells were assayed for luciferase activity, which was normalized to the corresponding β-gal activity. Data represent the mean ± SD of 3 or 4 independent experiments. $P < 0.05$.

4.4.3 BrdU incorporation inhibition

To investigate whether kamepferol promotes the differentiation of keratinocytes or not, BrdU incorporation experiment was performed. High calcium and vitamin D3, or protein kinase C (PKC) activator could induce keratinocyte differentiation from cell proliferation state.

To promote keratinocyte differentiation, kaempfrol on vehicle DMSO treated group relative to the proliferation inhibitory effect was calculated by the following equation by measuring the amount of HaCaT and NHEK that BrdU incorporated into DNA during cell division, thereby examined the extent.

$$\%\ \text{inhibition of proliferation relative to control} = 100 \times (\text{vehicle group} - \text{sample group}) / \text{vehicle group}$$

Calcium chloride induced cellular differentiation rather than proliferation, and thus BrdU incorportation was inhibited. As shown in **Figure 4.4.3**, kaempferol inhibited cell proliferation in HaCaT and normal human endothelical keratinocytes. WY-14643, a PPAR-α ligand and troglitazone, a PPAR-γ ligand were used as a positive control. Genistein is a well-known isoflavone that could be considered as a PPAR activator.

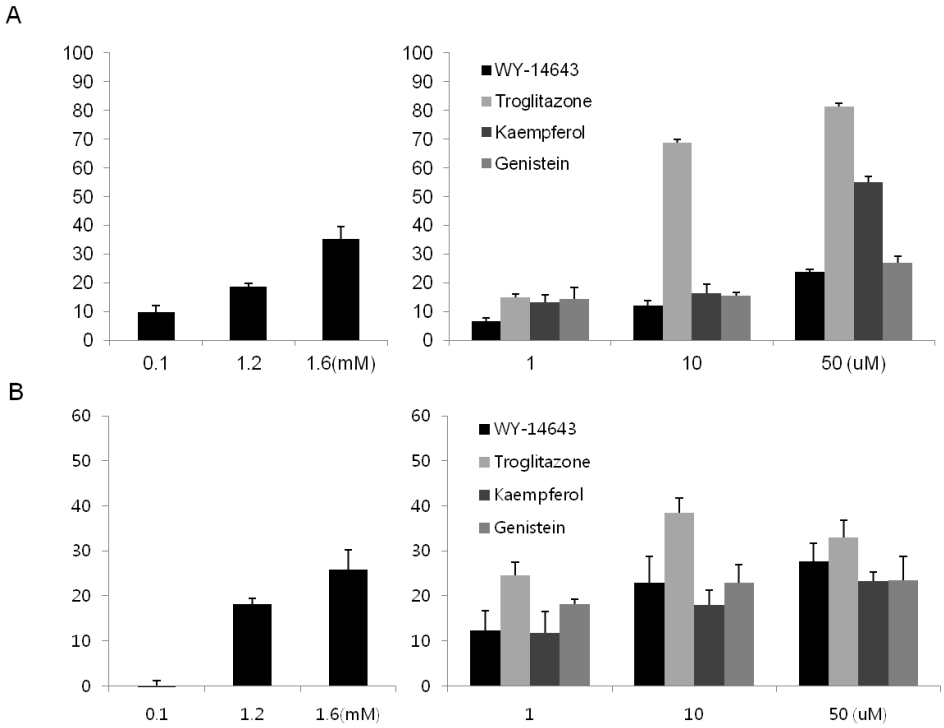

Figure 4.4.3 Inhibitory effect of kaempferol on BrdU incorporation

In BrdU incorporation assay, values are expressed as the percentage of cell proliferation relative to the control. Calcium treatment induced cellular differentiation (Left panel). (A) HaCaT cells, (B) Normal human endothelial keratinocytes.

4.4.4 TGM-1 protein expression

To examine if the kamepferol could promote the differentiation of keratinocytes, transglutaminase-1 (TGase-1) expression was observed at the protein level by Western blot. Cornified envelope formation and involucrin and TGase-1 protein and mRNA levels are increased by the activation of PPARα [138]. Keratinocyte specific TGase-1 catalyzes the cross-linking reaction between keratins and other structural proteins to form the chemically resistant cornified envelope structures of corneocytes [139]. As a result, kaempferol increased the expression of TGase-1 from 1μM. Facilitate the efficacy of a similar degree of increase in the 10um, 50μM showed concentration dependence was not observed. However, 1/10/50μM of genistein, another flavonol from GTSE increased TGase-1 in a concentration-dependent manner (**Figure 4.4.4**).

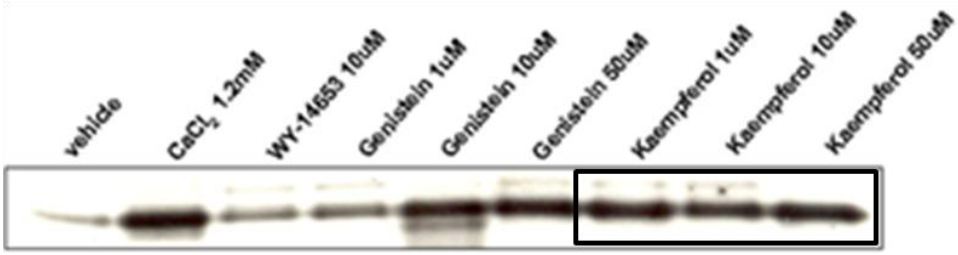

Figure 4.4.4 Effect of kaempferol on TGase-1 expression

Tranglutaminase-1 protein regulation by Western blotting analysis was performed after 72h treatment with WY-14643, Genistein, and kaempferol at the indicated doses. Vehicle is DMSO treated cells.

The epidermis is a self-renewing stratified epithelium populated primarily by keratinocytes that undergo a complex and dynamic program of terminal differentiation throughout life [140]. This process begins when proliferating keratinocytes of the basal layers stop dividing and begin migrating successively through the spinous, granular, and cornified cell layers [141]. The ability of keratinocytes to differentiate is regulated by a number of biological signals derived from cell–cell or cell–matrix interactions that act downstream of various signaling pathways [142]. The pathways that are particularly important for regulating keratinocyutes growth and differentiation include p63, IKKa, NF-κB, Notch, C/EBPb, KLF4, and EGFR-TK [143]. There was a previous report that 3,4 '-dihydroxy flavone (3,4'-DHF) induced cell proliferation, but other isoflavones such as genistein, isohamnetin, kaempferol inhibited cell growth in keratinocytes [144]. Based on these finding, it was examined that kaempferol could inhibit keratinocyte proliferation (BrdU incorporation) and induce differentiation (TGase-1 expression). Kaempferol treatment suppressed BrdU incorporation as a concentration-dependent manner in HaCaT and normal human keratinocytes. As the cells differentiate in culture, there is a successive increase in involucrin, transglutaminase, and cornified envelope formation [145]. Collectively, it could be able to contribute to the maintenance of epidermal homeostasis through promoting epidermal differentiation by kaempferol treatment on keratinocytes.

In summary, it was investigated kaempferol-induced alterations in the transcriptional profiles of immortalized human keratinocytes and analyzed the promoters of differentially regulated genes using bioinformatics. In this

study, it was identified altered gene expression profiles in response to kaempferol, and this information will be useful for establishing its regulatory network (**Figure 4.4.5**), as well as determining gene-nutrient interactions. Further studies of promoter occupancy and transcription factor perturbation are now required to provide a functional validation of the TREs identified in this study, as well as the TFs that bind to them.

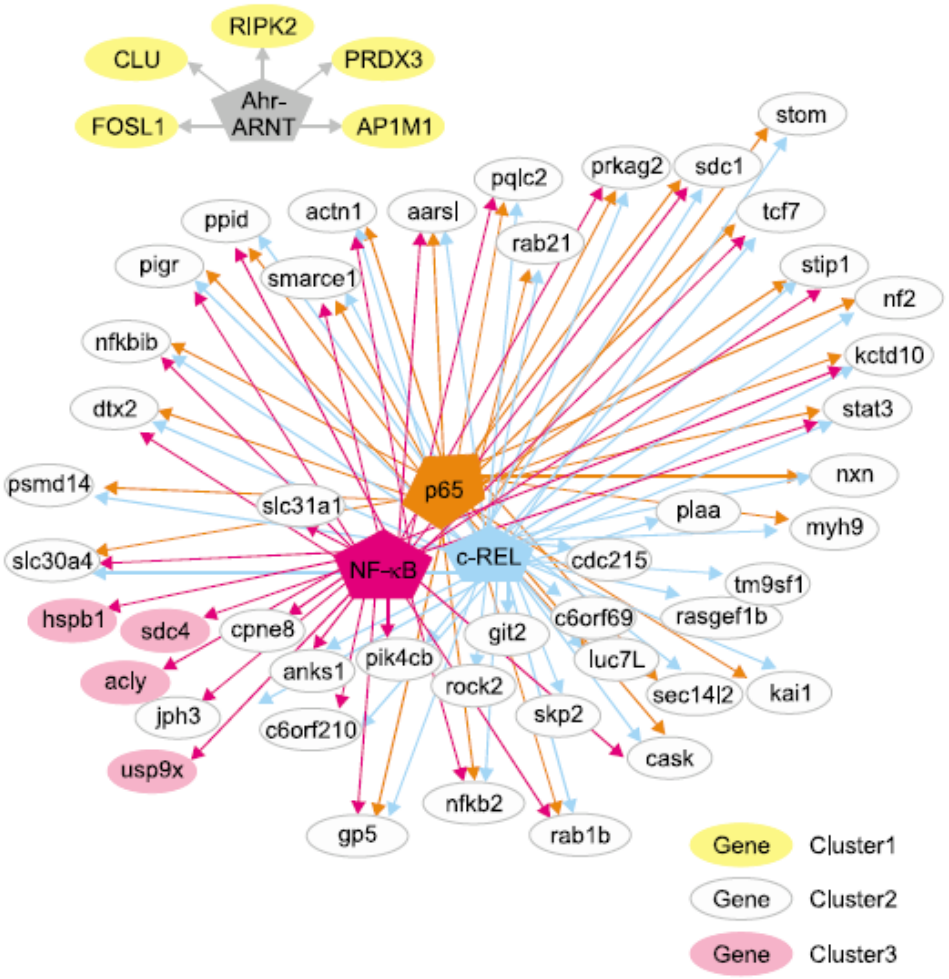

Figure 4.4.5 A network that is related to kaempferol treatment

This figure shows relations between the over-represented TREs (P value < 0.05) and differentially-expressed genes following treatment with kaempferol. The pentagonal boxes represent the TREs and ellipses represent the genes.

CHAPTER 5.

Conclusions

5.1 Conclusions

Kamepferol was prepared by enzymatic hydrolysis of two kaempferol glycosides, kaempferol-3-O-[2-O-β-D-galactopyranosyl-6-O-α-L-rhamnopyranosyl]-β-D-glucopyranoside (compound 1) and kaempferol-3-O-[2-O-β-D-xylopyranosyl-6-O-α-L-rhamnopyranosyl]-β-D-glucopyranoside (compound 2), obtained from extraction of green tea seeds. In order to get higher purity of kaempferol, the combination of two O-glycolytic enzymes, β-galactosidase and hesperidinase was selected. As a result, over 95% pure kaempferol was produced under the optimized condition.

In terms of antioxidant effect on skin aging, kaempferol aglycone showed a more efficient scavenger of DPPH radicals and a better inhibitor of xanthin/xanthine oxidase inhibition than the compound 1 and compound 2. The inhibitory effect of kaempferol on cellular lipid peroxidation induced by t-butyl hydroperoxide in keratinocytes was exhibited. Kaempferol treatment had a effect on significant inhibition ultraviolet-induced matrix metalloproteinase-1 (MMP-1) in mono-culture of normal human fibroblasts or keratinocytes/fibroblasts co-cultured system. Even though kaempferol did not change the level of type I pro-collagen synthesis in human fibroblasts, there was similar results in the case of retinol, well-known as increase of collagen synthesis in human dermis. Kaempferol inhibited TNF-α, which is well-known as an inducer of skin-aging affecting stimulation of MMP-1 fibroblasts production, in keratinocytes/fibroblasts co-culture system. Kaempferol showed to decrease wrinkles induced by sqaulene-

hydroperoxide in hairless mice. In the case of human clinical study, topical application of the emulsion containing kaempferol for 8 weeks decreased wrinkles in photo-aged skin such as crow's feet area.

To study the effects of kaempferol in the skin in detail, the transcriptional profiles of kaempferol-treated HaCaT cells were tested using cDNA microarray analysis. There were significant changes in the expression of 147 genes. 18 genes were up-regulated and 129 genes were down-regulated among them. Based on their function, those genes were classified into 12 categories: cell adhesion/cytoskeleton, cell cycle, redox homeostasis, immune/defense responses, metabolism, protein biosynthesis/modification, intracellular transport, RNA processing, DNA modification/replication, regulation of transcription, signal transduction and transport. After analyzing the promoter sequences of the differentially-regulated genes, c-REL, SAP-1, Ahr-ARNT, Nrf-2, Elk-1, SPI-B, NF-κB and p65 were identified as over-represented regulatory sites and candidate transcriptional factors (TFs) for gene regulation by kaempferol. To validate these microarray results and bioinformatic analysis, conventional method such as real-time PCR and ELISA-based transcriptional factor assay were examined. Kaempferol showed significant effect on NF-κB and RelB in HaCaT cells and normal human epidermal keratinocytes (NHEKs) irradiated with UVB by ELISA-based transcription factor assay. Since peroxisome proliferator-activated receptor (PPAR) activation can affect the decrease of NF-κB activity, the effect of kaempferol to increase the transcriptional activity of PPARs in HaCaT cells was studied. This experiment indicated that kaempferol stimulated PPAR transcriptional activity in HaCaT cells transiently transfected with the PPAR-*tk*-Luc

reporter gene. It suggested that kaempferol could act as a regulator of epidermal differentiation in human skin. To investigate whether or not kaempferol can promote the differentiation of keratinocytes, BrdU incorporation experiment and a Western blot analysis against transglutamase-1 protein were performed. As a result, kaempferol treatment had an effect on the inhibition of BrdU incorporation and the induction of transglutamse-1 protein in keratinocytes, which meant that kaempferol could be an inducer of the differentiation of epidermal keratinocytes.

In conclusion, kaempferol is demonstrated as a potentially effective anti-aging substance that can be used as an anti-aging ingredient in cosmeceutical products.

References

1. Formica, J.V. and W. Regelson, *Review of the biology of Quercetin and related bioflavonoids.* Food Chem Toxicol, 1995. **33**(12): p. 1061-80.
2. Dominguez, X.A., et al., *Kukulkanins A and B, new chalcones from Mimosa tenuefolia.* J Nat Prod, 1989. **52**(4): p. 864-7.
3. Anton, R., et al., *Pharmacognosy of Mimosa tenuiflora (Willd.) Poiret.* J Ethnopharmacol, 1993. **38**(2-3): p. 153-7.
4. Choi, J.S. and X. Li, *Enhanced diltiazem bioavailability after oral administration of diltiazem with quercetin to rabbits.* Int J Pharm, 2005. **297**(1-2): p. 1-8.
5. Rice-Evans, C., *Flavonoid antioxidants.* Curr Med Chem, 2001. **8**(7): p. 797-807.
6. Kesarwani, K., R. Gupta, and A. Mukerjee, *Bioavailability enhancers of herbal origin: An overview.* Asian Pac J Trop Biomed, 2013. **3**(4): p. 253-66.
7. Puizina-Ivic, N., *Skin aging.* Acta Dermatovenerol Alp Panonica Adriat, 2008. **17**(2): p. 47-54.
8. Park, S., et al., *Retinol binding protein-albumin domain III fusion protein deactivates hepatic stellate cells.* Mol Cells, 2012. **34**(6): p. 517-22.
9. Ahmad, N. and H. Mukhtar, *Green tea polyphenols and cancer: biologic mechanisms and practical implications.* Nutr Rev, 1999. **57**(3): p. 78-83.
10. Ahmad, N. and H. Mukhtar, *Cutaneous photochemoprotection by*

green tea: a brief review. Skin Pharmacol Appl Skin Physiol, 2001. **14**(2): p. 69-76.

11. Park, A.M. and Z. Dong, *Signal transduction pathways: targets for green and black tea polyphenols.* J Biochem Mol Biol, 2003. **36**(1): p. 66-77.
12. Hsu, S., *Green tea and the skin.* J Am Acad Dermatol, 2005. **52**(6): p. 1049-59.
13. Sekine, T., et al., *Two flavonol glycosides from seeds of Camellia sinensis.* Phytochemistry, 1991. **30**(3): p. 991-5.
14. de Vries, J.H., et al., *Consumption of quercetin and kaempferol in free-living subjects eating a variety of diets.* Cancer Lett, 1997. **114**(1-2): p. 141-4.
15. Murota, K., et al., *Unique uptake and transport of isoflavone aglycones by human intestinal caco-2 cells: comparison of isoflavonoids and flavonoids.* J Nutr, 2002. **132**(7): p. 1956-61.
16. Selloum, L., et al., *Effects of flavonols on the generation of superoxide anion radicals by xanthine oxidase and stimulated neutrophils.* Arch Biochem Biophys, 2001. **395**(1): p. 49-56.
17. Wang, I.K., S.Y. Lin-Shiau, and J.K. Lin, *Induction of apoptosis by apigenin and related flavonoids through cytochrome c release and activation of caspase-9 and caspase-3 in leukaemia HL-60 cells.* Eur J Cancer, 1999. **35**(10): p. 1517-25.
18. Samhan-Arias, A.K., F.J. Martin-Romero, and C. Gutierrez-Merino, *Kaempferol blocks oxidative stress in cerebellar granule cells and reveals a key role for reactive oxygen species production at the plasma membrane in the commitment to apoptosis.* Free Radic Biol

Med, 2004. **37**(1): p. 48-61.

19. Dobrzynska, M.M., A. Baumgartner, and D. Anderson, *Antioxidants modulate thyroid hormone- and noradrenaline-induced DNA damage in human sperm.* Mutagenesis, 2004. **19**(4): p. 325-30.
20. Noroozi, M., W.J. Angerson, and M.E. Lean, *Effects of flavonoids and vitamin C on oxidative DNA damage to human lymphocytes.* Am J Clin Nutr, 1998. **67**(6): p. 1210-8.
21. Brandner, J.M., et al., *Organization and formation of the tight junction system in human epidermis and cultured keratinocytes.* Eur J Cell Biol, 2002. **81**(5): p. 253-63.
22. Berge, U., P. Kristensen, and S.I. Rattan, *Hormetic modulation of differentiation of normal human epidermal keratinocytes undergoing replicative senescence in vitro.* Exp Gerontol, 2008. **43**(7): p. 658-62.
23. Wenk, J., et al., *UV-induced oxidative stress and photoaging.* Curr Probl Dermatol, 2001. **29**: p. 83-94.
24. Fisher, G.J., *The pathophysiology of photoaging of the skin.* Cutis, 2005. **75**(2 Suppl): p. 5-8; discussion 8-9.
25. Verdier-Sevrain, S., F. Bonte, and B. Gilchrest, *Biology of estrogens in skin: implications for skin aging.* Exp Dermatol, 2006. **15**(2): p. 83-94.
26. Shin, M.H., et al., *Modulation of collagen metabolism by the topical application of dehydroepiandrosterone to human skin.* J Invest Dermatol, 2005. **124**(2): p. 315-23.
27. Hall, G. and T.J. Phillips, *Estrogen and skin: the effects of estrogen, menopause, and hormone replacement therapy on the skin.* J Am

Acad Dermatol, 2005. **53**(4): p. 555-68; quiz 569-72.

28. Ghersetich, I., et al., *Hyaluronic acid in cutaneous intrinsic aging.* Int J Dermatol, 1994. **33**(2): p. 119-22.
29. Meyer, L.J. and R. Stern, *Age-dependent changes of hyaluronan in human skin.* J Invest Dermatol, 1994. **102**(3): p. 385-9.
30. Fligiel, S.E., et al., *Collagen degradation in aged/photodamaged skin in vivo and after exposure to matrix metalloproteinase-1 in vitro.* J Invest Dermatol, 2003. **120**(5): p. 842-8.
31. Calleja-Agius, J., Y. Muscat-Baron, and M.P. Brincat, *Skin ageing.* Menopause Int, 2007. **13**(2): p. 60-4.
32. Uitto, J., *Connective tissue biochemistry of the aging dermis. Age-related alterations in collagen and elastin.* Dermatol Clin, 1986. **4**(3): p. 433-46.
33. Baumann, L., *Skin ageing and its treatment.* J Pathol, 2007. **211**(2): p. 241-51.
34. Leyden, J.J., *Clinical features of ageing skin.* Br J Dermatol, 1990. **122 Suppl 35**: p. 1-3.
35. Uitto, J., *The role of elastin and collagen in cutaneous aging: intrinsic aging versus photoexposure.* J Drugs Dermatol, 2008. **7**(2 Suppl): p. s12-6.
36. Strom, S.S. and Y. Yamamura, *Epidemiology of nonmelanoma skin cancer.* Clin Plast Surg, 1997. **24**(4): p. 627-36.
37. Guinot, C., et al., *Reference ranges of skin micro-relief according to age in French Caucasian and Japanese women.* Skin Res Technol, 2006. **12**(4): p. 268-78.
38. Zou, Y., E. Song, and R. Jin, *Age-dependent changes in skin surface*

assessed by a novel two-dimensional image analysis. Skin Res Technol, 2009. **15**(4): p. 399-406.

39. Lee, H.K., et al., *Comparison between ultrasonography (Dermascan C version 3) and transparency profilometry (Skin Visiometer SV600).* Skin Res Technol, 2008. **14**(1): p. 8-12.
40. Giacomoni, P.U. and G. Rein, *A mechanistic model for the aging of human skin.* Micron, 2004. **35**(3): p. 179-84.
41. Waller, J.M. and H.I. Maibach, *Age and skin structure and function, a quantitative approach (II): protein, glycosaminoglycan, water, and lipid content and structure.* Skin Res Technol, 2006. **12**(3): p. 145-54.
42. Tzaphlidou, M., *The role of collagen and elastin in aged skin: an image processing approach.* Micron, 2004. **35**(3): p. 173-7.
43. Tsukahara, K., et al., *Effect of room humidity on the formation of fine wrinkles in the facial skin of Japanese.* Skin Res Technol, 2007. **13**(2): p. 184-8.
44. Goihman-Yahr, M., *Skin aging and photoaging: an outlook.* Clin Dermatol, 1996. **14**(2): p. 153-60.
45. Yin, L., A. Morita, and T. Tsuji, *Skin premature aging induced by tobacco smoking: the objective evidence of skin replica analysis.* J Dermatol Sci, 2001. **27 Suppl 1**: p. S26-31.
46. Darlenski, R., et al., *Non-invasive in vivo methods for investigation of the skin barrier physical properties.* Eur J Pharm Biopharm, 2009. **72**(2): p. 295-303.
47. Loden, M., I. Buraczewska, and K. Halvarsson, *Facial anti-wrinkle cream: influence of product presentation on effectiveness: a*

randomized and controlled study. Skin Res Technol, 2007. **13**(2): p. 189-94.

48. Callaghan, T.M. and K.P. Wilhelm, *A review of ageing and an examination of clinical methods in the assessment of ageing skin. Part I: Cellular and molecular perspectives of skin ageing.* Int J Cosmet Sci, 2008. **30**(5): p. 313-22.
49. Cravello, B. and A. Ferri, *Relationships between skin properties and environmental parameters.* Skin Res Technol, 2008. **14**(2): p. 180-6.
50. Makki, S., J.C. Barbenel, and P. Agache, *A quantitative method for the assessment of the microtopography of human skin.* Acta Derm Venereol, 1979. **59**(4): p. 285-91.
51. Gordon, K.D., *Pitting and bubbling artefacts in surface replicas made with silicone elastomers.* J Microsc, 1984. **134**(Pt 2): p. 183-8.
52. Iyer, V.R., et al., *The transcriptional program in the response of human fibroblasts to serum.* Science, 1999. **283**(5398): p. 83-7.
53. Brown, P.O. and D. Botstein, *Exploring the new world of the genome with DNA microarrays.* Nat Genet, 1999. **21**(1 Suppl): p. 33-7.
54. Alizadeh, A.A., et al., *Distinct types of diffuse large B-cell lymphoma identified by gene expression profiling.* Nature, 2000. **403**(6769): p. 503-11.
55. Li, D., et al., *Rays and arrays: the transcriptional program in the response of human epidermal keratinocytes to UVB illumination.* FASEB J, 2001. **15**(13): p. 2533-5.
56. Sesto, A., et al., *Analysis of the ultraviolet B response in primary human keratinocytes using oligonucleotide microarrays.* Proc Natl

Acad Sci U S A, 2002. **99**(5): p. 2965-70.

57. Curto, E.V., et al., *Biomarkers of human skin cells identified using DermArray DNA arrays and new bioinformatics methods.* Biochem Biophys Res Commun, 2002. **291**(4): p. 1052-64.
58. Gazel, A., et al., *Transcriptional profiling of epidermal keratinocytes: comparison of genes expressed in skin, cultured keratinocytes, and reconstituted epidermis, using large DNA microarrays.* J Invest Dermatol, 2003. **121**(6): p. 1459-68.
59. Bonnet-Duquennoy, M., et al., *Study of housekeeping gene expression in human keratinocytes using OLISA, a long-oligonucleotide microarray and q RT-PCR.* Eur J Dermatol, 2006. **16**(2): p. 136-40.
60. Kunz, M., et al., *DNA microarray technology and its applications in dermatology.* Exp Dermatol, 2004. **13**(10): p. 593-606.
61. Sellheyer, K. and T.J. Belbin, *DNA microarrays: from structural genomics to functional genomics. The applications of gene chips in dermatology and dermatopathology.* J Am Acad Dermatol, 2004. **51**(5): p. 681-92; quiz 693-6.
62. Blumenberg, M., *Skinomics.* J Invest Dermatol, 2005. **124**(4): p. viii-x.
63. Blumenberg, M., *DNA microarrays in dermatology and skin biology.* OMICS, 2006. **10**(3): p. 243-60.
64. Lu, J., et al., *Transcriptional profiling of keratinocytes reveals a vitamin D-regulated epidermal differentiation network.* J Invest Dermatol, 2005. **124**(4): p. 778-85.
65. Seo, E.Y., et al., *Analysis of calcium-inducible genes in*

keratinocytes using suppression subtractive hybridization and cDNA microarray. Genomics, 2005. **86**(5): p. 528-38.

66. Baron, J.M., et al., *Retinoic acid and its 4-oxo metabolites are functionally active in human skin cells in vitro.* J Invest Dermatol, 2005. **125**(1): p. 143-53.
67. Grossi, M., et al., *Negative control of keratinocyte differentiation by Rho/CRIK signaling coupled with up-regulation of KyoT1/2 (FHL1) expression.* Proc Natl Acad Sci U S A, 2005. **102**(32): p. 11313-8.
68. Duffy, C.L., S.L. Phillips, and A.J. Klingelhutz, *Microarray analysis identifies differentiation-associated genes regulated by human papillomavirus type 16 E6.* Virology, 2003. **314**(1): p. 196-205.
69. Thomas, J.T., et al., *Cellular changes induced by low-risk human papillomavirus type 11 in keratinocytes that stably maintain viral episomes.* J Virol, 2001. **75**(16): p. 7564-71.
70. Darbro, B.W., G.B. Schneider, and A.J. Klingelhutz, *Co-regulation of p16INK4A and migratory genes in culture conditions that lead to premature senescence in human keratinocytes.* J Invest Dermatol, 2005. **125**(3): p. 499-509.
71. Murakami, T., et al., *Expression profiling of cancer-related genes in human keratinocytes following non-lethal ultraviolet B irradiation.* J Dermatol Sci, 2001. **27**(2): p. 121-9.
72. Howell, B.G., et al., *Microarray analysis of UVB-regulated genes in keratinocytes: downregulation of angiogenesis inhibitor thrombospondin-1.* J Dermatol Sci, 2004. **34**(3): p. 185-94.
73. Koike, M., T. Shiomi, and A. Koike, *Identification of Skin injury-related genes induced by ionizing radiation in human keratinocytes*

using cDNA microarray. J Radiat Res, 2005. **46**(2): p. 173-84.

74. Lamartine, J., et al., *Activation of an energy providing response in human keratinocytes after gamma irradiation.* J Cell Biochem, 2005. **95**(3): p. 620-31.
75. Boukamp, P., et al., *Normal keratinization in a spontaneously immortalized aneuploid human keratinocyte cell line.* J Cell Biol, 1988. **106**(3): p. 761-71.
76. Gibson, D.F., A.V. Ratnam, and D.D. Bikle, *Evidence for separate control mechanisms at the message, protein, and enzyme activation levels for transglutaminase during calcium-induced differentiation of normal and transformed human keratinocytes.* J Invest Dermatol, 1996. **106**(1): p. 154-61.
77. Lee, K.H., et al., *Differential gene expression in retinoic acid-induced differentiation of acute promyelocytic leukemia cells, NB4 and HL-60 cells.* Biochem Biophys Res Commun, 2002. **296**(5): p. 1125-33.
78. Ahn, J.I., et al., *Comprehensive transcriptome analysis of differentiation of embryonic stem cells into midbrain and hindbrain neurons.* Dev Biol, 2004. **265**(2): p. 491-501.
79. Kim, J.H., H.Y. Kim, and Y.S. Lee, *A novel method using edge detection for signal extraction from cDNA microarray image analysis.* Exp Mol Med, 2001. **33**(2): p. 83-8.
80. Tusher, V.G., R. Tibshirani, and G. Chu, *Significance analysis of microarrays applied to the ionizing radiation response.* Proc Natl Acad Sci U S A, 2001. **98**(9): p. 5116-21.
81. Eisen, M.B., et al., *Cluster analysis and display of genome-wide*

expression patterns. Proc Natl Acad Sci U S A, 1998. **95**(25): p. 14863-8.

82. Ho Sui, S.J., et al., *oPOSSUM: identification of over-represented transcription factor binding sites in co-expressed genes.* Nucleic Acids Res, 2005. **33**(10): p. 3154-64.
83. Clamp, M., et al., *Ensembl 2002: accommodating comparative genomics.* Nucleic Acids Res, 2003. **31**(1): p. 38-42.
84. Katiyar, S.K., et al., *Inhibition of UVB-induced oxidative stress-mediated phosphorylation of mitogen-activated protein kinase signaling pathways in cultured human epidermal keratinocytes by green tea polyphenol (-)-epigallocatechin-3-gallate.* Toxicol Appl Pharmacol, 2001. **176**(2): p. 110-7.
85. Kliewer, S.A., et al., *Differential expression and activation of a family of murine peroxisome proliferator-activated receptors.* Proc Natl Acad Sci U S A, 1994. **91**(15): p. 7355-9.
86. Edwards, D.P., *The role of coactivators and corepressors in the biology and mechanism of action of steroid hormone receptors.* J Mammary Gland Biol Neoplasia, 2000. **5**(3): p. 307-24.
87. Lee, M.O., et al., *Repression of FasL expression by retinoic acid involves a novel mechanism of inhibition of transactivation function of the nuclear factors of activated T-cells.* Eur J Biochem, 2002. **269**(4): p. 1162-70.
88. Park, C.H., et al., *Heat shock-induced matrix metalloproteinase (MMP)-1 and MMP-3 are mediated through ERK and JNK activation and via an autocrine interleukin-6 loop.* J Invest Dermatol, 2004. **123**(6): p. 1012-9.

89. Aristidou, A. and M. Penttila, *Metabolic engineering applications to renewable resource utilization.* Curr Opin Biotechnol, 2000. **11**(2): p. 187-98.
90. Braca, A., et al., *Antioxidant and free radical scavenging activity of flavonol glycosides from different Aconitum species.* J Ethnopharmacol, 2003. **86**(1): p. 63-7.
91. Cos, P., et al., *Structure-activity relationship and classification of flavonoids as inhibitors of xanthine oxidase and superoxide scavengers.* J Nat Prod, 1998. **61**(1): p. 71-6.
92. Valentao, P., et al., *Antioxidant activity of Centaurium erythraea infusion evidenced by its superoxide radical scavenging and xanthine oxidase inhibitory activity.* J Agric Food Chem, 2001. **49**(7): p. 3476-9.
93. Heim, K.E., A.R. Tagliaferro, and D.J. Bobilya, *Flavonoid antioxidants: chemistry, metabolism and structure-activity relationships.* J Nutr Biochem, 2002. **13**(10): p. 572-584.
94. Autore, G., et al., *Inhibition of nitric oxide synthase expression by a methanolic extract of Crescentia alata and its derived flavonols.* Life Sci, 2001. **70**(5): p. 523-34.
95. Mitchell, J.H., et al., *Antioxidant efficacy of phytoestrogens in chemical and biological model systems.* Arch Biochem Biophys, 1998. **360**(1): p. 142-8.
96. Hou, L., et al., *Inhibition of human low density lipoprotein oxidation by flavonols and their glycosides.* Chem Phys Lipids, 2004. **129**(2): p. 209-19.
97. Dumont, P., et al., *Overexpression of apolipoprotein J in human*

fibroblasts protects against cytotoxicity and premature senescence induced by ethanol and tert-butylhydroperoxide. Cell Stress Chaperones, 2002. **7**(1): p. 23-35.

98. McCord, J.M., *Superoxide dismutase, lipid peroxidation, and bell-shaped dose response curves.* Dose Response, 2008. **6**(3): p. 223-38.
99. Tagoe, C.E., et al., *Annexin-1 mediates TNF-alpha-stimulated matrix metalloproteinase secretion from rheumatoid arthritis synovial fibroblasts.* J Immunol, 2008. **181**(4): p. 2813-20.
100. Wisithphrom, K. and L.J. Windsor, *The effects of tumor necrosis factor-alpha, interleukin-1beta, interleukin-6, and transforming growth factor-beta1 on pulp fibroblast mediated collagen degradation.* J Endod, 2006. **32**(9): p. 853-61.
101. Monteleone, G., et al., *Control of matrix metalloproteinase production in human intestinal fibroblasts by interleukin 21.* Gut, 2006. **55**(12): p. 1774-80.
102. Jian, J., et al., *Iron sensitizes keratinocytes and fibroblasts to UVA-mediated matrix metalloproteinase-1 through TNF-alpha and ERK activation.* Exp Dermatol, 2011. **20**(3): p. 249-54.
103. Kligman, L.H., *The ultraviolet-irradiated hairless mouse: a model for photoaging.* J Am Acad Dermatol, 1989. **21**(3 Pt 2): p. 623-31.
104. Pinnell, S.R., *Cutaneous photodamage, oxidative stress, and topical antioxidant protection.* J Am Acad Dermatol, 2003. **48**(1): p. 1-19; quiz 20-2.
105. Fisher, G.J., et al., *c-Jun-dependent inhibition of cutaneous procollagen transcription following ultraviolet irradiation is reversed by all-trans retinoic acid.* J Clin Invest, 2000. **106**(5): p.

663-70.

106. Jung, E., et al., *Effect of Camellia japonica oil on human type I procollagen production and skin barrier function.* J Ethnopharmacol, 2007. **112**(1): p. 127-31.

107. Fisher, G.J., et al., *Molecular basis of sun-induced premature skin ageing and retinoid antagonism.* Nature, 1996. **379**(6563): p. 335-9.

108. Visse, R. and H. Nagase, *Matrix metalloproteinases and tissue inhibitors of metalloproteinases: structure, function, and biochemistry.* Circ Res, 2003. **92**(8): p. 827-39.

109. Lauer-Fields, J.L., D. Juska, and G.B. Fields, *Matrix metalloproteinases and collagen catabolism.* Biopolymers, 2002. **66**(1): p. 19-32.

110. McCawley, L.J. and L.M. Matrisian, *Matrix metalloproteinases: they're not just for matrix anymore!* Curr Opin Cell Biol, 2001. **13**(5): p. 534-40.

111. Brennan, M., et al., *Matrix metalloproteinase-1 is the major collagenolytic enzyme responsible for collagen damage in UV-irradiated human skin.* Photochem Photobiol, 2003. **78**(1): p. 43-8.

112. Li, M., et al., *Keratinocyte-releasable factors increased the expression of MMP1 and MMP3 in co-cultured fibroblasts under both 2D and 3D culture conditions.* Mol Cell Biochem, 2009. **332**(1-2): p. 1-8.

113. Ghaffari, A., et al., *Fibroblast extracellular matrix gene expression in response to keratinocyte-releasable stratifin.* J Cell Biochem, 2006. **98**(2): p. 383-93.

114. Palmer, D.M. and J.S. Kitchin, *Oxidative damage, skin aging,*

antioxidants and a novel antioxidant rating system. J Drugs Dermatol, 2010. **9**(1): p. 11-5.

115. Saurat, J.H., *Side effects of systemic retinoids and their clinical management.* J Am Acad Dermatol, 1992. **27**(6 Pt 2): p. S23-8.
116. Lehman, P.A., J.T. Slattery, and T.J. Franz, *Percutaneous absorption of retinoids: influence of vehicle, light exposure, and dose.* J Invest Dermatol, 1988. **91**(1): p. 56-61.
117. Ferguson, J. and B.E. Johnson, *Retinoid associated phototoxicity and photosensitivity.* Pharmacol Ther, 1989. **40**(1): p. 123-35.
118. Flynn, C. and B.A. McCormack, *Simulating the wrinkling and aging of skin with a multi-layer finite element model.* J Biomech, 2010. **43**(3): p. 442-8.
119. Kambayashi, H., et al., *N-retinoyl-D-glucosamine, a new retinoic acid agonist, mediates topical retinoid efficacy with no irritation on photoaged skin.* Br J Dermatol, 2005. **153 Suppl 2**: p. 30-6.
120. Boswell, C.B., *Skincare science: update on topical retinoids.* Aesthet Surg J, 2006. **26**(2): p. 233-9.
121. Kim, H., et al., *Synthesis and in vitro biological activity of retinyl retinoate, a novel hybrid retinoid derivative.* Bioorg Med Chem, 2008. **16**(12): p. 6387-93.
122. Uchino, T., et al., *Effect of squalene monohydroperoxide on cytotoxicity and cytokine release in a three-dimensional human skin model and human epidermal keratinocytes.* Biol Pharm Bull, 2002. **25**(5): p. 605-10.
123. Chiba, K., et al., *Characteristics of skin wrinkling and dermal changes induced by repeated application of squalene*

monohydroperoxide to hairless mouse skin. Skin Pharmacol Appl Skin Physiol, 2003. **16**(4): p. 242-51.

124. Chen, F., et al., *Phosphorylation of PPARgamma via active ERK1/2 leads to its physical association with p65 and inhibition of NF-kappabeta.* J Cell Biochem, 2003. **90**(4): p. 732-44.

125. Ashburner, M., et al., *Gene ontology: tool for the unification of biology. The Gene Ontology Consortium.* Nat Genet, 2000. **25**(1): p. 25-9.

126. Kim, H.K., et al., *Effects of naturally occurring flavonoids on nitric oxide production in the macrophage cell line RAW 264.7 and their structure-activity relationships.* Biochem Pharmacol, 1999. **58**(5): p. 759-65.

127. Kim, S.J., H. Park, and H.P. Kim, *Inhibition of nitric oxide production from lipopolysaccharide-treated RAW 264.7 cells by synthetic flavones: structure-activity relationship and action mechanism.* Arch Pharm Res, 2004. **27**(9): p. 937-43.

128. Xagorari, A., et al., *Luteolin inhibits an endotoxin-stimulated phosphorylation cascade and proinflammatory cytokine production in macrophages.* J Pharmacol Exp Ther, 2001. **296**(1): p. 181-7.

129. Blonska, M., Z.P. Czuba, and W. Krol, *Effect of flavone derivatives on interleukin-1beta (IL-1beta) mRNA expression and IL-1beta protein synthesis in stimulated RAW 264.7 macrophages.* Scand J Immunol, 2003. **57**(2): p. 162-6.

130. Blonska, M., et al., *Effects of ethanol extract of propolis (EEP) and its flavones on inducible gene expression in J774A.1 macrophages.* J Ethnopharmacol, 2004. **91**(1): p. 25-30.

131. Comalada, M., et al., *Inhibition of pro-inflammatory markers in primary bone marrow-derived mouse macrophages by naturally occurring flavonoids: analysis of the structure-activity relationship.* Biochem Pharmacol, 2006. **72**(8): p. 1010-21.
132. Pang, J.L., et al., *Differential activity of kaempferol and quercetin in attenuating tumor necrosis factor receptor family signaling in bone cells.* Biochem Pharmacol, 2006. **71**(6): p. 818-26.
133. Carroll, J.S., et al., *Genome-wide analysis of estrogen receptor binding sites.* Nat Genet, 2006. **38**(11): p. 1289-97.
134. Kim, H.K., et al., *Down-regulation of iNOS and TNF-alpha expression by kaempferol via NF-kappaB inactivation in aged rat gingival tissues.* Biogerontology, 2007. **8**(4): p. 399-408.
135. Liang, Y.C., et al., *Suppression of inducible cyclooxygenase and inducible nitric oxide synthase by apigenin and related flavonoids in mouse macrophages.* Carcinogenesis, 1999. **20**(10): p. 1945-52.
136. Blanquart, C., et al., *Peroxisome proliferator-activated receptors: regulation of transcriptional activities and roles in inflammation.* J Steroid Biochem Mol Biol, 2003. **85**(2-5): p. 267-73.
137. Lewis, D.A., et al., *Aberrant NF-kappaB activity in HaCaT cells alters their response to UVB signaling.* J Invest Dermatol, 2006. **126**(8): p. 1885-92.
138. Feingold, K.R., M. Schmuth, and P.M. Elias, *The regulation of permeability barrier homeostasis.* J Invest Dermatol, 2007. **127**(7): p. 1574-6.
139. Kalinin, A.E., A.V. Kajava, and P.M. Steinert, *Epithelial barrier function: assembly and structural features of the cornified cell*

envelope. Bioessays, 2002. **24**(9): p. 789-800.

140. Fuchs, E., *Epidermal differentiation.* Curr Opin Cell Biol, 1990. **2**(6): p. 1028-35.

141. Eckert, R.L., *Structure, function, and differentiation of the keratinocyte.* Physiol Rev, 1989. **69**(4): p. 1316-46.

142. Szabowski, A., et al., *c-Jun and JunB antagonistically control cytokine-regulated mesenchymal-epidermal interaction in skin.* Cell, 2000. **103**(5): p. 745-55.

143. Sugiura, K., et al., *The unfolded protein response is activated in differentiating epidermal keratinocytes.* J Invest Dermatol, 2009. **129**(9): p. 2126-35.

144. Lee, E.R., et al., *Modulation of apoptosis in HaCaT keratinocytes via differential regulation of ERK signaling pathway by flavonoids.* J Biol Chem, 2005. **280**(36): p. 31498-507.

145. Pillai, S., D.D. Bikle, and P.M. Elias, *1,25-Dihydroxyvitamin D production and receptor binding in human keratinocytes varies with differentiation.* J Biol Chem, 1988. **263**(11): p. 5390-5.

Abstract in Korean

녹차에서 발견되는 flavonol 중에서 캄페롤은 다양한 생물학적 활성을 갖고 있다. 그러나 식물에서 유래하는 캄페롤은 가격이 비싸서 상업적인 사용에 문제가 있었다. 최근에 녹차씨 (green tea seed, GTS)에 많은 양의 캄페롤 당유도체가 있음이 확인되었다. 구조 분석 결과, 두 가지의 캄페롤 당유도체를 확인했는데 이는 각각 kaempferol-3-O-[2-O-β-D-galatctopyranosyl-6-O-α-L-rhamnopyranosyl]-β-D-glucopyranoside (화합물 1)과 kaempferol-3-O-[2-O-β-D-xylopyranosyl-6-O-α-L-rhamnopyranosyl]-β-D-glucopyranoside (화합물 2)이다. 본 연구를 통해 상업적으로 유용한 효소 가수분해 반응을 통해 캄페롤을 확보할 수 있는 방법을 제안하였다. 이 때 최적의 효소조합은 β-galactosidase 와 hesperidinase 인데, 몇 개의 효소 반응 후에 화합물 1, 화합물 2 의 완전한 전환을 통해 95% 이상의 순도를 가진 캄페롤을 얻을 수 있었다.

캄페롤 성분을 확보한 후, 다양한 방법을 통해 항노화 활성을 평가하였다. 우선 위에서 언급한 2 개의 GTS 플라보노이드 (화합물 1, 화합물 2)와 그것의 아글리콘인 캄페롤의 항산화 효능을 비교하였다. 그 결과 캄페롤이 더 높은 DPPH 라디칼 소거능을 갖고 있음을 확인하였다. 또한 xanthine/xanthine oxidase 억제 효능도 화합물 1 과 화합물

2 보다 높았다. 캄페롤은 각질형성세포에 처리된 t-BHP 에 의해 유도되는 지질 과산화 현상도 억제하는 효능을 보였다. 자외선 B 는 세포 외 기질을 분해하는 중요 효소인 MMP-1 의 발현을 유도하는데, 캄페롤 처리에 의해 MMP-1 의 발현이 유의성 있게 감소하는 현상을 확인하였다. 이러한 효능은 인간유래 섬유아세포 단독배양 및 섬유아세포-각질형성세포 공배양계 모두 동일하였다. 그러나 섬유아세포에서 콜라겐 type I 의 전구체 형성을 유도하는 효능은 없었다. TNF-α 역시 피부노화를 유발하는 인자로서, 각질형성세포에서 유래하여 섬유아세포의 MMP-1 발현을 유도한다. 캄페롤은 섬유아세포-각질형성세포 공배양계에서 TNF-α의 발현을 억제하였다.

마지막으로 무모쥐와 인체 대상의 임상실험을 통해 피부 주름을 개선하는 캄페롤의 효능을 확인하였다. 피부주름 개선 효과는 모사판 분석을 통해 정량화하였다. 무모쥐에서 스쿠알렌 히드로과산화물로 유도되는 주름이 캄페롤 도포에 의해 감소되었다. 또한, 8 주간 인체 시험에서 캄페롤이 함유된 에멀전의 피부 도포는 광노출로 생성된 눈가 주름을 감소시키는 효과도 보였다.

표피에 대한 캄페롤의 효능을 확인하기 위하여 캄페롤을 처리한 인간유래 각질형성세포주 (HaCaT)를 대상으로 cDNA 마이크로어레이를 수행하였고, 그 결과 유의적인 변화가 있는

147 개의 유전자를 발견하였다. 이들 중 18 개는 증가하는 경향을, 129 개는 감소하는 경향을 보였다. 이 유전자들은 다음과 같이 12 개 카테고리로 분류되었다: 세포부착 및 세포 구조체, 세포주기, 산화-환원 항상성, 면역/방어 작용, 세포 대사, 단백질 생합성 및 변형, 세포 내 수송, RNA 프로세싱, DNA 변형 및 복제, 전사 조절, 세포 내 신호전달 등이다. 캄페롤에 의해 발현이 변화되는 유전자를 조절하는 전사인자를 확인하기 위해서 생물정보학 방법을 이용하여 유전자의 프로모터 영역을 분석한 결과 c-REL, SAP-1, Ahr-ARNT, Nrf-2, Elk-1, SPI-B, NF-κB, p65 의 전사조절을 발굴하였다. 마이크로어레이의 분석 결과와 생물정보학 분석 결과는 실시간 PCR 과 ELISA 를 기반으로 하는 리포터 유전자 분석법에 의해 재확인되었다. 캄페롤에 의한 NH-κB 전사활성 억제 현상이 PPAR 전사인자의 전사 활성에 의한 것임을 PPAR 리포터 유전자 분석을 통해 확인하였다. 각질형성세포에서 PPAR 전사 활성 증가는 각질형성세포의 분화를 유도하므로 BrdU incorporation 과 표피분화 마커 발현에 영향을 미치는 캄페롤의 효과를 확인하였다. 캄페롤은 각질형성세포에서 BrdU 결합을 저해할 뿐만 아니라, transglutaminase-1 의 단백질 발현을 유도하는데, 이와 같은 결과는 캄페롤이 각질형성세포의 분화를 유도하는데 도움을 준다는 것을 보여준다. 마이크로어레이 분석결과는 캄페롤에 의해 조절되는 유전자들의 네트워크를 확인하는데 큰 도움이 되었다. 또한 이러한 접근 방법은 유전자와

식물유래 약용성분 사이의 상호작용을 확인하는데 유용하게 활용될 수 있다.

결론적으로, 캄페롤은 매우 유용한 항노화 소재가 될 수 있는 가능성이 매우 높으며, 코스메슈티컬 제품에 적용될 수 있는 주요 후보 물질이라고 기대한다.

주요어: 캄페롤, 피부, 노화, 항산화, DNA 마이크로어레이, 주름

학 번: 2003-30270